



DESIGN AND SYNTHESIS OF BENZHYDROL DERIVATIVES AS  
ANTITUBERCULOSIS AGENTS



By  
MISS Pitikan KANJANAPRUK

A Thesis Submitted in Partial Fulfillment of the Requirements  
for Doctor of Philosophy PHARMACEUTICAL SCIENCES  
Graduate School, Silpakorn University  
Academic Year 2022  
Copyright of Silpakorn University

การออกแบบและการสังเคราะห์อนุพันธ์เบนซไฮดรอลเพื่อเป็นสารต้านไวรัสโรค



โดย  
นางสาวปติกาญจน์ กาญจนพฤกษ์

วิทยานิพนธ์นี้เป็นส่วนหนึ่งของการศึกษาตามหลักสูตรปรัชญาดุษฎีบัณฑิต  
สาขาวิชาวิทยาการทางเภสัชศาสตร์ แบบ 1.2 ปรัชญาดุษฎีบัณฑิต  
บัณฑิตวิทยาลัย มหาวิทยาลัยศิลปากร  
ปีการศึกษา 2565  
ลิขสิทธิ์ของมหาวิทยาลัยศิลปากร

DESIGN AND SYNTHESIS OF BENZHYDROL DERIVATIVES AS  
ANTITUBERCULOSIS AGENTS



A Thesis Submitted in Partial Fulfillment of the Requirements  
for Doctor of Philosophy PHARMACEUTICAL SCIENCES  
Graduate School, Silpakorn University  
Academic Year 2022  
Copyright of Silpakorn University

Title                    Design and Synthesis of Benzhydrol Derivatives as Antituberculosis Agents  
By                        MISS Pitikan KANJANAPRUK  
Field of Study        PHARMACEUTICAL SCIENCES  
Advisor                Assistant Professor Sathit Niratisai, Ph.D.  
Co advisor            Assistant Professor Kanawan Pochanakom, Dr.rer.nat.

---

Graduate School Silpakorn University in Partial Fulfillment of the Requirements for the Doctor of Philosophy

..... Dean of the Graduate School  
(Assistant Professor Sathit Niratisai, Ph.D)                    (Acting)

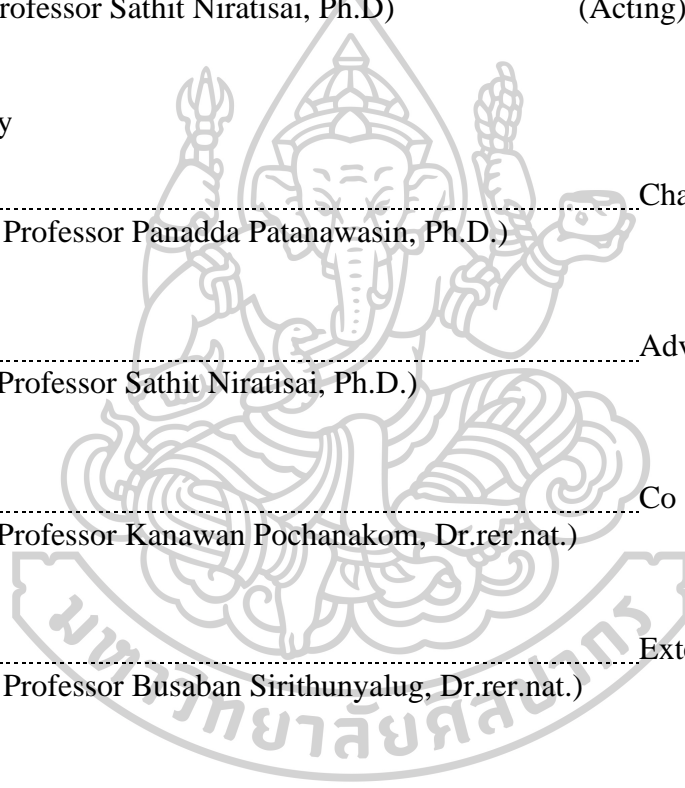
Approved by

..... Chair person  
(Associate Professor Panadda Patanawasin, Ph.D.)

..... Advisor  
(Assistant Professor Sathit Niratisai, Ph.D.)

..... Co advisor  
(Assistant Professor Kanawan Pochanakom, Dr.rer.nat.)

..... External Examiner  
(Associate Professor Busaban Sirithunyalug, Dr.rer.nat.)



57356802 : Major PHARMACEUTICAL SCIENCES

Keyword : benzhydrol, antituberculosis, Fries rearrangement

MISS PITIKAN KANJANAPRUK : DESIGN AND SYNTHESIS OF BENZHYDROL DERIVATIVES AS ANTITUBERCULOSIS AGENTS THESIS ADVISOR : ASSISTANT PROFESSOR SATHIT NIRATISAI, Ph.D.

Benzhydrol derivatives were designed, synthesized, and evaluated for antituberculosis activities. Benzhydrol derivatives (compounds 4a-f, 9, 10, 13a-c) and its diacetylated derivatives (compounds 5a, 5c, 5f), which are analogs of the natural product 1'-acetoxychavicol acetate (ACA) from *Alpinia galangal* rhizome, were designed as new antituberculosis agents. In this synthetic approach, compounds 4a-f, 9 were synthesized in three steps, i.e. (1) coupling reactions between benzoic acid or substituted benzoic acids and phenol to form ester linkages, (2) Fries rearrangement of phenylbenzoates using aluminium chloride as a catalyst to get benzophenones, and (3) reduction of ketones with sodium borohydride to obtain benzhydrol compounds. Compounds 4a-f and 9 had overall yields of 20.26%, 26.98%, 56.59%, 49.71%, 31.41%, 23.97%, and 40.54%, respectively. Benzhydrol 10 was prepared by amide hydrolysis of compound 4f with a 6.57% overall yield. By acetylating 4a, 4c, and 4f with acetic anhydride, the diacetylated derivatives 5a, 5c, and 5f were obtained with overall yields of 18.82%, 39.22%, and 21.96%, respectively. The amide derivatives 13a-c were prepared: (1) amide formation between 4-aminobenzophenone and alkyl, aryl, or long-chain aryl acids, and (2) ketone reduction. Compounds 13a-c had overall yields of 57.53%, 29.74%, and 24.26%, respectively. The structures of desired compounds were elucidated by spectral data (<sup>1</sup>H NMR, <sup>13</sup>C NMR and IR). These synthesized benzhydrol compounds were evaluated for antituberculosis activities by agar-dilution method. It was found that they had antituberculosis efficacy on 20 clinical isolates and MTB H37Rv reference strains (ATCC 27294). Compound 4d, 4-hydroxy- $\alpha$ -(4'-butylphenyl)benzyl alcohol possessed the highest inhibitory activity in this series with an MIC value of 20-40  $\mu$ g/ml. The structure-activity of the synthesized benzhydrol derivatives were also summarized.

## ACKNOWLEDGEMENTS

First of all, I especially would like to express my deepest gratitude to my advisor Asst. Prof. Dr. Sathit Niratisai, for his encouragement, valuable advice, guidance, and support throughout my study. My sincere gratitude also goes to my co-advisors, Asst. Prof. Dr. Kanawan Pochanakom, for her supervision, valuable advice, encouragement, and kindness throughout my study. Besides my advisors, I would like to thank my thesis committees, Assoc. Prof. Dr. Panadda Patanawasin and Assoc. Prof. Dr. Busaban Sirithunyalug for giving me insightful comments and suggestions.

My special acknowledgment is extended to all teachers who share their education with me and the Department of Pharmaceutical Chemistry, Faculty of Pharmacy, Silpakorn University for the research facilities and their kind assistance. I would like to thank Dr. Therdsak Prammananan, Tuberculosis Research Laboratory, National Center for Genetic Engineering and Biotechnology, National Science and Technology Development Agency, Thailand, sincerely acknowledged for his kind and helpful cooperation for activity testing.

I would like to thank my supervisor and my friends at the Department of Medical Sciences, Ministry of Public Health, for helping me to support materials and equipments for my thesis and Miss Ei Ei THIN for invaluable help, encouragement, and our friendship.

I would like to acknowledge the Graduate School of Silpakorn University for the Thesis Development Scholarship.

Finally, my deepest appreciation goes to my family for everything, especially your love, care, encouragement, and support all the time.

MISS Pitikan KANJANAPRUK

## TABLE OF CONTENTS

	<b>Page</b>
ABSTRACT.....	D
ACKNOWLEDGEMENTS.....	E
TABLE OF CONTENTS.....	F
LIST OF TABLES.....	I
LIST OF FIGURES.....	J
CHAPTER 1 INTRODUCTION.....	1
1.1 Statement and significance of the research problem.....	1
1.2 Objectives of the study.....	3
1.3 Hypotheses of the study.....	3
1.4 Scope of the study.....	5
CHAPTER 2 LITERATURE REVIEW.....	8
2.1 Tuberculosis.....	8
2.1.1 Tuberculosis Overview.....	8
2.1.2 Causes of Tuberculosis.....	9
2.2 Anti-tuberculosis drugs.....	11
2.2.1 Targets and mode of action of current anti-TB drugs.....	12
2.3 1'-S-Acetoxychavicol acetate (ACA).....	15
2.3.1 ACA modification for anti-TB activity.....	15
2.3.2 Stability of ACA.....	17
2.4 Chemical synthesis.....	20
2.4.1 Benzhydrol synthesis.....	20
2.4.2 Benzophenone synthesis.....	21
2.4.3 Fries rearrangement reaction.....	22
2.4.4 Reduction.....	24
2.5 Chemical structure of anti-TB agents.....	25

CHAPTER 3 MATERIALS AND METHODS .....	30
3.1 Materials .....	30
3.1.1 Instruments .....	30
3.1.2 Chemical reagents and Instruments.....	30
3.1.3 Chemical preparations .....	32
3.2 Methods .....	33
3.2.1 General methods for chemistry .....	33
3.2.2 Synthesis of designed compounds.....	35
3.2.2.1 Synthesis of phenyl benzoate derivatives (2a-f).....	35
3.2.2.2 Synthesis of 4-hydroxy benzophenone derivatives (3a-f).....	37
3.2.2.3 Synthesis of (4-Hydroxyphenyl)phenylmethanol derivatives (4a-f) .....	39
3.2.2.4 4-acetoxy- $\alpha$ -(phenyl)benzyl acetate derivatives (5a, 5d, 5g) .....	42
3.2.2.5 2-Naphthyl benzoate (7) .....	43
3.2.2.6 4-hydroxyphenyl(2-naphthyl)methanone (8) .....	44
3.2.2.7 4-hydroxyphenyl(2-naphthyl)methanol (9).....	44
3.2.2.8 4-((4-aminophenyl)(hydroxy)methyl)phenol (10).....	45
3.2.2.9 4-amido benzophenone derivatives (12a-c).....	45
3.2.2.10 4-amido benzhydrol derivatives (13a-c).....	47
3.3 Evaluation of antitubercular activities .....	48
CHAPTER 4 RESULTS AND DISCUSSION.....	50
4.1 Chemical synthesis .....	52
4.1.1 Phenyl benzoate compounds (2a-f) .....	52
4.1.2 Benzophenone compounds (3a-m).....	54
4.1.2.1 Fries rearrangement reaction investigation by DSC analysis.....	54
4.1.3 Benzhydrol compounds (4a-f) and 9 .....	59
4.1.4 Diacetyl benzhydrol compounds (5a, 5c, 5f) .....	60
4.1.5 4-hydroxy- $\alpha$ -(4'-amino phenyl)benzyl alcohol (10).....	60
4.1.6 Amidobenzhydrol compounds (13a-c).....	61

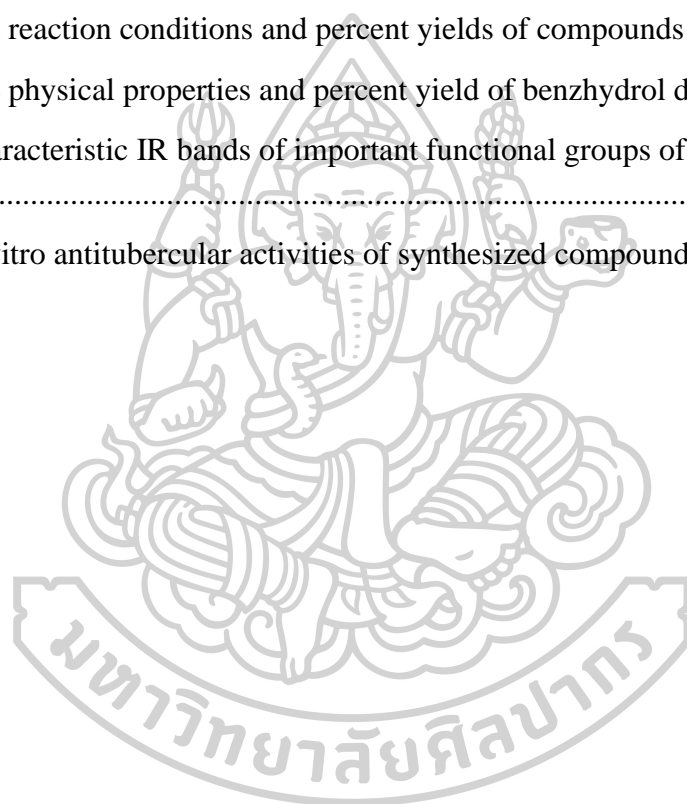


4.2 Structural characterizations .....	64
4.2.1 IR spectroscopic characterization.....	64
4.2.2 NMR spectroscopic characterization.....	69
4.3 Structure-activity relationship of synthesized compounds and anti-tuberculosis activity .....	74
CHAPTER 5 CONCLUSION.....	78
REFERENCES .....	81
APPENDIX.....	88
VITA.....	117



## LIST OF TABLES

	<b>Page</b>
Table 1 Synthesized benzhydrol derivatives.....	6
Table 2 Anti-TB drugs and their targets .....	13
Table 3 % Compositions of Fries rearrangement products by LC-MS analysis at variable temperatures .....	56
Table 4 The reaction conditions and percent yields of compounds 3a-f and 8.....	59
Table 5 The physical properties and percent yield of benzhydrol derivatives .....	63
Table 6 Characteristic IR bands of important functional groups of synthesized compounds .....	68
Table 7 In vitro antitubercular activities of synthesized compounds against MTB <sup>a</sup> ...	77



## LIST OF FIGURES

	<b>Page</b>
Figure 1 Chemical structure of 1'S-1'-Acetoxychavicol acetate (ACA).....	1
Figure 2 Design of benzhydrol derivatives.....	2
Figure 3 Proposed benzhydrol derivatives.....	3
Figure 4 Design strategy used for benzhydrol derivatives.....	4
Figure 5 The Mycobacterial cell wall structure.....	10
Figure 6 Mycolic acids in MTB.....	11
Figure 7 ACA and its analogs possessing anti-TB activities.....	16
Figure 8 Hydrolysis of 1'-Acetoxychavicol acetate.....	17
Figure 9 Proposed sigmatropic rearrangement of 1'-Acetoxychavicol acetate.....	18
Figure 10 Chemical structure of 1'-Acetoxychavicol acetate (ACA), benzhydrol and benzhydrol diacetate.....	18
Figure 11 Diarylmethane and diarylmethanone derivatives possessing anti-TB activities.....	19
Figure 12 Synthesis of benzhydrol analogs.....	20
Figure 13 Synthesis of benzhydrol and acetoxylbenzhydrol analogs.....	21
Figure 14 Synthesis of benzophenone derivatives.....	22
Figure 15 Mechanism of Fries rearrangement reaction.....	23
Figure 16 Mechanism of ketone reduction by NaBH <sub>4</sub> .....	25
Figure 17 Structure of amino containing anti-TB compounds.....	25
Figure 18 Structure of amide containing anti-TB compounds.....	26
Figure 19 Structure of halogen containing anti-TB compounds.....	27
Figure 20 Structure of cinnamyl containing anti-TB compounds.....	28
Figure 21 Structure of long chain containing anti-TB compounds.....	29
Figure 22 The scope of research project.....	51
Figure 23 The reaction mechanism of the esterification.....	53
Figure 24 DSC curves of the mixtures of compounds 2b, 2e, 2f and AlCl <sub>3</sub> .....	55

Figure 25 The reaction mechanism of Fries rearrangement. ....	58
Figure 26 The reaction mechanism of sodium borohydride reduction .....	60
Figure 27 The reaction mechanism of the base-catalyzed hydrolysis .....	61
Figure 28 The reaction mechanism of the amide formation .....	62
Figure 29 The structure of active benzhydrol derivatives of this series .....	80



## CHAPTER 1 INTRODUCTION

### 1.1 Statement and significance of the research problem

In recent years, tuberculosis (TB) remains as one of the ten leading causes of death worldwide in 2021.[1] There are an estimated 10.4 million new incident of TB annually, and the number of deaths is around 1.8 million. The high susceptibility of human immunodeficiency virus-infected persons to the disease, the emergence of multi-drug-resistant (MDR-TB) strains and extensively drug-resistant (XDR-TB) ones have brought this infectious disease into the focus of urgent scientific interest. However, the development of new anti-TB drugs has been slow, therefore, importantly efforts to discover new classes of chemical compounds acting with different mechanisms from currently used.

1'S-1'-Acetoxychavicol acetate (ACA) (Figure 1), the major constituent isolated from *Alpinia galangal* rhizome, and its derivatives were reported to be efficacious antituberculosis agents. ACA was studied against *M. tuberculosis* H37Ra and *M. tuberculosis* H37Rv strains with minimum inhibitory concentrations (MIC) 0.1-0.5 µg/mL and 0.6-1.6 µg/mL, respectively.[2] ACA is reasonably a lead compound for the development of new potent anti-TB drugs. However, ACA still has a few disadvantages i.e. poor water solubility and degradation in aqueous solution. Because of unstable structure, it is hard to develop ACA as edible drugs and modification of chemical structure is needed to improve stability. Thus, while the possibility to develop ACA itself as an oral anti-TB drug may be remote, synthetic compounds that contain the ACA pharmacophore were considered to be viable lead.

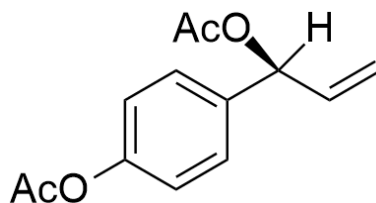


**Figure 1** Chemical structure of 1'S-1'-Acetoxychavicol acetate (ACA)

To avoid the instability of ACA, our attempt began to investigate the replacement effect of the vinyl on ACA with phenyl, as shown in Figure 2. In a review study, benzhydrol diacetate analog was reported as a stable analog of natural ACA.[3] Therefore, in this research, benzhydrol derivatives were designed to obtain promising stable compounds, synthesized, and tested for anti-TB activity. Benzhydrol was selected as a scaffold for designing of proposed compounds. To further understanding the SAR of the benzhydrol derivatives, substitution at aromatic ring A and B was explored. The benzhydrol derivatives were designed and synthesized into three groups. 1) 4-Hydroxybenzhydrols containing the *para*- position of ring A was substituted with hydroxyl group. The acetamido substitution at ring B was substituted at *meta*- or *para*- to compare the effects of substitution positions on anti-TB activities. At the *para*- position of ring B, various functional groups, including halide, amino, amide, aromatic, and aliphatic groups, were attached. 2) Benzhydrol diacetates were designed to mimic the ACA structure to evaluate the acetoxy group's necessity. The di-hydroxy compounds that show effective activity were converted to di-acetoxy compounds to investigate their anti-TB activities further. 3) 4-Amidobenzhydrols were generated from the coupling between benzhydrol and the alkyl, aryl, or cinnamyl to explore the molecular target. (Figure 3) In addition, interesting intermediate compounds, benzophenone derivatives were tested for anti-TB activity.

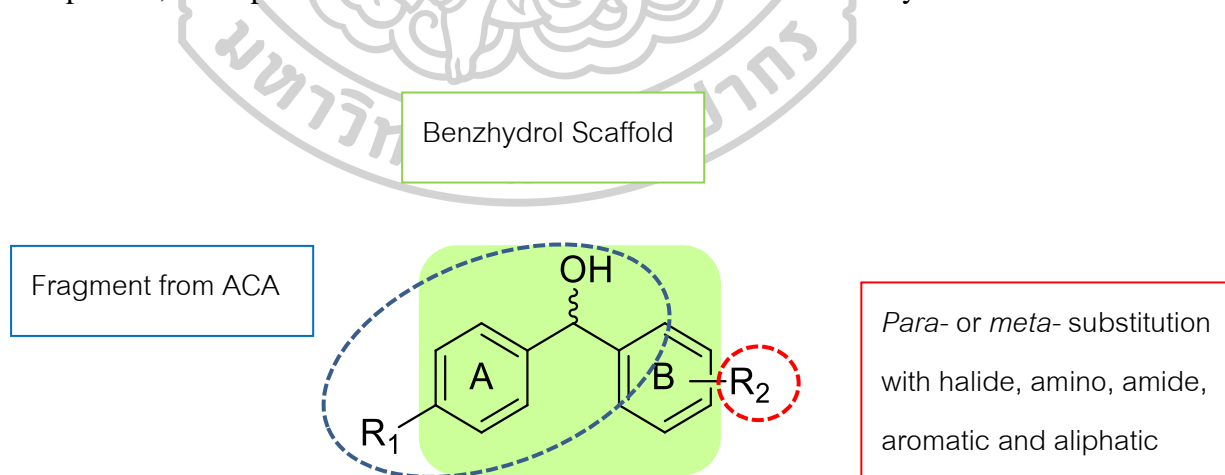


**Figure 2** Design of benzhydrol derivatives

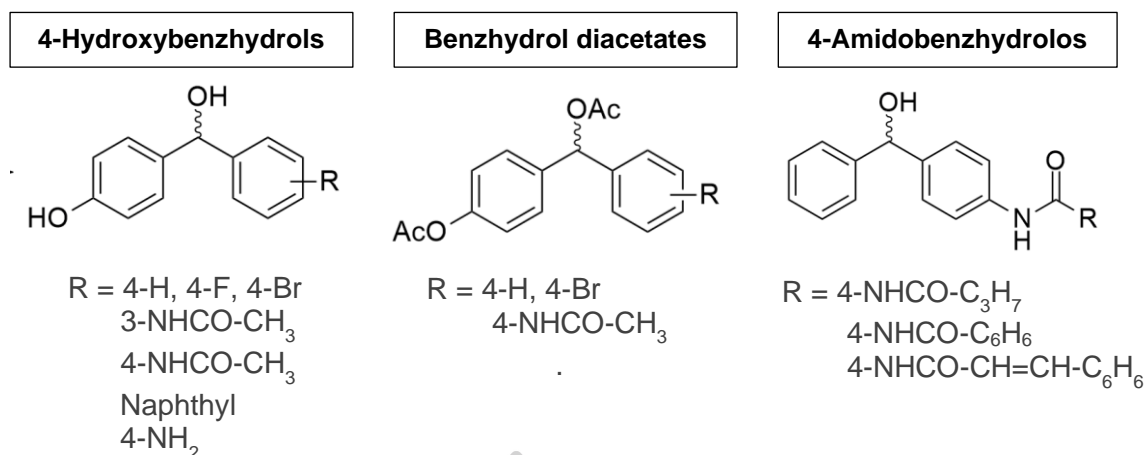


**Figure 3** Proposed benzhydrol derivatives

### 1.2 Objectives of the study

The goal of the study is to design and synthesize benzhydrol derivatives as antituberculosis agents. Objectives of research in order to achieve this goal are

1. To design and synthesize benzhydrol derivatives
2. To evaluate antitubercular activities of the synthesized benzhydrol derivatives
3. To determine the structure-activity relationship (SAR) of the synthesized benzhydrol derivatives after evaluation of MIC values against *M.tuberculosis* strains

### 1.3 Hypotheses of the study

A literature survey described that both ACA and diphenyl compounds possess anti-TB activity with good MIC values on *M. tuberculosis* strains. [2, 4-6] The two structural fragments, i.e., 1'-hydroxychavicol obtained from ACA and diphenyl rings, were structurally combined to generate benzhydrol derivatives, which can be employed to explore target sites. (Figure 4). The benzhydrol derivatives were modified as follows:

1. Substitution of halogen atoms, fluorine and bromine, at *meta*- or *para*-positions of the benzene ring (R3) may enhance anti-TB activity due to attractive interaction between the high electronegativity nature of halogen atoms with electrophilic regions of target sites. The different sizes of halogen atoms may describe the size of the binding sites of biological targets.

2. Substitution at R3 with various chemical groups, e.g., alkyl long chain or replacing benzene ring with naphthalene ring (compound 9), may also give information on the size and shape of binding sites as in hydrophobic pockets of the targets.

3. Amide substitution (R3) may be employed, assuming that its ionization giving positive ions at physiological pH may attract negative ions of target binding sites. In addition, the amino group can be coupled with various side-chain acids, e.g., aliphatic acid, aromatic acid, or cinnamic acid, by forming an amide linkage to explore the interaction of amide side chains with biological targets.

4. Acetoxy substitution at  $\alpha$ -carbon (R1) and benzene ring (R2) positions may increase biological activity with promising acetyl groups as essential substituents similar to that of the lead compound (ACA).

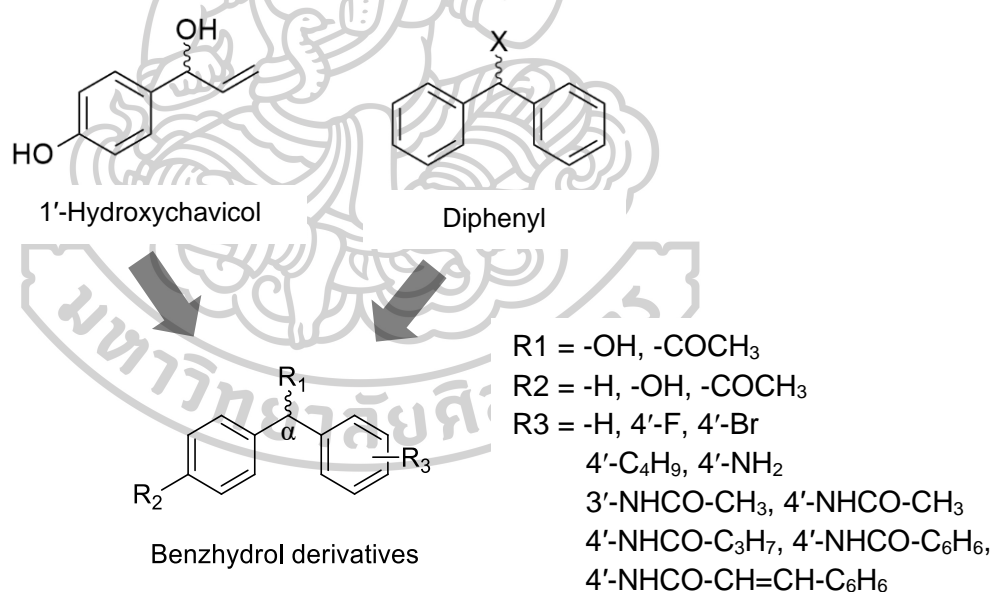
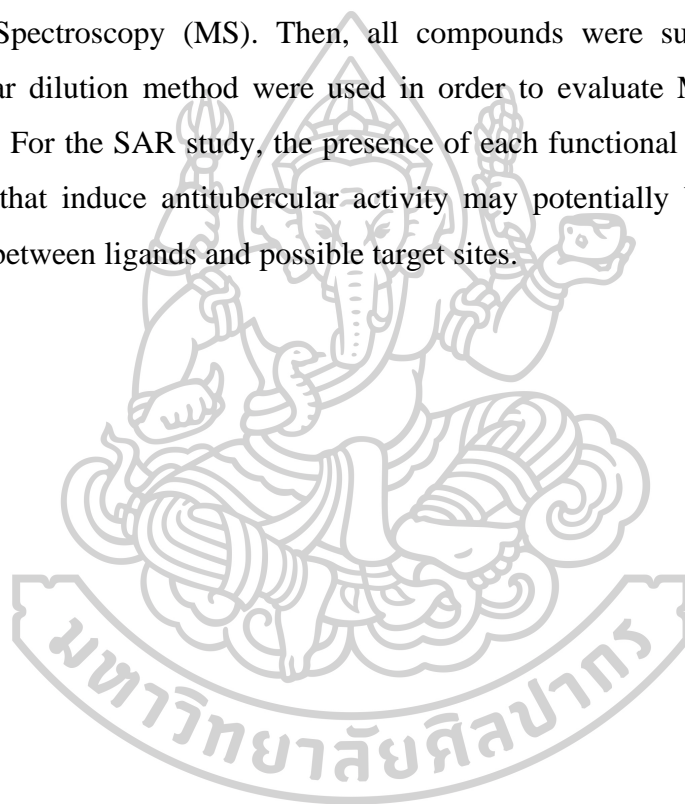


**Figure 4** Design strategy used for benzhydryl derivatives

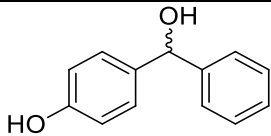
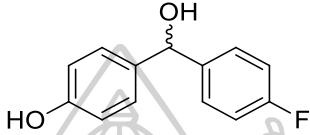
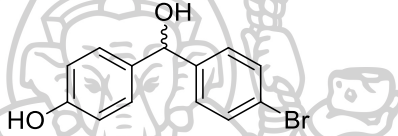
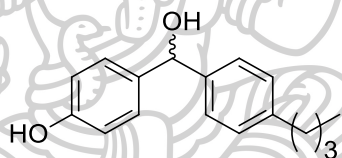
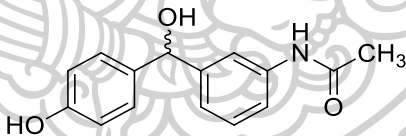
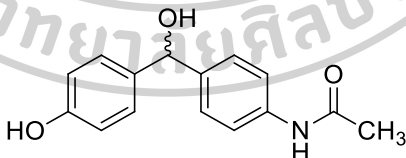
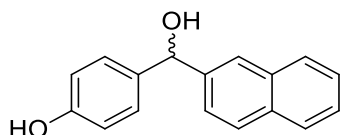
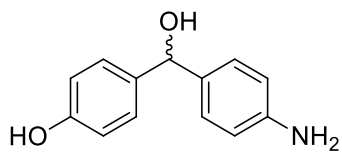


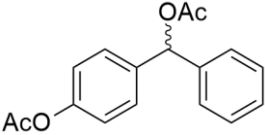
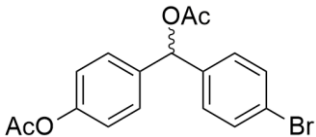
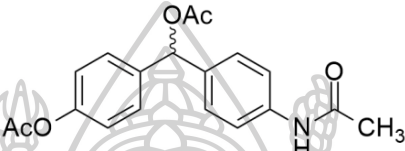
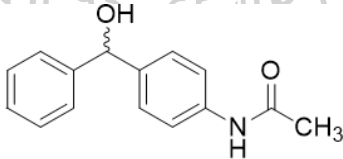
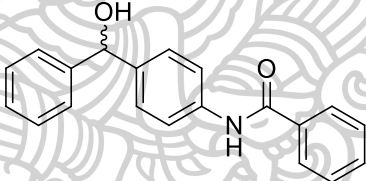
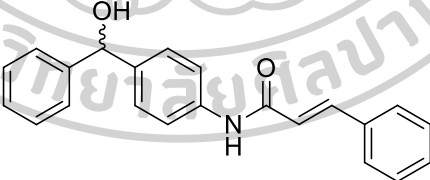
#### 1.4 Scope of the study

A set of new analogs were designed and synthesized to evaluate the structural requirements for the antituberculosis activity. Benzhydrol derivatives prepared from organic synthesis are shown in Table 1. All synthesized compounds were purified by chromatography. Percent yields of products were calculated for each purified compound. Chemical structures were elucidated by using spectroscopic methods i.e. Fourier Transform Infrared Spectroscopy (FTIR), Proton Nuclear Magnetic Spectroscopy ( $^1\text{H-NMR}$ ), Carbon-13 Nuclear Magnetic Spectroscopy ( $^{13}\text{C-NMR}$ ), and Mass Spectroscopy (MS). Then, all compounds were subjected for anti-TB testing. Agar dilution method were used in order to evaluate MICs of synthesized compounds. For the SAR study, the presence of each functional group of benzhydrol derivatives that induce antitubercular activity may potentially be explained by the interaction between ligands and possible target sites.



**Table 1** Synthesized benzhydryl derivatives

Entry	Compound code	Chemical structures	Molecular formula	Molecular weight
1	4a		$C_{13}H_{12}O_2$	200.23
2	4b		$C_{13}H_{11}FO_2$	218.22
3	4c		$C_{13}H_{11}BrO_2$	279.13
4	4d		$C_{17}H_{20}O_2$	256.34
5	4e		$C_{15}H_{15}NO_3$	257.28
6	4f		$C_{15}H_{15}NO_3$	257.28
7	9		$C_{17}H_{14}O_2$	250.29
8	10		$C_{13}H_{13}NO_2$	215.25

Entry	Compound code	Chemical structures	Molecular formula	Molecular weight
9	5a		C <sub>17</sub> H <sub>16</sub> O <sub>4</sub>	284.31
10	5d		C <sub>17</sub> H <sub>15</sub> BrO <sub>4</sub>	363.20
11	5f		C <sub>19</sub> H <sub>19</sub> NO <sub>5</sub>	341.36
12	13a		C <sub>15</sub> H <sub>14</sub> NO <sub>2</sub>	240.28
13	13b		C <sub>20</sub> H <sub>17</sub> NO <sub>2</sub>	303.35
14	13c		C <sub>22</sub> H <sub>19</sub> NO <sub>2</sub>	329.39

## CHAPTER 2 LITERATURE REVIEW

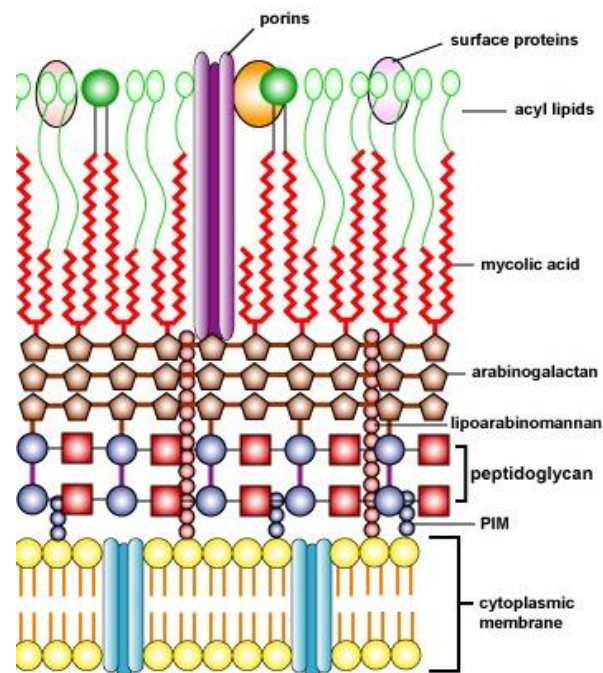
### 2.1 Tuberculosis

#### 2.1.1 Tuberculosis Overview

Tuberculosis (TB) is a threat to worldwide public health, mainly caused by *Mycobacterium tuberculosis* (MTB) bacteria species. In 2021, an estimated 10.4 million people fell ill with TB worldwide and the largest number of new TB cases occurred in the South-East Asian region with 44% of new cases. TB has led to an estimated death of around 1.3 million including human immune deficiency virus (HIV) positive people in 2021 and is the second leading cause of deaths among the infectious disease [1]. With its high death rate, tuberculosis remains a difficult disease to treat. There are other forms of tuberculosis that affect the kidney, brain, lungs, etc., but mycobacteria mostly damage the lungs because MTB, an aerobic mycobacterium, receives a great deal of oxygen from the lungs. Due to the emergence of MDR-TB, XDR-TB, and TDR-TB, the directly observed treatment short therapy (DOTS) with the first line anti-TB medications isoniazid (INH), rifampin (RIF), ethambutol (EMB), and pyrazinamide (PZA) is no longer sufficient to combat this lethal disease. [7-9]. Bedaquiline recommended by United States Food and Drug Administration (USFDA) [10] and delamanid approved by European Medical Agency (EMA) [11] for treatment of MDR-TB have shown cases of resistance. In addition to QT prolongation, bedaquiline and delamanid cause hepatotoxicity [12] and CNS toxicity [13, 14], respectively. There have been reports that long-term treatment with bedaquiline is related with cardiac arrhythmia as a fatal side effect [15]. Recently, USFDA has approved pretomanid, a nitroimidazopyran derivative, in conjunction with bedaquiline and linezolid for XDR-TB or MDR-TB to treat adult TB patients [16]. Due to the deteriorating tuberculosis condition, there has been an urgent need for the discovery of novel antitubercular agents. Poor chemotherapeutics, cross-resistance, and the dearth of effective anti-TB medications highlight the need for the discovery of innovative anti-tuberculous agents that may have a novel mode of action. Novel anti-TB drugs with benzhydryl as its pharmacophoric characteristic are described here.

### 2.1.2 Causes of Tuberculosis

Tuberculosis is caused by the bacillus *Mycobacterium tuberculosis* (MTB). MTB is a rather large, non-motile, rod-shaped bacterium, measuring 2 to 4  $\mu\text{m}$  in length and 0.2 to 0.5  $\mu\text{m}$  in width, and dividing every 16 to 20 hours, which is a very slow rate compared to other bacteria. MTB is neither Gram-positive nor Gram-negative because it lacks the chemical characteristics of either category. Its cell wall possesses both Gram-positive and Gram-negative features.[17] They are categorized as acid-fast Gram-positive bacteria (AFB) because they lack an outer cell membrane and their fatty cell walls prevent acid solutions from decolorizing the cells during diagnostic staining. The cell wall structure of MTB deserves special attention because it appears to allow MTB to survive in its preferred environment. It is a major determinant of virulence for the bacterium. The cell walls of all *Mycobacterium* species are thicker than those of most other bacteria, being hydrophobic, waxy, and abundant in mycolic acids/mycolates. The cell wall consists of the hydrophobic mycolate layer and a peptidoglycan layer held together by a polysaccharide, arabinogalactan.[18, 19] The arabinogalactan and mycolic acid layer is covered by a polypeptide layer. Other glycolipids include phosphatidylinositol mannosides and lipoarabinomannan. Porins are involved in the movement of tiny hydrophilic molecules through the cell wall's outer membrane. (Figure 5)

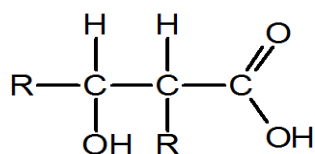


Source: From <http://student.cbcemd.edu/courses/bio141/lecguide/unit1/prostruct/u1fig11.html>

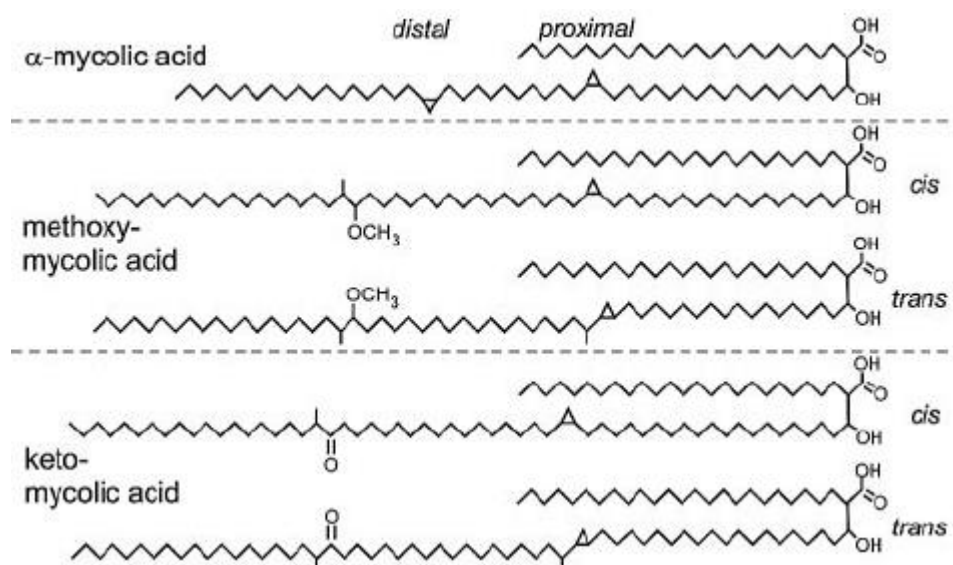
**Figure 5** The Mycobacterial cell wall structure

Lipids make up more than sixty percent of the mycobacterial cell wall. Mycolic acids, cord factor, and wax-D are the three primary components that make up the lipid fraction of the MTB cell wall [20, 21]. Mycolic acids impart *M. tuberculosis* with unique properties that defy medical treatment. They increase an organism's resistance to chemical damage and dehydration and reduce the efficacy of hydrophilic antibiotics and biocides [22].

Mycolic acids are high-molecular weight fatty acid. They are composed of a longer beta-hydroxy chain with a shorter alpha-alkyl side chain. Each molecule contains between 60 and 90 carbon atoms. Three main types of mycolic acids are alpha-, methoxy-, and keto-mycolic acid. Alpha-mycolic acids constitute at least 70% of the organism's mycolic acids and include several cyclopropane rings. Between 10 and 15 percent of the mycolic acids in an organism are methoxy-mycolic acids, which contain several methoxy groups. 10% to 15% of the remaining mycolic acids are keto-mycolic acids, which contain several ketone groups (Figure 6).



Mycolic Acid



Source: From <https://pl.csl.sri.com/mycolate-overview.html>

**Figure 6** Mycolic acids in MTB

## 2.2 Anti-tuberculosis drugs

In 1944, chemotherapy for tuberculosis was initiated using the natural substance streptomycin. Then, in the early 1950s, the alternative synthetic chemicals isoniazid and pyrazinamide were discovered, followed by ethambutol and rifampicin in 1961 and 1963, respectively.[23, 24] After the approval of rifampicin in 1967, no new anti-tubercular drugs were developed until the introduction of bedaquiline as an anti-tubercular medicine in 2012. There was a forty-year gap in identifying innovative drugs to treat this disease. TB is a priority disease for the discovery and development of novel, safe compounds because MDR and XDR strains are emerging at a rapid rate. It is synergistic of the HIV pandemic, pharmacokinetic interaction between anti-TB and anti-retroviral drugs, complex regimens for MDR-TB, longer treatment duration, relapse, and toxic side effects.[25] The first-line drugs, including isoniazid, rifampin,

ethambutol and pyrazinamide, are the most effective and have the lowest toxicity. The second-line drugs are less effective and have more toxic effects than first-line drugs. These drugs may not be available in many developing countries. There are streptomycin, *p*-amino salicylic acid, ciprofloxacin, and moxifloxacin. The third-line drugs are Amikacin, linezolid, clarithromycin, kanamycin, cycloserine, and capreomycin. These drugs were categorized as "third-line treatments" because they are not highly effective or their efficacy has not been demonstrated.

Novel drugs required to combat tuberculosis must contain bactericidal activity against both drug-susceptible and drug-resistant MTB strains and be effective in real-world settings. In general, novel and safe anti-TB drugs aim to decrease treatment duration, develop new mechanisms of action against drug-resistant strains, be effective against MDR-TB and XDR-TB, prevent drug-drug interactions, and reduce toxic side effects. In addition, new anti-tuberculosis medications must be oral-only regimens in adults, children, and HIV patients. Their posology must be once daily or less frequently for treatment course tolerability. The next challenge is to be cost competitive with current drugs.

### **2.2.1 Targets and mode of action of current anti-TB drugs**

Current standard treatment for tuberculosis (TB) involves drugs that interfere with bacterial metabolism, particularly those that prevent cell wall production. Cell wall inhibitors include isoniazid, ethambutol, ethionamide, and cycloserine; nucleic acid synthesis inhibitors include rifampicin and quinolones; protein synthesis inhibitors include streptomycin and kanamycin; and second-line TB medications include those that block the metabolism of membrane energy (pyrazinamide) [26]. New drugs have emerged recently as potential candidates for the treatment of TB. The new anti-tuberculosis agents are targeting mycolic acid biosynthesis, protein biosynthesis, cofactor biosynthesis, menaquinone biosynthesis, ATP biosynthesis, regulatory proteins, and the stringent response enzyme [27]. Targets and mechanisms of action of current TB drugs are summarized in Table 2.



**Table 2** Anti-TB drugs and their targets

No.	Drug	Chemical class	Mechanism of action	MIC ( $\mu\text{g/ml}$ )	Ref.
1	Isoniazid	Isonicotinic acid derivative	Inhibits cell wall mycolic acid biosynthesis	0.02-020	[26]
2	Rifampicin	Amide derivatives	Inhibits of RNA synthesis	0.05-0.50	[26]
3	Pyrazinamide	Niacinamide derivative	Depletion of membrane energy	5.5-6.0	[26]
4	Ethambutol	Ethylenediamine	Inhibits cell-wall arabinogalactan synthesis	1.0-5.0	[26]
5	Streptomycin	Amino-glycoside	Inhibits protein synthesis	1.0-8.0	[26]
6	Kanamycin	Amino-glycoside	Inhibits protein synthesis	1.0-4.0	[26]
7	Amicacin	Semi-synthetic aminoglycoside	Inhibits protein synthesis	1.0-4.0	[26]
8	Capreomycin	Cyclic peptide	Inhibits protein synthesis	2.0-4.0	[26]
9	Quinolones	Fluroquinolone	Inhibits DNA replication and transcription	0.2-4.0	[28]
10	Ethionamide	Isonicotinic acid derivative	Inhibits mycolic acid synthesis	2.5-10.0	[26]
11	Prothionamide	Thioamide derivative	Disrupts cell wall biosynthesis	0.5	[29]
12	Para-amino salicylic acid	Salicylic acid	Inhibits folate biosynthesis	0.50-8.0	[26]
13	D-cycloserine	D-analine analogue	Inhibits peptidoglycan biosynthesis in the cell wall	1.5-40.0	[26]
14	Rifabutin	A rifamycin class	Inhibits RNA synthesis	0.015 - 0.125	[30]
15	Rifapentine	Cyclopentyl rifampicin	Inhibits RNA synthesis	0.06-0.5	[31]

**Table 2** Anti-TB drugs and their targets (continued)

No.	Drug	Chemical class	Mechanism of action	MIC ( $\mu\text{g/ml}$ )	Ref.
16	Clofazimine	A lipophilic riminophena-zine antibiotic	Probably acts on membrane transport	0.01-0.25	[26]
17	Bedaquiline	Diarylquinoline	Inhibits ATP synthesis	0.03-0.12	[32]
18	Delamanid	Dihydronitroimidazo oxazole derivative	Probably inhibiting cell wall	0.006-0.024	[33]
19	Linezolid	Oxazolidinone	Inhibits protein synthesis	0.06-1.0	[34]
20	Thioacetazone	Thiosemicarbazone	Inhibits cell wall synthesis	0.1	[35]
21	Pretomanid	Nitroimidazole	Probably inhibition of cell wall synthesis and causing respiratory	0.015-0.25	[33]
22	Tedizolid	Oxazolidinone	Inhibits protein synthesis	0.015-16	[36]
23	Sutezolid	Oxazolidinone	Inhibits protein synthesis	$\leq 0.062$	[37]
24	SQ 109	1,2-ethylenediamine	Inhibits cell wall synthesis	0.7-1.56 ( $\mu\text{M}$ )	[38]
25	TBA-354	Pyridine biaryl nitroimidazole	Inhibits cell wall synthesis and causing respiratory poisoning	0.011	[39]
26	CPZEN-45	Caprazamycin derivative	Inhibits cell wall biosynthesis	1.56	[40]
27	Q203	Imidazopyridine amide	Oxidative phosphorylation	10 nM	[41]
28	SQ641	Carboxamide	Inhibits cell wall biosynthesis	1.0	[42]

### 2.3 1'-S-Acetoxychavicol acetate (ACA)

1'-S-Acetoxychavicol acetate (ACA) is the major constituent isolated from *Alpinia galangal* (Kha) rhizome. Greater galangal is also known as *Alpinia galangal* (L.) Sw. (Zingiberaceae), and it is a perennial herb that has rhizomatous root stocks and tall stems that are covered with leaves. The plant has been discovered in the Western Ghats, Mysore, Goa, Malabar, and Gujarat, as well as Thailand, Indonesia, China, and Malaysia. ACA was reported to possess activities as antioxidant, anticancer, antifungal, antimicrobial, anti-inflammatory, gastroprotective agent, anti-HIV, and anti-TB.[2, 3, 43-58]

For anti-TB activity, ACA was studied against *M. tuberculosis* H37Ra and *M. tuberculosis* H37Rv strains with minimum inhibitory concentrations (MIC) 0.1-0.5 µg/mL and 0.6-1.6 µg/mL, respectively.[2] In addition, ACA was reported that it could inhibit efflux pump in *M. smegmatis* mc2 cells.[44] This is highly advantageous because inhibition of efflux pump can decrease the resistance of bacteria to antibiotic and reduce the frequency of the emergence of resistant mutant strains, while the toxic level of ACA is low in various mammalian cells with higher MICs than the MIC against *M.tb* H37Ra.[2]

#### 2.3.1 ACA modification for anti-TB activity

Due to the various advantages of ACA, it is a likely candidate for creating new effectively anti-tuberculosis drugs. Bunthitsakda W. reported the study of anti-TB of ACA analogs to clarify the structure–activity relationship for drug design. There were four compounds (**I**, **II**, **III**, and **IV**) showed potent anti-TB activity against *M. tuberculosis* H37Ra (Figure 7). This report showed that the presence of two acetyl groups replacing hydroxyl groups did not significantly affect anti-TB activity.[43] Electron-withdrawing halogen substitutions at the *para*- and *ortho*- position of benzene ring of compounds (**I**, **II**) showed high inhibitory activity against *M. tuberculosis* H37Ra. The presence of the aliphatic side chain at C1' of chavicol of compounds (**III**, **IV**) was important for improving activity.[59] This research informed that the essential anti-tuberculosis structure of ACA analogs should contain the following structural requirements: 1) the *para*-substitution of halide atom at the benzene ring was required; 2) the presence of aliphatic side chain at C1' of chavicol should have fewer than 8 carbons; 3) The presence of an acetyl group rather than a

hydroxyl group at the C1' position of an active molecule (with an eight-carbon aliphatic side chain) was crucial for enhancing its biological activity; 4) A phenyl group connected to a carbon atom with a highly electronegative group at the *para*-position of the benzene ring, such as a chloride or bromide atom, possesses the physical properties necessary to enter the target cell more effectively than other aromatics. [43] The MICs of *S*-ACA against *M. tuberculosis* H37Ra and H37Rv were lower than those of the racemic ACA. Both *S*- and *rac*-ACA had potent bactericidal activity and were able to kill the *M. tuberculosis* H37Rv strain.[4] The structural requirements of ACA for displaying activity have described that phenyl acetate moiety was important, substitution of vinyl group by phenyl still possessed the activity and the chirality was not influential factor for eliciting the response. [46]

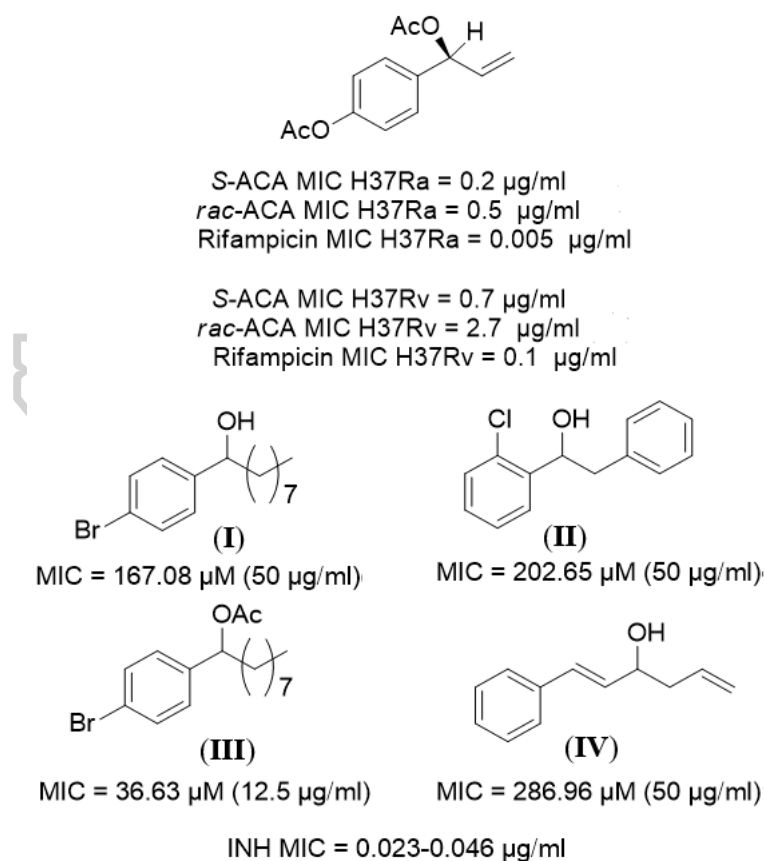


**Figure 7** ACA and its analogs possessing anti-TB activities

### 2.3.2 Stability of ACA

In an aqueous solution, ACA lacked stability. After a few hours at room temperature, ACA undergoes hydrolysis and structural rearrangement. Three degraded products were identified as 1'-hydroxychavicol acetate, *p*-coumaryl diacetate, and *p*-acetoxycinnamic alcohol (Figure 8) [60]. It can also be postulated that ACA is metabolically unstable compound. As hydrolysis products, *p*-acetoxycinnamic alcohol is the result of ACA's SN1 reaction mechanism, and *p*-coumaryl diacetate is the consequence of [3,3]-sigmatropic isomerization (Figure 9) [62]. Kubota K. and co-workers reported the antioxidant activity of ACA and its related compounds from *A. galanga* fresh rhizomes imported from Thailand. They heated rhizomes in aqueous medium or lard and antioxidant assay was investigated by ferric thiocyanate and thiobarbituric acid (TBA) method. It was found degraded compounds of *A. galanga* after heating in aqueous medium or lard [61]. As a result, the clinical applications of ACA as an antituberculosis drug are limited by some restrictions.

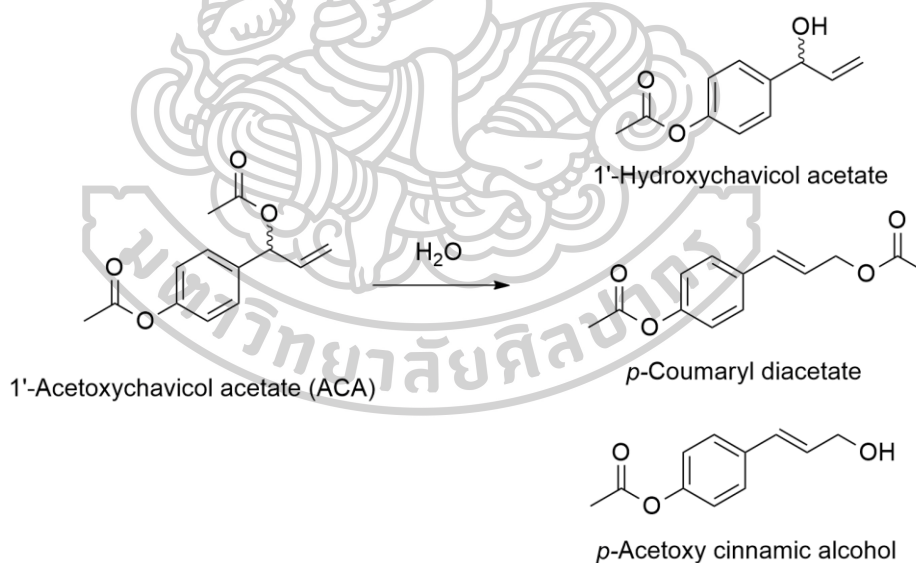


**Figure 8** Hydrolysis of 1'-Acetoxychavicol acetate.

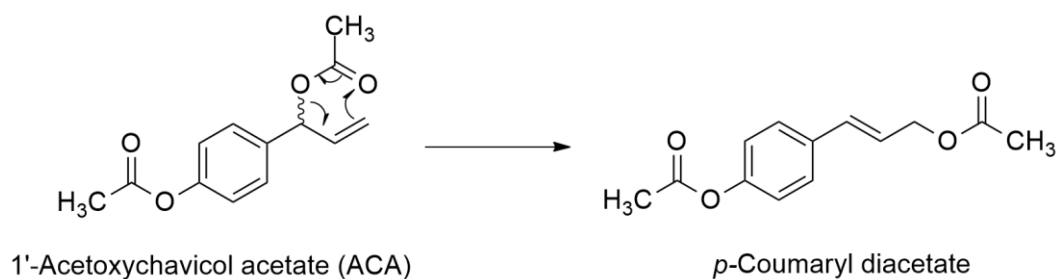


**Figure 9** Proposed sigmatropic rearrangement of 1'-Acetoxychavicol acetate.

Because ACA has a few disadvantages, i.e. poor water solubility and degradation in aqueous solution, it is hard to develop ACA as edible drugs and chemical structure modification is needed to improve stability. While the possibility of developing ACA as an oral anti-TB medication is remote, synthesized molecules containing the ACA pharmacophore may be a feasible lead. Benzhydryl derivatives were designed as stable ACA analogs. The vinyl group of ACA was substituted by the phenyl group, converting to benzhydryl diacetate (Figure 10). Benzhydryl derivatives were reported to possess antiallergic and anticancer activities. [3, 46] It has been proved that these derivatives are stable and become promising lead compounds for anti-TB activity for this study.

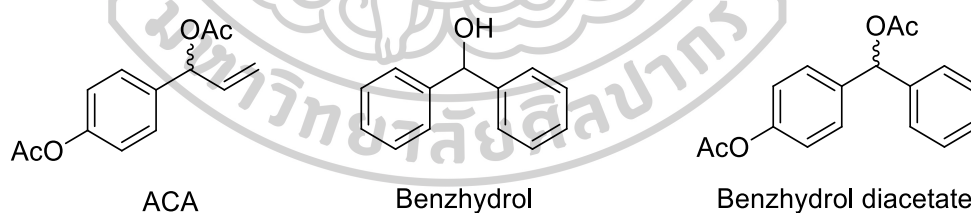


**Figure 10** Chemical structure of 1'-Acetoxychavicol acetate (ACA), benzhydryl and benzhydryl diacetate

Due to the advantages of diaryl containing benzhydryl scaffold, design and synthesis of benzhydryl derivatives were investigated in several studies. Furthermore, diarylmethane and diarylmethanone derivatives with promising antitubercular activities were also well documented (Figure 11). [4-6]

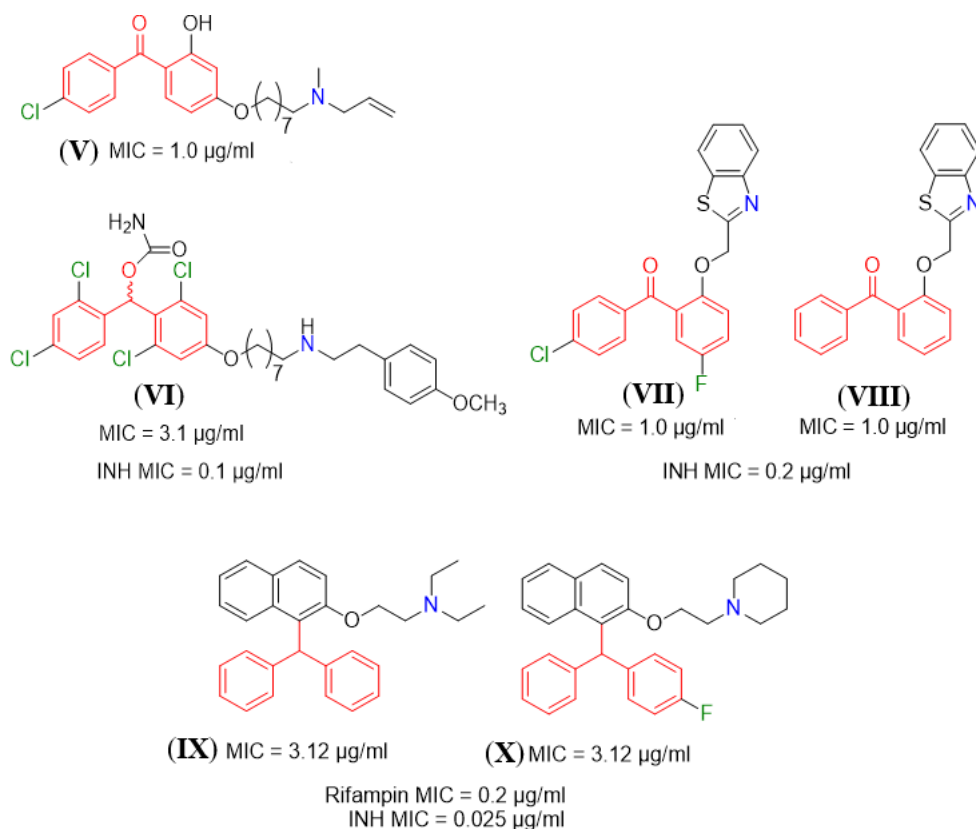


**Figure 11** Diarylmethane and diarylmethanone derivatives possessing anti-TB activities

From literature reviews [4-6], it was found that most of compounds containing diaryl rings with nitrogen atom and halogen atom showed effective anti-TB activity. The electron donating and electron withdrawing groups of nitrogen and halogen atoms show a significant effect on anti-TB activity. However, the mechanism of action of these compounds on *M. tuberculosis* is unknown and there are only few SAR studies of ACA and benzhydrol derivatives on anti-TB activity. Hence, it is of great interest to discover novel compounds with high potency for *M. tuberculosis* inhibition. Based on the structures of ACA and benzhydrol, we attempted to design and synthesis a series of benzhydrol derivatives and determine the SAR of novel benzhydrol derivatives against *M. tuberculosis* H37Rv activities.

## 2.4 Chemical synthesis

### 2.4.1 Benzhydrol synthesis

Benzhydrol or diphenylmethanol can be synthesized by the reduction of benzophenone or by a Grignard reaction between phenyl magnesium bromide and benzaldehyde. The synthesis pathway of benzhydrol type 1'-acetoxychavicol acetate (ACA) analogs was reported by Misawa et al. [3] The hydroxyl group of 4-hydroxybenzaldehyde was protected with *tert*-butyldimethylchlorosilane (TBS-Cl). The intermediates were then made by treating 4-hydroxybenzaldehyde with the right Grignard or aryl lithium reagents. The TBS group was deprotected with tetra-*n*-butylammonium fluoride (TBAF), and acetylation with acetic anhydride yielded benzhydrols and their acetyl analogs. On the other hand, the hydroxyl group of 4-bromophenol was protected with TBS-Cl, followed by treatment with *n*-butyllithium, yielding aryllithium species, which were quenched with different benzaldehydes to yield intermediates. TBS group deprotection with TBAF and subsequent acetylation with acetic anhydride yielded benzhydrols and acetylated compounds (Figure 12).

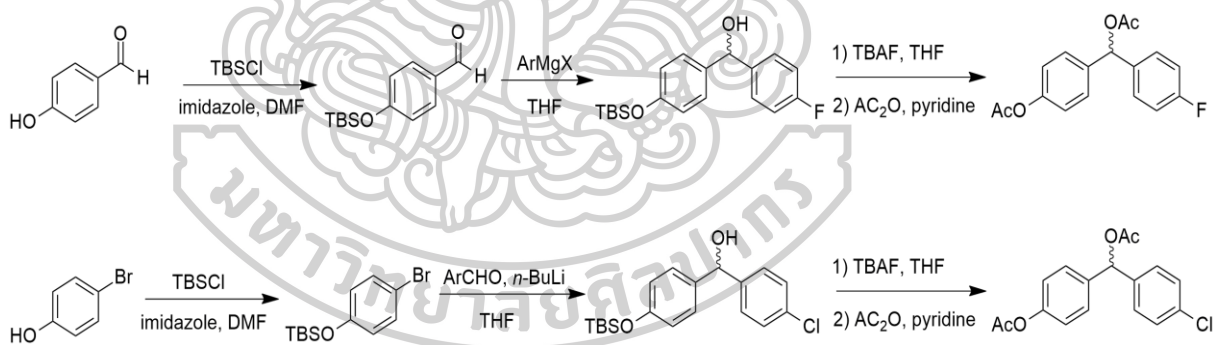


**Figure 12** Synthesis of benzhydrol analogs

Yasuhara et al. synthesized the acetoxybenzhydrols as a potent antiallergic. The benzhydrol analogues were created by protecting the hydroxyl of 4-hydroxybenzophenone with *tert*-butyldimethylsilyl chloride (TBSCl), which resulted in the corresponding silyl ether compound, which was then reduced with sodium borohydride to yield a racemic mixture of TBS-O-benzhydrol. 4-hydroxybenzhydrol was produced by treating protected benzhydrol with tetrabutylammonium fluoride in THF. Under usual conditions, 4-hydroxybenzhydrol was treated with acetic



anhydride, suitable acyl chlorides, or methyl chlorocarbonate to obtain corresponding acetoxybenzhydrols. (Figure 13).

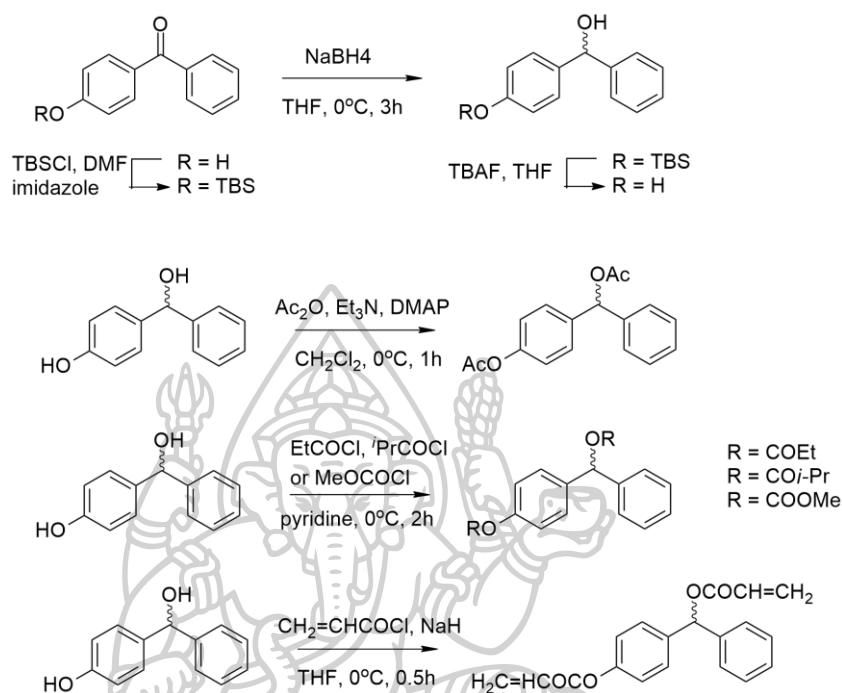


**Figure 13** Synthesis of benzhydrol and acetoxybenzhydrol analogs

#### 2.4.2 Benzophenone synthesis

According to the benzhydrol synthesis, benzophenone can be reduced to create benzhydrol. In 2012, Kwon and coworkers [62] synthesized the anti-inflammatory activity of a benzophenone derivative by inhibiting IFN- $\gamma$ -induced ICAM-1 expression. Figure 14 depicts the straightforward synthesis of benzoyloxy benzophenone derivatives, which consists of the dicyclohexyl carbodiimide coupling of benzoic acid with phenol, the Fries rearrangement of ester to aryl ketone, and the esterification of benzophenone and acyl chloride to yield benzoyloxy benzophenone. Fries rearrangement and esterification of benzoic acids produced benzoyloxy benzophenones with yields ranging from 24 to 89%.

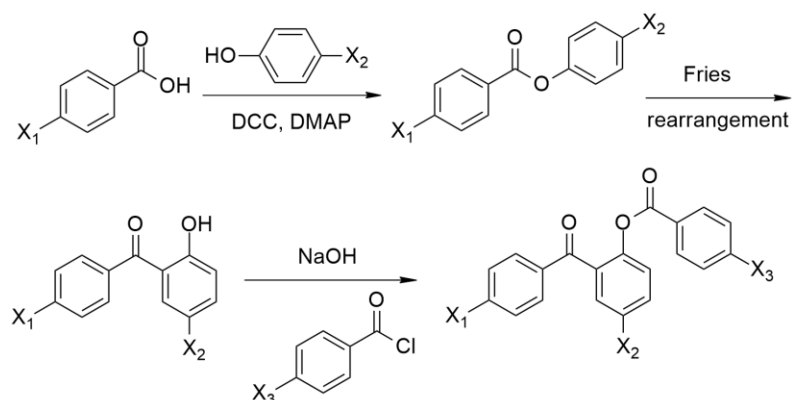


**Figure 14** Synthesis of benzophenone derivatives

### 2.4.3 Fries rearrangement reaction

The Fries rearrangement is an organic process in which phenolic esters are converted into hydroxyaryl ketones by heating in the presence of a catalyst. Phenolic esters on heating with aluminium trichloride (Lewis acid) give *ortho* and *para* acyl phenol. Solvent is generally not required for the reaction. Utilizing Nitrobenzene, DMF, and Zylene decreases the reaction temperature. Fries rearrangement has also been observed to be catalysed by light (photo Fries rearrangement). Fries rearrangement is well documented. However, the regioselectivity between the formation of 2- or 4-hydroxybenzophenones is still in question because of the versatility of substituents in the structure, which results in a low yield. [63] The *para* isomer is generally generated preferentially at temperatures below 100 C, but above this temperature, the *ortho* isomer predominates. The most commonly employed Lewis acids for the Fries rearrangement reaction are  $\text{AlCl}_3$ ,  $\text{FeCl}_3$ ,  $\text{MsOH}$ , and  $\text{ZnCl}_3$  at temperatures between 100°C to 210 °C [62].

Due to the wide ranges of reaction temperatures, Yerande S. and co-workers investigated the various reaction temperatures to obtain the ratio of *ortho*-/*para*-isomer. Toward this goal, Fries rearrangement was performed using  $\text{AlCl}_3$  as a catalyst at various temperatures ranging from 40 °C to 170 °C. They discovered that temperatures below 100°C result in partial conversion, while temperatures above 150°C result in lower isolated yields due to the considerable formation of other side products. Hence all the optimizations were carried out to do Fries rearrangement using 1.5 equiv of  $\text{AlCl}_3$  at 120 °C [64].

The precise process of Fries rearrangement remains unclear. Both intermolecular and intramolecular reaction processes are supported by evidence. Therefore, it appears that both mechanisms are acting concurrently. A two-step mechanism may be taken to be Friedel-Crafts acylation in which the acylium ion, (MeCO) is supplied by the substrate, i.e., it is self-acylation. Initially,  $\text{AlCl}_3$  binds with the oxygen of the phenoxy group to create the acylium ion. As depicted in Figure 15, the acylium ion attacks the benzene ring. An acyl group of phenol ester migrates to the aryl ring. The reaction is *ortho* and *para* selective, and modifying reaction conditions, such as temperature and solvent, might prefer one of the two products.

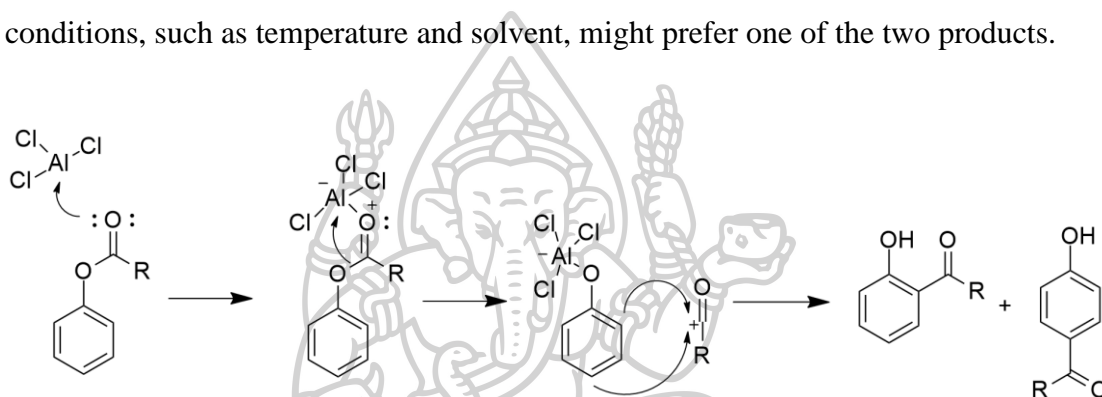


**Figure 15** Mechanism of Fries rearrangement reaction

In this study, benzhydrol derivatives were synthesized from corresponding phenyl benzoates through Fries rearrangement and reduction reaction. In order to carry out the synthesis using the non-solvent technique, the Fries rearrangement reaction was decided to be used. As Fries rearrangement is an endothermic reaction [65], the reaction mixtures of phenyl benzoates and  $\text{AlCl}_3$  heated at constant rates were analyzed by differential scanning calorimetry (DCS) to establish the ideal temperature for phenyl benzoates.

#### **Differential scanning calorimetry (DSC) analysis**

Differential scanning calorimetry (DSC) is a thermal analytical measuring how a sample's physical or chemical properties change, along with temperature, against time. This technique involves the calorimetry of heat released in a chemical process, either a reaction or a conformational alteration. It can be utilized to calculate metrics such as the Heat of Reaction ( $\Delta_rH$ ), the change in enthalpy associated with a chemical reaction. When  $\Delta_rH$  is negative, the process is exothermic and heat is released; when  $\Delta_rH$  is positive, the process is endothermic and heat input is required.

[66]. In the literature, DSC uses include evaluating structural-phase transition, melting point, and assessing molecular interaction between solid components [67, 68]. Litwinienko and co-workers [69] demonstrated that DSC can be used to investigate the oxidative stability of both simple [linolenic acid (LNA)] and complex (lecithin) lipids. By comparing the kinetics of soy lecithin autoxidation to that of LNA, it is possible to learn about the differences between the thermal oxidative behaviors of simple and complex lipids. Sopade et al. [70] investigated gelatinization in mixtures of sugars offers a promising frontier in clarifying the process. According to DSC research, this process is endothermic, with two stages: breaking of existing hydrogen bonds (endothermic) and creation of new bonds to produce a less-ordered structure (exothermic). DSC techniques could be useful to provide new data about the structural thermodynamics of reaction intermediates.[71] In particular, some reactions, such as isothermal amplification of nucleic acids, can be processed in DSC to obtain new thermodynamic information about polymerizing nucleic acid molecules [72]. A DSC thermograph might represent the complex process involving dehydration of the saccharide rings, depolymerization, and disintegration of the acetylated and deacetylated units of the polymer [73, 74] As a DSC application, to investigate the optimal temperature for the endothermic Fries rearrangement, our research utilized DSC as a promising screening tool for determining the optimal temperature.

#### **2.4.4 Reduction**

Reduction is the chemical reactions where one or more electrons are gained. When an atom gains one or more electrons during a chemical process, this is referred to as reduction. That suggests its oxidation number is decreasing.

Alcohols can be prepared from carbonyl compounds such as aldehydes, ketones, esters, acid chlorides and even carboxylic acids by hydride reductions. These reductions are the result of two net hydrogen atom additions to the C=O bond. Lithium aluminum hydride ( $\text{LiAlH}_4$ ) and sodium borohydride are the most prevalent hydride-reducing agents ( $\text{NaBH}_4$ ).  $\text{LiAlH}_4$  is one of the most potent reducing agents, effectively reducing carbonyl.  $\text{NaBH}_4$  is less reactive and can be used to convert aldehydes and ketones to alcohols selectively. Since  $\text{NaBH}_4$  is not especially reactive, the reaction is often carried out in protic solvents such as ethanol or methanol. [75] the sodium ion is a weaker Lewis acid than the lithium ion, and the hydrogen bonding

between the alcohol and the carbonyl group serves as a catalyst to activate the carbonyl group. This reaction takes place as a result of the activation of the carbonyl group, as shown in Figure 16.

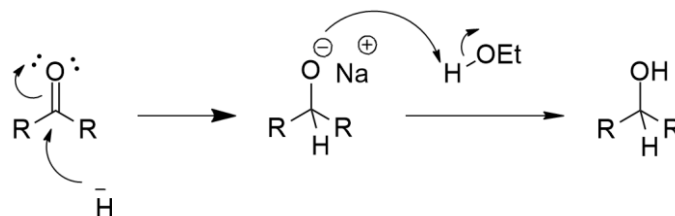


**Figure 16** Mechanism of ketone reduction by NaBH<sub>4</sub>

## 2.5 Chemical structure of anti-TB agents

Based on anti-TB drugs, amino aromatic compounds are organic molecules with an amine (-NH<sub>2</sub>) group, which is a significant functional group in drug design. There are many well-known drugs containing amino aromatic structure such as antibiotic isoniazid, ethionamide, prothionamide, *para*-amino salicylic acid. In addition, compounds containing amino groups have been reported in the discovery of leads as new anti-tuberculosis agents (Figure 17). Some compounds containing amide functional group with therapeutic efficacy showed in Figure 18 [76, 77]. Chemically, amide is a powerful electron-withdrawing group that, by attracting electrons nearby, can generate localized or regional electron-deficient zones within molecules. Electrophilic amide groups can react with biological nucleophiles such as proteins, amino acids, enzymes, and nucleic acids in the target sites.

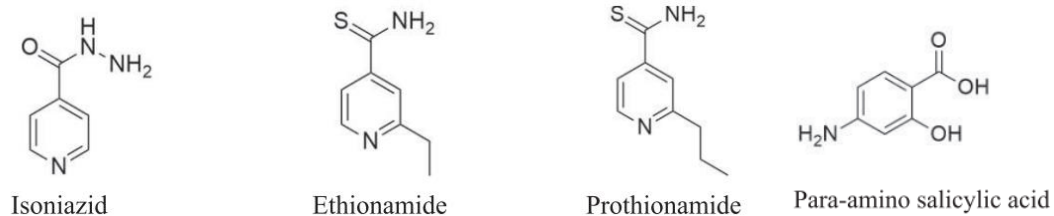


**Figure 17** Structure of amino containing anti-TB compounds

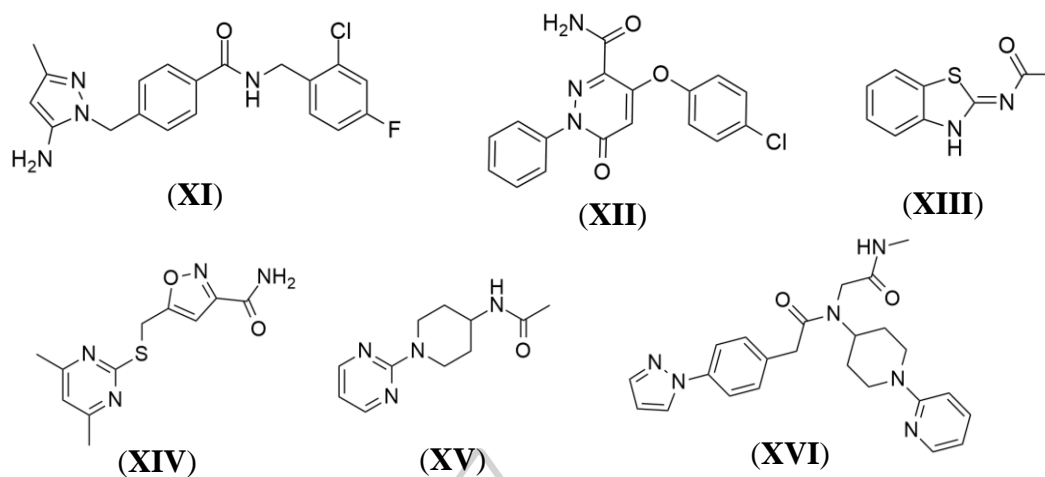


**Figure 18** Structure of amide containing anti-TB compounds

The addition of a halogen atom in the molecule is commonly used in drug design because halogen is the most electronegative element. Its electron-withdrawing effect can be attributed to changing the acidity, lipophilicity and conformation and modifying the interaction of halogenated compounds with the biological receptor or enzyme, all of which may be influenced by biological and pharmacological properties. As lead modification, halogen atom was incorporated at the different position of phenyl ring and it was observed that antituberculosis activities was reported as shown in Figure 19. [78, 79]

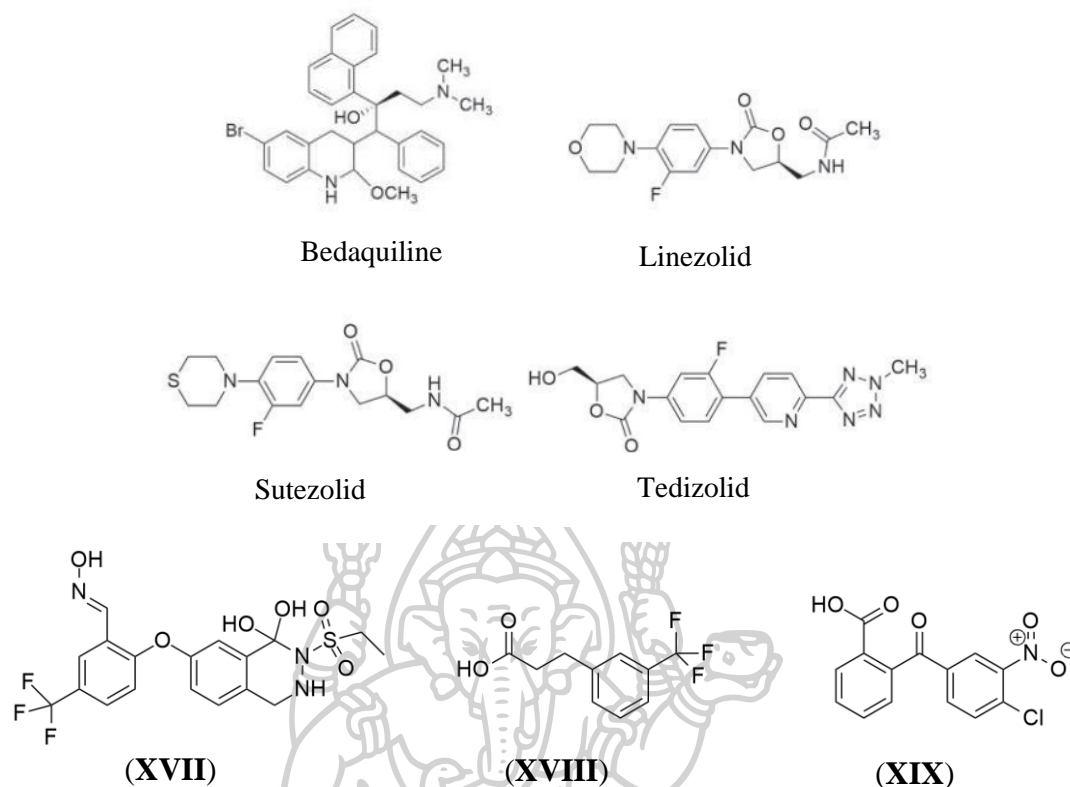


**Figure 19** Structure of halogen containing anti-TB compounds

Cinnamic acid has been documented as a conventional anti-tuberculosis drug. [80] The development of 3-(4-cinnamylpiperazinyl iminomethyl) rifamycin SV (**XX**) was the first study to describe the synergistic action of the cinnamyl moiety on the piperazinyl group of the existing antituberculosis rifamycin. This investigation was supported by the enhancement of *trans*-cinnamic acid's activity in medication combinations with rifampin, amikacin, and clofazimine for tuberculosis infection [81]. The molecular hybridization between isoniazid and *trans*-cinnamic acid was described, and the MIC of the produced compound (**XXI**) was 3.12  $\mu\text{g}/\text{mL}$  compared to 0.20  $\mu\text{g}/\text{mL}$  for isoniazid [82]. Degani et al. developed novel molecular hybrids of cinnamic acid and guanyl hydrazone as compound (**XXII**) that demonstrated MIC of 6.49  $\mu\text{M}$  against MTB H37Rv with an excellent safety profile [83]. The published literature indicates that *trans*-cinnamic acid-containing compounds had synergistic effects on existing antibiotics and promising activities on resistance strains. Therefore, cinnamic derivatives can be potential leads in the design and synthesis of antimycobacterial agents.

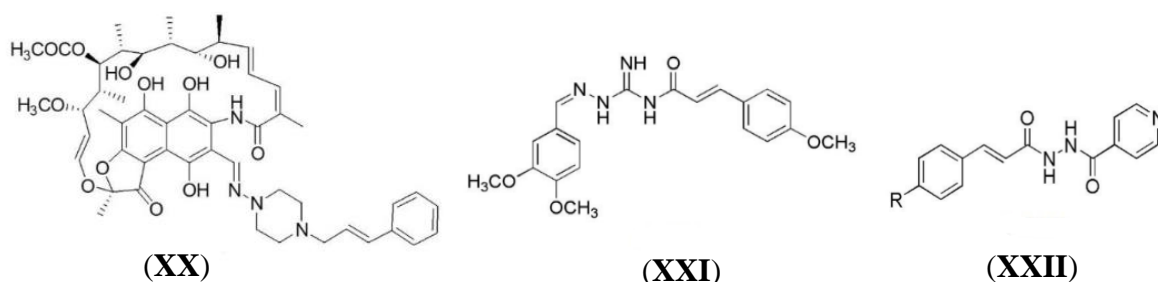


**Figure 20** Structure of cinnamyl containing anti-TB compounds

The mycobacteria cell wall consists of highly long chain (C<sub>60</sub>-C<sub>90</sub>) a-branched fatty acids esterified to the arabinogalactan component of the cell wall or trehalose. Its thick cell wall is one of the mechanisms preventing drugs from reaching the mycobacterial cytoplasm. Generally, lipophilic medicines penetrate through the cell membrane more easily and are more active [84]. Therefore, chemical modification of the compound structure to increase the permeability property of cell wall is quite challenging task. Stec J. et al. synthesized the triclosan derivatives to inhibit the enoyl-acyl carrier protein reductase InhA of MTB drug-sensitive and drug-resistance strains. It was found that n-butyl attached triazole ring containing compound (XXIII) showed the promising activity with MIC value 0.6 µg/ml when in compare with triclosan (12.5 µg/ml) [85]. It has also been demonstrated that the long-chain synthesis compounds XXIV and XXV inhibit *M. tuberculosis* H37Rv *in vitro* with a MIC<sub>90</sub> value of 29 µM. In contrast, the parent thiolactomycin has a MIC<sub>90</sub> value of 125 µM. It suggested that the addition of a long chain could increase activity. In addition, it was discovered that increasing the potency of compounds against *M. tuberculosis* by modifying the hydrophobicity of the side chain by varying its length and saturation.



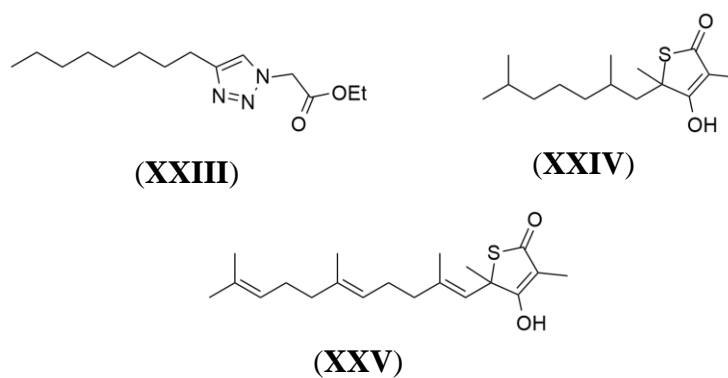
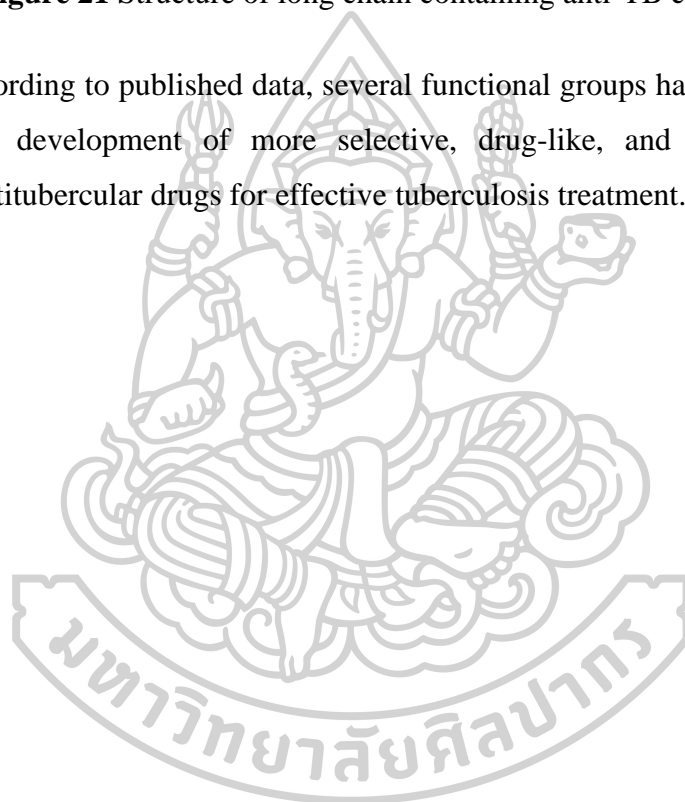


**Figure 21** Structure of long chain containing anti-TB compounds

According to published data, several functional groups have contributed to the design and development of more selective, drug-like, and pharmacokinetically effective antitubercular drugs for effective tuberculosis treatment.



## CHAPTER 3 MATERIALS AND METHODS

### 3.1 Materials

#### 3.1.1 Instruments

Name	Source
Analytical balance	Mettler Toledo, Switzerland
Infrared spectrophotometer (FT-IR 4100)	Jasco, Japan
Magnetic stirrer heating plate (IKA <sup>®</sup> C-MAG HS7)	IKA, USA
Differential Scanning Calorimeter (823e)	Mettler Toledo, Switzerland
High performance liquid chromatography- Mass spectrometer (UPLC-PDA-QDa)	Waters, USA
Nuclear magnetic resonance spectrophotometer (300 MHz)	Bruker, USA
Rotary evaporator BÜCHI Heating Bath B 490 BÜCHI Rotavapor R-205	BÜCHI, Switzerland

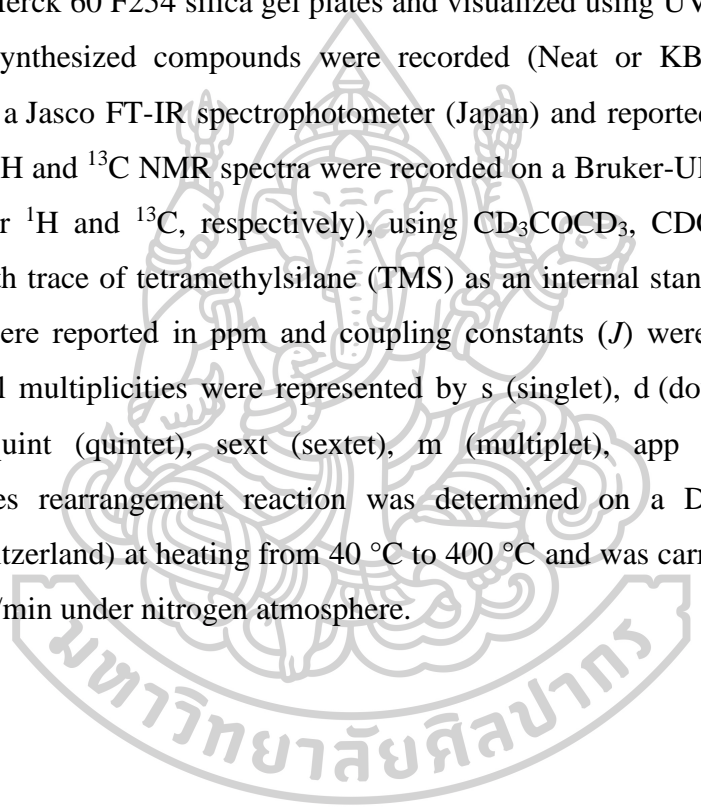
#### 3.1.2 Chemical reagents and Instruments

Name	Source
Benzoic acid	Fluka, Switzerland
4-Fluorobenzoic acid	Sigma Aldrich, Germany
3-Bromobenzoic acid	Sigma Aldrich, Germany
4-Bromobenzoic acid	Sigma Aldrich, Germany
4-Butylbenzoic acid	Sigma Aldrich, Germany
3-Acetamidobenzoic acid	Sigma Aldrich, Germany
4-Acetamidobenzoic acid	Sigma Aldrich, Germany
Phenol	Sigma Aldrich, Germany
2-Naphthoic acid	Sigma Aldrich, Germany
4-Aminobenzophenone	Sigma Aldrich, Germany
Butyric acid	Sigma Aldrich, Germany

Name	Source
trans-cinnamic acid	Ajax FineChem Pty Ltd. Australia
N-(3-Dimethylaminopropyl)-N'-ethylcarbodiimide hydrochloride (EDC·HCl)	Sigma Aldrich, Germany
4-(Dimethylamino)pyridine (DMAP)	Sigma Aldrich, Germany
Aluminium Chloride	Sigma Aldrich, Germany
Sodium borohydride	Sigma Aldrich, Germany
Benzyl chloroformate	Sigma Aldrich, Germany
Sodium hydroxide	Merck, Germany
Acetic anhydride	J.T.Baker, USA
Sodium sulfate anhydrous	Ajax FineChem Pty Ltd. Australia
Molecular sieve (4A° beads 8-12 mesh)	Sigma Aldrich, Germany
Silica gel 60 (0.063-0.2 mm)	Merck, Germany
Silica gel 60 (0.04-0.06 mm)	Merck, Germany
TLC silica gel 60 F254	Merck, Germany
Dichloromethane AR grade	J.T.Baker, USA
Ethyl acetate AR grade	J.T.Baker, USA
Hexane AR grade	J.T.Baker, USA
Methanol AR grade	J.T.Baker, USA
Ethanol AR grade	J.T.Baker, USA
Toluene	Carlo Erba, France
Tetrahydrofuran	Carlo Erba, France
Methanol HPLC grade	Honeywell, Burdick&Jackson, USA
Acetonitrile HPLC grade	Honeywell, Burdick&Jackson, USA
Nitrogen gas	Masser Speciality Gas Co.Ltd, Thailand
Carbon dioxide gas	Masser Speciality Gas Co.Ltd, Thailand

### 3.1.3 Chemical preparations

All solvents and starting materials were purchased from Acros Organics, Fluka, Merck KGaA, Ajax Finechem and Sigma-Aldrich. Dichloromethane for esterification was stored over molecular sieves 4Å. The purification of the compounds were isolated by column chromatography on silica gel 60 (0.063-0.2 mm and 0.04-0.06 mm, Merck) by using stated solvent systems and equilibrated with those systems prior to use. The reactions were monitored by thin-layer chromatography (TLC) on precoated Merck 60 F254 silica gel plates and visualized using UV light (254 nm). IR spectra of synthesized compounds were recorded (Neat or KBR pellets or nujol mulllets) on a Jasco FT-IR spectrophotometer (Japan) and reported as a wavenumber ( $\text{cm}^{-1}$ ). All  $^1\text{H}$  and  $^{13}\text{C}$  NMR spectra were recorded on a Bruker-Ultra Shield (300 and 75 MHz for  $^1\text{H}$  and  $^{13}\text{C}$ , respectively), using  $\text{CD}_3\text{COCD}_3$ ,  $\text{CDCl}_3$  and  $\text{CD}_3\text{OD}$  as solvents with trace of tetramethylsilane (TMS) as an internal standard. The chemical shifts ( $\delta$ ) were reported in ppm and coupling constants ( $J$ ) were reported as Hertz (Hz). Signal multiplicities were represented by s (singlet), d (doublet), t (triplet), q (quartet), quint (quintet), sext (sextet), m (multiplet), app (apparent) and br (broad). Fries rearrangement reaction was determined on a DSC 823e (Mettler Toledo, Switzerland) at heating from 40 °C to 400 °C and was carried out at a heating rate of 5 °C/min under nitrogen atmosphere.

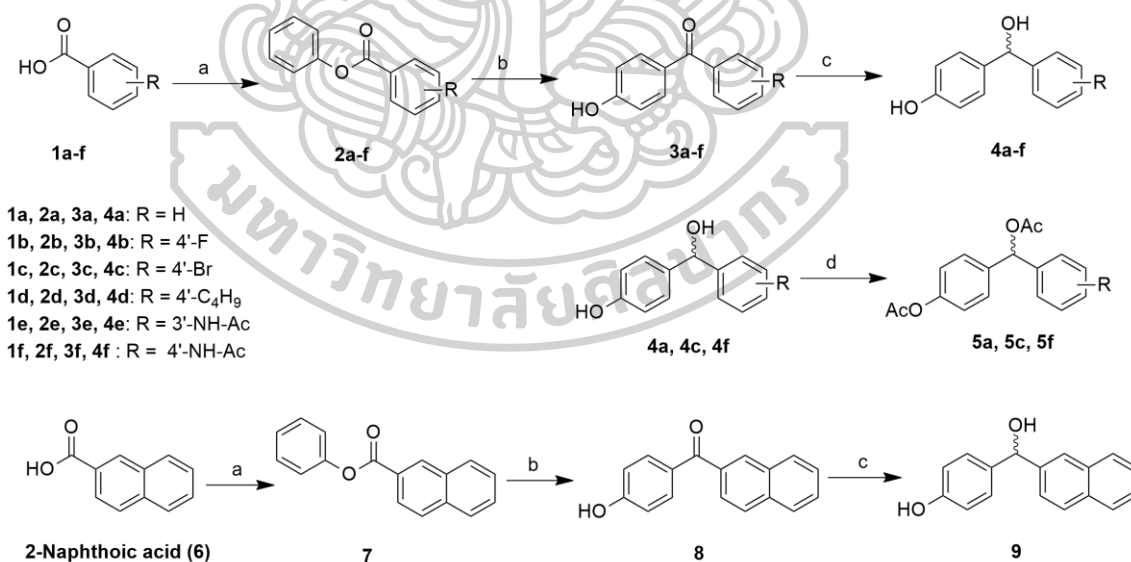


## 3.2 Methods

### 3.2.1 General methods for chemistry

Synthetic routes of benzhydryl derivatives are depicted in schemes 1-3. Esterification reaction and Fries rearrangement in scheme 1 were used for synthesis of compounds **4a-f** and **9**. In the synthesis of aminobenzhydryl derivatives **10** in scheme 2, amino functional groups could be obtained from hydrolysis of acetamide group by aqueous base reaction. In case of amide derivatives in scheme 3, 4-amino benzophenone was coupled with butyric acid, benzoic acid, and cinnamic acid via amide formation to give compounds **13a-c**.

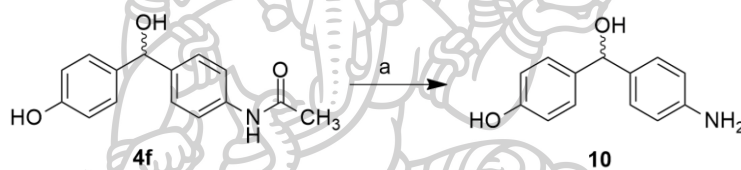
All reagents and solvents were used from commercial sources, and all reactions were monitored by TLC using silica plates with fluorescence F254 and UV light visualization. All crude products were confirmed the molar mass of desired compounds with LC-MS. All synthesized compounds were purified by column chromatography. Their structures were characterized by spectral data ( $^1\text{H}$ ,  $^{13}\text{C}$  NMR, IR and MS).



Reactions and conditions : (a) Phenol, EDC, DMAP, CH<sub>2</sub>Cl<sub>2</sub>, rt, overnight; (b) AlCl<sub>3</sub>, 120-140°C, 2h; (c) NaBH<sub>4</sub>, MeOH, rt, 3h; (d) AcO<sub>2</sub>, EDC, DMAP, CH<sub>2</sub>Cl<sub>2</sub>, rt, overnight

**Scheme 1.** Synthesis of compounds **4a-f**, **5a**, **5c**, **5f** and **9**

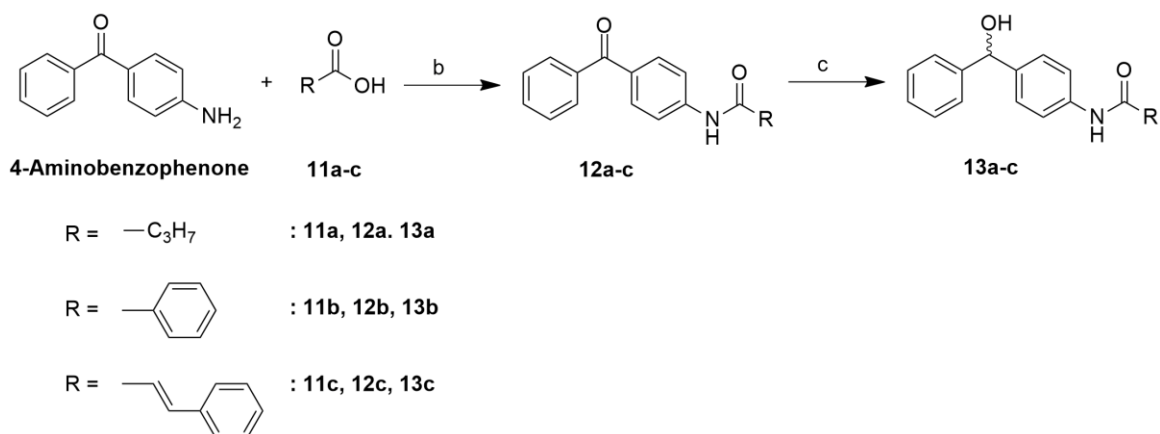
In scheme 1, first, the synthesis of compound **4a-f**, benzoic acid and substituted benzoic acid (**1a-f**) were used as starting materials. Its carboxylic acid group was coupled with phenol in the presence of EDC·HCl and DMAP to form phenyl benzoate. The benzoate derivatives were changed to 4-hydroxy benzophenone (**3a-f**) by performing Fries rearrangement reaction using  $\text{AlCl}_3$ . After that, benzophenones were converted to benzhydrols by reduction using  $\text{NaBH}_4$  to give benzhydrol derivatives (**4a-f**). Due to their significant anti-TB properties, benzhydrol derivatives (**4a**, **4c**, and **4f**) were chosen as starting materials for the synthesis of diacetate compounds (**5a**, **5c**, and **5f**). Diacetylation was performed by adding acetyl groups into hydroxyl groups of benzhydrol derivatives using acetic anhydride as an acetylating agent. In the synthesis of compound **9**, 2-naphthoic acid served as starting material and was converted to compound **9** via reactions a, b and c.



Reaction and conditions: (a) aq. NaOH, EtOH,  $50^\circ\text{C}$ , 12 h

### Scheme 2. Synthesis of compound **10**

In scheme 2, the synthesis of compound **10**, 4-acetamido-4'-acetylbenzhydrol acetate (**4f**) was used as starting material, and the acetyl group at N position was removed by base-catalysed hydrolysis to provide 4-amino-4'-acetylbenzhydrol acetate (**10**).



Reaction and conditions: (a) EDC, DMAP,  $\text{CH}_2\text{Cl}_2$ , rt, overnight; (b)  $\text{NaBH}_4$ , MeOH, rt, 3h.

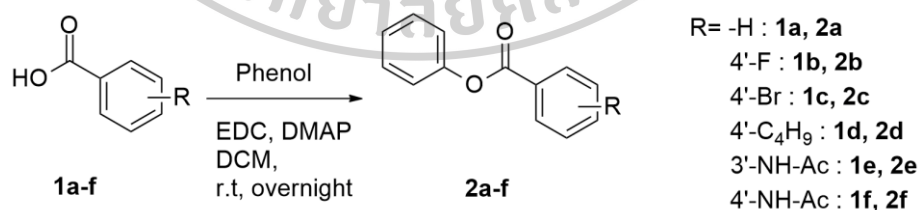
### Scheme 3. Proposed synthesis of compound 13a-c

In scheme 3, 4-amino benzophenone was used as a starting material. Its amino group was linked with an alkylcarboxylic acid or an arylcarboxylic acid (**11a-c**) to form amide derivatives (**12a-c**). Then, benzophenone scaffolds were changed to benzhydrol derivatives (**13a-c**) by means of the reduction reaction.

## 3.2.2 Synthesis of designed compounds

### 3.2.2.1 Synthesis of phenyl benzoate derivatives (2a-f)

#### General procedure for esterification



A general procedure for coupling reaction with ester bonds was performed as follows. [86, 87] All glassware were dried in hot-air oven at  $120\text{ }^\circ\text{C}$  for 4 hours. DCM was dried by storing over freshly dried and cooled 4A molecular sieves for overnight. Aromatic acids (**1a-g**) (1 equiv), EDC·HCl (2 equiv), and DMAP (2 equiv) were weighed separately and dissolved in dried DCM. The mixture was stirred for 1h

or until the mixture was dissolved completely. Then, phenol (1 equiv) in dried DCM was added by stirring to the round-bottomed flask containing acids, EDC and DMAP. Reaction was run overnight at room temperature and monitored by TLC. After complete reaction, the reaction mixture was worked-up with water and evaporated DCM. Water layer was extracted with EtOAc (30mLx3). Organic layer then was washed with water until pH of water layer is neutral and then dried with anhydrous Na<sub>2</sub>SO<sub>4</sub>, filtered, and concentrated under reduced pressure. The desired products (**2a-g**) were used directly in the next step without purification.

#### **Phenyl benzoate (2a)**

To a solution of benzoic acid **1a** (626 mg, 5 mmol, 1 equiv), EDC·HCl (1552 mg, 10 mmol, 2 equiv) and DMAP (1220 mg, 10 mmol, 2 equiv) in dried DCM, stirred for 1h, added phenol (477 mg, 5 mmol, 1 equiv). Reaction was performed according to general procedure for esterification. Compound **2a** as white crystalline powder (849 mg, 78.9%). FT-IR (KBr),  $\nu$ : 1729 cm<sup>-1</sup> (C=O stretching in ester).

#### **4-Fluorophenyl benzoate (2b)**

To a solution of 4-fluoro benzoic acid **1b** (1,405 mg, 10 mmol, 1.4 equiv), EDC·HCl (2,643 mg, 17 mmol, 2.3 equiv) and DMAP (1,865 mg, 15 mmol, 2.1 equiv) in dried DCM, stirred for 1h, added phenol (680 mg, 7.2 mmol, 1 equiv). Reaction was performed according to general procedure for esterification. Compound **2b** as white crystalline powder (1,492 mg, 95.8%). FT-IR (KBr),  $\nu$ : 1737 cm<sup>-1</sup> (C=O stretching in ester).

#### **4-Bromophenyl benzoate (2c)**

To a solution of 4-bromo benzoic acid **1c** (1,312 mg, 6 mmol, 1.2 equiv), EDC·HCl (4,800 mg, 25 mmol, 5 equiv) and DMAP (3,087 mg, 25 mmol, 5 equiv) in dried DCM, stirred for 1h, added phenol (498 mg, 5 mmol, 1 equiv). Reaction was performed according to general procedure for esterification. Compound **2b** as off-white powder (1,339 mg, 96.7%). FT-IR (KBr),  $\nu$ : 1731 cm<sup>-1</sup> (C=O stretching in ester); LC-MS (ESI, m/z) [M+H]<sup>+</sup>: 278.



#### 4-Butylphenyl benzoate (2d)

To a solution of 4-butyl benzoic acid **1d** (1,785 mg, 10 mmol, 1.25 equiv), EDC·HCl (3,700 mg, 22.5 mmol, 2.8 equiv) and DMAP (2,740 mg, 22.5 mmol, 2.8 equiv) in dried DCM, stirred for 1h, added phenol (770 mg, 8 mmol, 1 equiv). Reaction was performed according to general procedure for esterification. Compound **2d** as pale-yellow liquid (1,900 mg, 93.9%). FT-IR (KBr),  $\nu$ : 1713  $\text{cm}^{-1}$  (C=O stretching in ester).

#### 3-Acetamidophenyl benzoate (2e)

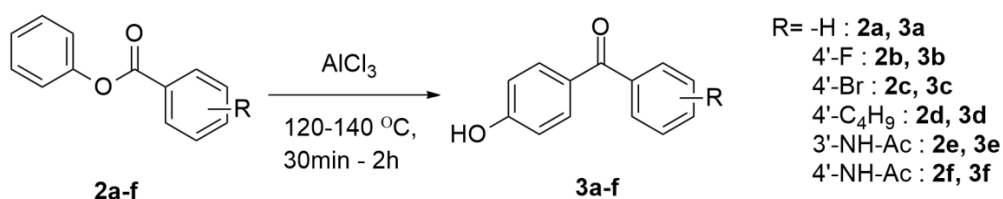
To a solution of 3-acetamido benzoic acid **1e** (1,865 mg, 10.4 mmol, 1.1 equiv), EDC·HCl (3,135 mg, 20 mmol, 2.1 equiv) and DMAP (2,370 mg, 19.4 mmol, 2 equiv) in dried DCM, stirred for 1h, added phenol (908 mg, 9.6 mmol, 1 equiv). Reaction was performed according to general procedure for esterification. Compound **2e** as white powder (2,048 mg, 83.6%). FT-IR (KBr),  $\nu$ : 1724  $\text{cm}^{-1}$  (C=O stretching in ester).

#### 4-Acetamidophenyl benzoate (2f)

To a solution of 4-acetamido benzoic acid **1f** (1,802 mg, 10 mmol, 1 equiv), EDC·HCl (2,765 mg, 17.8 mmol, 1.8 equiv) and DMAP (1,890 mg, 15.5 mmol, 1.6 equiv) in dried DCM, stirred for 1h, added phenol (936 mg, 10 mmol, 1 equiv). Reaction was performed according to general procedure for esterification. Compound **2e** as white powder (2,104 mg, 82.5%). FT-IR (KBr),  $\nu$ : 1726  $\text{cm}^{-1}$  (C=O stretching in ester).

### 3.2.2.2 Synthesis of 4-hydroxy benzophenone derivatives (3a-f)

#### General procedure for synthesis of Fries rearrangement



Substituted phenyl benzoates (**2a-g**) (1 equiv) and AlCl<sub>3</sub> (10 equiv) were crushed and mixed together in mortar. The mixture was stirred at 120-140 °C for 2h and reaction was monitored by TLC. After 2 hours, reaction was quenched with water and the reaction mixture then was extracted with EtOAc (30mLx3). The combined organic phase was washed with water (50mL) until pH of water is about 7, dried with anhydrous Na<sub>2</sub>SO<sub>4</sub>, filtered and evaporated. Crude products (**3a-g**) were purified by column chromatography (SiO<sub>2</sub>, EtOAc:Hex:MeOH, 5:5:1) [62, 88]

#### **4-Hydroxy benzophenone (3a)**

The mixture of phenylbenzoate **2a** (849 mg, 3.9 mmol, 1 equiv) and AlCl<sub>3</sub> (5,070 g, 40 mmol, 10 equiv) was stirred at 140 °C for 45 min. Reaction was performed according to general procedure of Fries rearrangement. Crude products (**3a**) were purified by column chromatography (SiO<sub>2</sub>, EtOAc:Hex:MeOH, 5:5:1). Compound **3a** as white crystalline powder (284 mg, 33.7%). FT IR (KBr),  $\nu$ : 1673 cm<sup>-1</sup> (C=O stretching in ketone).

#### **4-Fluoro-4'-hydroxybenzophenone (3b)**

The mixture of 4-fluorophenyl benzoate **2b** (864 mg, 4 mmol, 1 equiv) and AlCl<sub>3</sub> (5,300 mg, 40 mmol, 10 equiv) was stirred at 140 °C for 45 min. Reaction was performed according to general procedure of Fries rearrangement. Crude products (**3b**) were purified by column chromatography (SiO<sub>2</sub>, EtOAc:Hex:MeOH, 2:8:1). Compound **3b** as white crystalline powder (410 mg, 47.5%). FT IR (KBr),  $\nu$ : 1604 cm<sup>-1</sup> (C=O stretching in ketone).

#### **4-Bromo-4'-hydroxybenzophenone (3c)**

The mixture of 4-bromophenyl benzoate **2c** (1,339 mg, 4.8 mmol, 1 equiv) and AlCl<sub>3</sub> (6,445 mg, 48 mmol, 10 equiv) was stirred at 140 °C for 30 min. Reaction was performed according to general procedure of Fries rearrangement. Crude products (**3c**) were purified by column chromatography (SiO<sub>2</sub>, EtOAc:Hex:MeOH, 2:8:1). Compound **3b** as pale-yellow powder (867 mg, 65.1%). FT IR (KBr),  $\nu$ : 1650 cm<sup>-1</sup> (C=O stretching in ketone).

#### 4-Butyl-4'-hydroxybenzophenone (3d)

The mixture of 4-butylphenyl benzoate **2d** (1,900 mg, 7.47 mmol, 1 equiv) and AlCl<sub>3</sub> (9,965 mg, 74.7 mmol, 10 equiv) was stirred at 130 °C for 30 min. Reaction was performed according to general procedure of Fries rearrangement. Crude products (**3d**) were purified by column chromatography (SiO<sub>2</sub>, EtOAc:Hex:MeOH, 2:8:1). Compound **3b** as pale-yellow liquid (1,502 mg, 78.9%). FT IR (KBr),  $\nu$ : 1665 cm<sup>-1</sup> (C=O stretching in ketone); LC-MS (ESI,  $m/z$ ) [M+H]<sup>+</sup>: 255.

#### 3-Acetamido-4'-hydroxybenzophenone (3e)

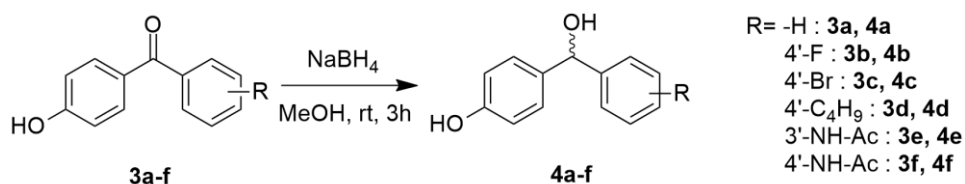
The mixture of 3-acetamidophenyl benzoate **2e** (517 mg, 2 mmol, 1 equiv) and AlCl<sub>3</sub> (3,242 mg, 24.3 mmol, 12 equiv) was stirred at 140 °C for 30 min. Reaction was performed according to general procedure of Fries rearrangement. Crude products (**3e**) were purified by column chromatography (SiO<sub>2</sub>, EtOAc:Hex:MeOH, 5:5:1). Compound **3e** as pale yellow liquid (203 mg, 44.9%). FT IR (KBr),  $\nu$ : 1665 cm<sup>-1</sup> (C=O stretching in ketone); LC-MS (ESI,  $m/z$ ) [M+H]<sup>+</sup>: 226.

#### 4-Acetamido-4'-hydroxybenzophenone (3f)

The mixture of 4-acetamidophenyl benzoate **2f** (1104 mg, 4.3 mmol, 1 equiv) and AlCl<sub>3</sub> (5,53 mg, 38.6 mmol, 9 equiv) was stirred at 140 °C for 60 min. Reaction was performed according to general procedure of Fries rearrangement. Crude products (**3f**) were purified by column chromatography (SiO<sub>2</sub>, EtOAc:Hex:MeOH, 5:5:1). Compound **3e** as pale yellow liquid (473 mg, 43.1%). FT IR (KBr),  $\nu$ : 1665 cm<sup>-1</sup> (C=O stretching in ketone); LC-MS (ESI,  $m/z$ ) [M+H]<sup>+</sup>: 226.

### 3.2.2.3 Synthesis of (4-Hydroxyphenyl)phenylmethanol derivatives (4a-f)

#### General procedure for reduction



To a solution of substituted benzophenones (**3a-g**, **17a-c**) (1 equiv) in MeOH, NaBH<sub>4</sub> (10 equiv) was added. The mixture was stirred at room temperature for 3h or until starting material disappeared. After that, the solvent was evaporated by rotary evaporator. Water was added to the mixture for working-up and the mixture was extracted with EtOAc (50mLx2). The organic layers were combined and washed with water (50mLx3). After drying over Na<sub>2</sub>SO<sub>4</sub>, EtOAc was removed under reduced pressure to yield desired products (**4a-g**, **9**, **18a-c**) [89]. Crude products (**4a-g**) were purified by column chromatography.

#### **4-hydroxy- $\alpha$ -(phenyl)benzyl alcohol (4a)**

To a solution of 4-hydroxy benzophenone (**3a**) (284 mg, 1.3 mmol, 1 equiv) in dried MeOH, added NaBH<sub>4</sub> (492 mg, 13 mmol, 10 equiv). Reaction was performed according to general procedure for reduction reaction. Compound **4a** as white crystalline powder (215 mg, 76.2%). IR (cm<sup>-1</sup>): OH str. 3335 (broad); <sup>1</sup>H NMR (300 MHz), CD<sub>3</sub>COCD<sub>3</sub>  $\delta$  (ppm): 8.21 (1H, s), 7.40 (2H, d, J = 8.7 Hz), 7.28 (3H, t, J = 7.8 Hz), 7.21 (2H, d, J = 8.7 Hz), 6.76 (2H, d, J = 8.7 Hz), 5.73 (1H, s), 4.64 (1H, s); LC-MS (ESI) [M+H]<sup>+</sup> m/z 200

#### **4-hydroxy- $\alpha$ -(4'-fluorophenyl)benzyl alcohol (4b)**

To a solution of 4-fluoro-4'-hydroxybenzophenone (**3b**) (821 mg, 3.8 mmol, 1 equiv) in dried MeOH, added NaBH<sub>4</sub> (1,436 mg, 38 mmol, 10 equiv). Reaction was performed according to general procedure for reduction reaction. Compound **4b** as white crystalline powder (489 mg, 59.3%). FT-IR (cm<sup>-1</sup>): OH str. 3384 (broad), 3180 (broad); <sup>1</sup>H NMR (300 MHz), CD<sub>3</sub>OD,  $\delta$  (ppm): 7.35 (2H, dd, J = 5.5, 2.9 Hz, H-Ar), 7.15 (2H, d, J = 8.3 Hz, H-Ar), 7.02 (2H, t, J = 8.9 Hz, H-Ar), 6.73 (2H, d, J = 8.6 Hz, H-Ar), 5.69 (1H, s, CH-OH); <sup>13</sup>C NMR (75 MHz, CD<sub>3</sub>OD),  $\delta$  (ppm): 165.0, 161.8, 157.9, 142.4, 142.4, 136.8, 129.6, 129.5, 129.2, 116.2, 116.0, 115.7, 76.1. LC-MS (ESI, m/z): 217.06

#### **4-hydroxy- $\alpha$ -(4'-bromophenyl)benzyl alcohol (4c)**

To a solution of 4-bromo-4'-hydroxybenzophenone (**3c**) (867mg, 3.1 mmol, 1 equiv) in dried MeOH, added NaBH<sub>4</sub> (586 mg, 15.5 mmol, 5 equiv). Reaction was

performed according to general procedure for reduction reaction. Compound **4c** as pale-yellow powder (778 mg, 89.9%). FT-IR ( $\text{cm}^{-1}$ ): OH str. 3384 (broad), 3150 (broad);  $^1\text{H}$  NMR (300 MHz),  $\text{CD}_3\text{COCD}_3$ ,  $\delta$  (ppm): 8.30 (1H, bs), 7.47 (2H, d,  $J = 8.4$  Hz), 7.35 (2H, d,  $J = 8.7$  Hz), 7.19 (2H, d,  $J = 8.4$  Hz), 6.77 (2H, d,  $J = 8.7$  Hz), 5.73 (1H, s), 4.82 (1H, s); LC-MS (ESI,  $m/z$ ): 279

#### **4-hydroxy- $\alpha$ -(4'-butylphenyl)benzyl alcohol (4d)**

To a solution of 4-butyl-4'-hydroxybenzophenone (**3d**) (489 mg, 2 mmol, 1 equiv) in dried MeOH, added  $\text{NaBH}_4$  (756 mg, 20 mmol, 10 equiv). Reaction was performed according to general procedure for reduction reaction. Compound **4d** as pale-yellow liquid (342 mg, 67.1%). IR ( $\text{cm}^{-1}$ ): OH str. 3340 (broad), 3168 (broad);  $^1\text{H}$  NMR (300 MHz),  $\text{CD}_3\text{OD}$ ,  $\delta$  (ppm): 7.23 (2H, d,  $J = 8.0$  Hz), 7.14 (4H, q), 6.73 (2H, d,  $J = 8.6$  Hz), 5.66 (1H, s, CH-OH), 2.58 (2H, t,  $J = 7.5$  Hz,  $-\text{CH}_2-$ ), 1.57 (2H, q,  $J = 7.6$  Hz,  $-\text{CH}_2-$ ), 1.34 (2H, sext,  $J = 7.6$  Hz,  $-\text{CH}_2-$ ), 0.92 (3H, t,  $J = 7.3$  Hz,  $-\text{CH}_3-$ ).

#### **4-hydroxy- $\alpha$ -(3'-acetamidophenyl)benzyl alcohol (4e)**

To a solution of 3-acetamido-4'-hydroxybenzophenone (**3e**) (203 mg, 0.9 mmol, 1 equiv) in dried MeOH, added  $\text{NaBH}_4$  (586 mg, 15.5 mmol, 15 equiv). Reaction was performed according to general procedure for reduction reaction. Compound **4e** as pale yellow liquid (171 mg, 83.7%). IR ( $\text{cm}^{-1}$ ): OH str. 3307 (broad), 3189 (broad) 1673 ( $\text{C}=\text{O}$  str.);  $^1\text{H}$  NMR (300 MHz),  $\text{CD}_3\text{COCD}_3$ ,  $\delta$  (ppm): 9.08 (NH, br s), 8.22 (OH, br s), 7.60 (1H, d,  $J = 9.0$  Hz, H-Ar), 7.54 (1H, s, H-Ar), 7.21 (3H, m, HAr), 7.08 (1H, d,  $J = 9.0$  Hz, H-Ar), 6.76 (2H, dt,  $J = 9.0$  Hz, H-Ar), 5.69 (1H, s, CH-OH), 4.65 (OH, d), 2.89 (3H, s,  $\text{CH}_3$ ). LC-MS (ESI,  $m/z$ ): 257.03

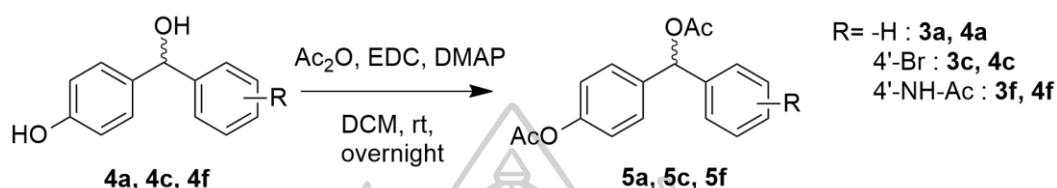
#### **4-hydroxy- $\alpha$ -(4'-acetamidophenyl)benzyl alcohol (4f)**

To a solution of 4-acetamido-4'-hydroxybenzophenone (**3f**) (270 mg, 1.1 mmol, 1 equiv) in dried MeOH, added  $\text{NaBH}_4$  (501 mg, 13.3 mmol, 12.1 equiv). Reaction was performed according to general procedure for reduction reaction. Compound **4f** as pale yellow liquid (189 mg, 67.4%). IR ( $\text{cm}^{-1}$ ): OH str. 3307 (broad), 1668 ( $\text{C}=\text{O}$  str.);  $^1\text{H}$  NMR (300 MHz),  $\text{CD}_3\text{OD}$ ,  $\delta$  (ppm): 7.67 (6H, m,  $J = 8.7$  Hz, H-Ar), 6.85

(2H, d,  $J = 8.7$  Hz, H-Ar), 5.74 (1H, s, CH-OH), 4.88 (OH, s), 2.14 (3H, s, CH<sub>3</sub>). LC-MS (ESI,  $m/z$ ): 257.06

### 3.2.2.4 4-acetoxy- $\alpha$ -(phenyl)benzyl acetate derivatives (5a, 5d, 5g)

#### General procedure for acetylation



A general procedure for acetylation of dihydroxy-containing compounds was performed as follows. Oven-dried glassware was used for the reaction. Acetic anhydride (1 equiv), EDC·HCl (3 equiv), and DMAP (3 equiv) were dissolved in dry DCM and stirred for 1 hour. Compound **4a**, **4c**, and **4f** in dry DCM was added to the reaction mixture. The mixtures were stirred overnight at room temperature. After that, DCM was evaporated and water was added. Water layer was extracted with EtOAc (50mLx2), EtOAc layer was washed by water (50mL), dried over Na<sub>2</sub>SO<sub>4</sub>, filtered and concentrated under reduced pressure. The desired products (**5a**, **5c**, **5f**) were purified by column chromatography.

#### 4-acetoxy- $\alpha$ -(phenyl)benzyl acetate (5a)

To a solution of acetic anhydride (51 mg, 0.5 mmol, 1 equiv), EDC·HCl (780 mg, 5 mmol, 10 equiv) and DMAP (611 mg, 5 mmol, 10 equiv) in dried DCM, stirred for 1h, added a solution of 4-hydroxy- $\alpha$ -(phenyl)benzyl alcohol (**4a**) (105 mg, 0.49 mmol, 1 equiv) in dried DCM. Reaction was performed according to general procedure for acetylation. Compound **4a** as white crystalline powder (138 mg, 92.9%). FT-IR (KBr),  $\nu$ : C=O str. 1735 (sharp); <sup>1</sup>H NMR (300 MHz, CDCl<sub>3</sub>)  $\delta$ : 7.36-7.26 (7H, m), 7.05 (2H, d,  $J = 8.7$  Hz), 6.88 (1H, s), 2.28 (3H, s), 2.15 (3H, s)

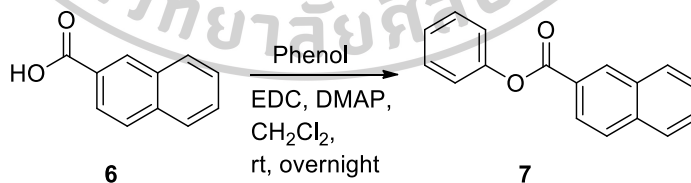
#### 4-acetoxy- $\alpha$ -(4'-bromophenyl)benzyl acetate (**5c**)

To a solution of acetic anhydride (245 mg, 2.4 mmol, 1.2 equiv), EDC·HCl (1,970 mg, 10 mmol, 5 equiv) and DMAP (1,230 mg, 10 mmol, 5 equiv) in dried DCM, stirred for 1h, added a solution of 4-hydroxy- $\alpha$ -(4'-bromophenyl)benzyl alcohol (**4c**) (554 mg, 2 mmol, 1 equiv) in dried DCM. Reaction was performed according to general procedure for acetylation. Compound **5c** as white crystalline powder (502 mg, 69.3%). FT-IR (KBr),  $\nu$ : C=O str. 1735.9 (sharp);  $^1\text{H}$  NMR (300 MHz,  $\text{CDCl}_3$ )  $\delta$ : 7.46 (2H, d,  $J = 8.4$  Hz), 7.31 (2H, d,  $J = 8.7$  Hz), 7.20 (2H, d,  $J = 8.4$  Hz), 7.06 (2H, d,  $J = 8.7$  Hz), 6.82 (1H, s), 2.28 (3H, s), 2.15 (3H, s)

#### 4-acetoxy- $\alpha$ -(4'-acetamidophenyl)benzyl acetate (**5f**)

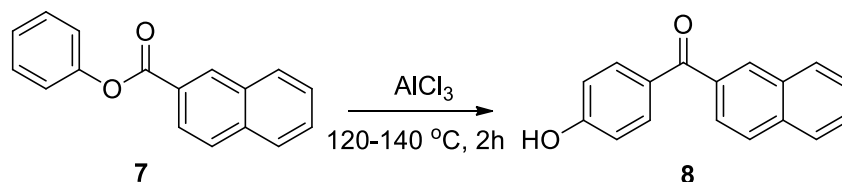
To a solution of acetic anhydride (40 mg, 0.4 mmol, 1 equiv), EDC·HCl (629 mg, 4 mmol, 11.4 equiv) and DMAP (487 mg, 4 mmol, 11.4 equiv) in dried DCM, stirred for 1h, added a solution of 4-hydroxy- $\alpha$ -(4'-acetamidophenyl)benzyl alcohol (**4f**) (90 mg, 0.35 mmol, 1 equiv) in dried DCM. Reaction was performed according to general procedure for acetylation. Compound **5f** as pale-yellow liquid (110 mg, 91.6%). FT-IR (KBr),  $\nu$ : C=O str. 1701 (sharp);  $^1\text{H}$  NMR (300 MHz,  $\text{CD}_3\text{OD}$ )  $\delta$ : 7.63 (6H, d,  $J = 8.7$  Hz), 6.89 (2H, d,  $J = 8.7$  Hz), 6.82 (1H, s), 2.28 (3H, s), 2.15 (6H, s)

#### 3.2.2.5 2-Naphthyl benzoate (**7**)



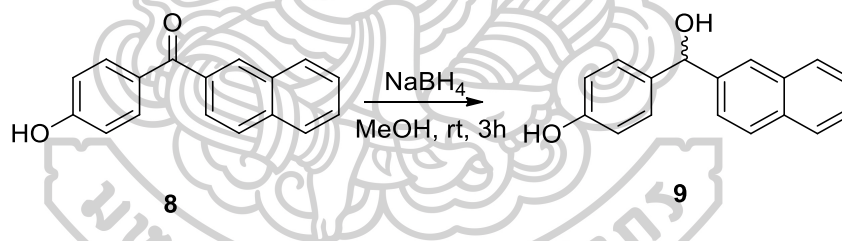
The synthesis of 2-Naphthyl benzoate (**7**) using 2-naphthoic acid (**6**) (1,725 mg, 10 mmol, 1 equiv), EDC·HCl (2,511 mg, 15 mmol, 1.5 equiv), and DMAP (1,860 mg, 15 mmol, 1.5 equiv) in dried DCM, stirred for 1h, added phenol (741 mg, 8 mmol, 0.8 equiv), was followed as general procedure of esterification. The obtained product, 2-Naphthyl benzoate (**7**), were used directly in the next step without purification. Compound **7** as white crystalline powder (1,734 mg, 87.4%). FT-IR (KBr),  $\nu$ : 1724  $\text{cm}^{-1}$  (C=O stretching in ester); LC-MS (ESI,  $m/z$ )  $[\text{M}+\text{H}]^+$ : 249.

### 3.2.2.6 4-hydroxyphenyl(2-naphthyl)methanone (**8**)



2-Naphthyl benzoate (**7**) (1,334 mg, 5 mmol, 1 equiv) and  $\text{AlCl}_3$  (6,868 mg, 50 mmol, 10 equiv) were crushed and mixed. The reaction mixture was stirred at  $130\text{ }^\circ\text{C}$  for 1h. The rest of the preparation method was followed as general procedure of Fries rearrangement. Crude products **8** were purified by column chromatography ( $\text{SiO}_2$ , EtOAc:Hex:MeOH, 3:7:1). Compound **8** as pale-yellow crystalline powder (740 mg, 59.7%). FT-IR (KBr),  $\nu$ :  $1600\text{ cm}^{-1}$  (C=O stretching in ketone); LC-MS (ESI,  $m/z$ )  $[\text{M}+\text{H}]^+$ : 249.

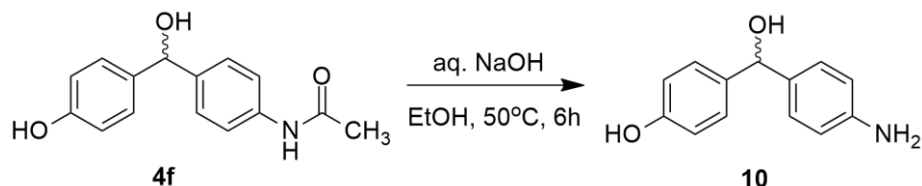
### 3.2.2.7 4-hydroxyphenyl(2-naphthyl)methanol (**9**)



The synthesis of 4-hydroxyphenyl(2-naphthyl)methanol (**9**) using 2-naphthyl ketone (**8**) (380 mg, 1.5 mmol, 1 equiv) in MeOH,  $\text{NaBH}_4$  (587 mg, 15 mmol, 10 equiv) was followed as general procedure of reduction. The desired product (**9**) were purified by column chromatography ( $\text{SiO}_2$ , EtOAc:Hex:MeOH, 2:8:1). Compound **9** as off-white crystalline powder (289 mg, 77.7%).  $^1\text{H}$  NMR (300 MHz),  $\text{CD}_3\text{OD}$ ,  $\delta$  (ppm): 7.86-7.75 (4H, m, Ar-H), 7.43 (3H, m, Ar-H), 7.21 (2H, d,  $J = 8.4\text{ Hz}$ ), 6.75 (2H, d,  $J = 8.6\text{ Hz}$ ), 5.56 (1H, s, CH-OH).  $^{13}\text{C}$  NMR (75 MHz,  $\text{CD}_3\text{OD}$ ),  $\delta$  (ppm): 116.18-157.90 (Ar-C), 76.86 (C-OH); LC-MS (ESI,  $m/z$ )  $[\text{M}-\text{OH}]^+$ : 233.



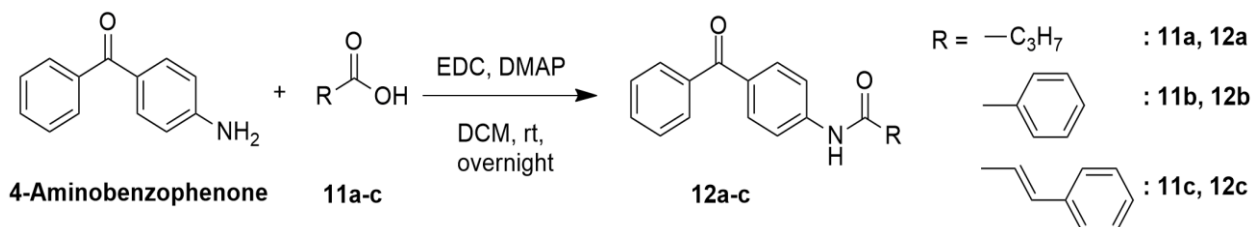
### 3.2.2.8 4-((4-aminophenyl)(hydroxy)methyl)phenol (**10**)



Amide hydrolysis was performed under alkaline condition using aqueous NaOH as catalyst. The solution of NaOH (3,086 mg, 77 mmol, 10 equiv) was added by stirring to the round-bottomed flask containing solution of compound **4f** (1,950 mg, 7.6 mmol, 1 equiv) in EtOH at 50 °C for 12h (Shimizu et al. 2014). The reaction was monitored by TLC. After complete reaction, EtOH was evaporated and then water was added for working-up. EtOAc (50mlx2) was used for extraction. The combined organic layer was washed with water until pH of water phase is neutral. Then, organic layer was dried over anhydrous Na<sub>2</sub>SO<sub>4</sub>, filtered, and dried by evaporation of solvent. Crude product (**10**) was purified by column chromatography (SiO<sub>2</sub>, EtOAc:Hex:MeOH, 3:7:1). Compound **10** as pale yellow powder (446 mg, 27.4%). FT-IR (cm<sup>-1</sup>),  $\nu$ : N-H str. 3328 (sharp), O-H str. about 3300 (board), C-H str. 3023, N-H bend 1618, C=C str. 1617-1450, C-O str. 1176, 1122, C-N str. 1018. LC-MS (ESI,  $m/z$ ) [M]<sup>+</sup>: 214.

### 3.2.2.9 4-amido benzophenone derivatives (**12a-c**)

#### General procedure for amide formation



A general procedure for coupling reaction with amide bonds is performed as follows. All glassware were dried in hot-air oven at 120 °C for 4 hours. DCM was dried by storing over freshly dried and cooled 4A molecular sieves for overnight.

Aliphatic acids or aromatic acids (**11a-c**) (1 equiv), EDC·HCl (3 equiv), and DMAP (1 equiv) were weighed separately and dissolved in dried DCM. The mixture was stirred for 1h or until the mixture is dissolved completely. Then, 4-aminobenzophenone (1 equiv) in dried DCM was added by stirring to the round-bottomed flask containing acids, EDC and DMAP. Reaction was run overnight at room temperature and monitored by TLC. After complete reaction, the reaction mixture was worked-up with water and evaporated DCM. Water layer was extracted with EtOAc (30mLx3). Organic layer then was washed with water until pH of water layer is neutral and then dried with anhydrous Na<sub>2</sub>SO<sub>4</sub>, filtered, and concentrated under reduced pressure. The desired products (**12a-c**) were purified by column chromatography (SiO<sub>2</sub>, EtOAc:Hex:MeOH, 3:7:1).

#### **4-butylramido benzophenone (12a)**

To a solution of butyric acid **11a** (881 mg, 10 mmol, 1.25 equiv), EDC·HCl (2,376 mg, 15 mmol, 1.88 equiv) and DMAP (1,859 mg, 15 mmol, 1.88 equiv) in dried DCM, stirred for 1h, added a solution of 4-aminobenzophenone (1,577 mg, 8 mmol, 1 equiv) in dried DCM. Reaction was performed according to general procedure for amide formation. Compound **12a** as off-white powder (1,538 mg, 72.0%). FT-IR (cm<sup>-1</sup>),  $\nu$ : 3305 (N-H str.), 1658(C=O str. in amide), 1600 (C=O str. in ketone). LC-MS (ESI, m/z) [M]<sup>+</sup>: 268.

#### **4-benzamido benzophenone (12b)**

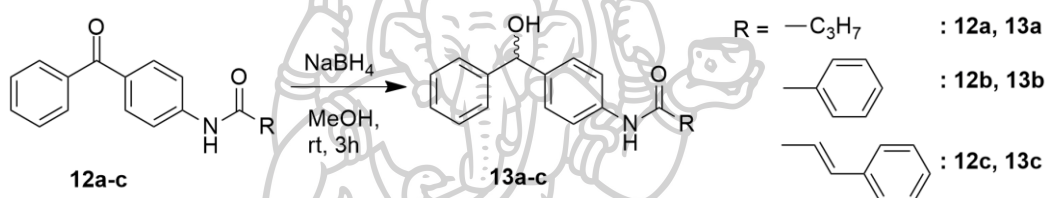
To a solution of benzoic acid **11b** (1,220 mg, 10 mmol, 2 equiv), EDC·HCl (1,563 mg, 10 mmol, 2 equiv) and DMAP (1,230 mg, 10 mmol, 2 equiv) in dried DCM, stirred for 1h, added a solution of 4-aminobenzophenone (993 mg, 5 mmol, 1 equiv) in dried DCM. Reaction was performed according to general procedure for amide formation. Compound **12b** as off-white powder (897 mg, 59.6%). FT-IR (cm<sup>-1</sup>),  $\nu$ : 3312 (N-H str.), 1650 (C=O str. in amide), 1590 (C=O str. in ketone).

#### 4-cinnamido benzophenone (**12c**)

To a solution of *trans*-cinnamic acid **11c** (459 mg, 3 mmol, 1.5 equiv), EDC·HCl (623 mg, 4 mmol, 2 equiv) and DMAP (494 mg, 4 mmol, 2 equiv) in dried DCM, stirred for 1h, added a solution of 4-aminobenzophenone (405 mg, 2 mmol, 1 equiv) in dried DCM. Reaction was performed according to general procedure for amide formation. Compound **12c** as off-white powder (206 mg, 31.5%). FT-IR ( $\text{cm}^{-1}$ ),  $\nu$ : 3323 (N-H str.), 1658 (C=O str. in amide), 1660 (C=O str. in ketone).

#### 3.2.2.10 4-amido benzhydryl derivatives (**13a-c**)

##### General procedure for synthesis of **13a-c**



The synthesis of benzhydryl compounds (**13a-c**) using benzophenone compounds (**12a-c**) (1 equiv) dissolved in MeOH, NaBH<sub>4</sub> (10 equiv) was followed as general procedure of reduction. The desired product (**13a-c**) were purified by column chromatography (SiO<sub>2</sub>, EtOAc:Hex:MeOH, 3:7:1)

#### 4-butyramido- $\alpha$ -(phenyl)benzyl alcohol (**13a**)

To a solution of 4-butyramido benzophenone (**12a**) (249 mg, 0.9 mmol, 1 equiv) and NaBH<sub>4</sub> (412 mg, 9 mmol, 10 equiv) in MeOH, stirred at room temperature for 1h, was followed as general procedure of reduction. Compound **13a** as off-white powder (192 mg, 79.9%). FT-IR ( $\text{cm}^{-1}$ ),  $\nu$ : 3303 (N-H str.), 3328 (O-H str.), 3124 (sp<sup>2</sup> C-H), 3057 (sp<sup>2</sup> C-H), 2962-2871 (sp<sup>3</sup> C-H str.), 1660 (C=O str. in amide); <sup>1</sup>H NMR (300 MHz), CD<sub>3</sub>OD,  $\delta$  (ppm): 7.50 (2H, d, Ar-H), 7.37-7.18 (7H, m, Ar-H), 5.78 (1H, s, CH-OH), 2.32 (2H, t, J = 7.4 Hz), 1.70 (2H, sext, J = 7.4 Hz), 0.98 (3H, t, J = 7.4 Hz). <sup>13</sup>C NMR (75 MHz, CD<sub>3</sub>OD),  $\delta$  (ppm): 174.68 (C=O), 145.98-121.25 (Ar-C), 76.68 (C-OH); LC-MS (ESI, *m/z*) [M-OH]<sup>+</sup>: 252.

#### 4-benzamido- $\alpha$ -(phenyl)benzyl alcohol (13b)

To a solution of 4-benzamido benzophenone (**12b**) (897 mg, 3 mmol, 1 equiv) and NaBH<sub>4</sub> (1134 mg, 30 mmol, 10 equiv) in MeOH, stirred at room temperature for 1h, was followed as general procedure of reduction. Compound **13a** as off-white powder (451 mg, 49.9%). FT-IR (cm<sup>-1</sup>),  $\nu$ : 3318 (N-H str.), 3300 board (O-H str.), 3060 (sp<sup>2</sup> C-H), 3030 (sp<sup>2</sup> C-H), 1651 (C=O str. in amide), 1182 (C-O str.); <sup>1</sup>H NMR (300 MHz), CD<sub>3</sub>OD,  $\delta$  (ppm): 7.92 (2H, d, J = 8.1 Hz, Ar-H), 7.64 (2H, d, J = 11.0 Hz, Ar-H), 7.60 -7.47 (3H, m, Ar-H), 7.40 -7.20 (7H, m, Ar-H), 5.78 (1H, s, CH-OH); <sup>13</sup>C NMR (75 MHz, CD<sub>3</sub>OD),  $\delta$  (ppm): 169.04 (C=O), 146.04 -122.32 (Ar-C), 76.73 (C-OH).

#### 4-cinnamido- $\alpha$ -(phenyl)benzyl alcohol (13c)

To a solution of 4-cinnamido benzophenone (**12c**) (200 mg, 0.6 mmol, 1 equiv) and NaBH<sub>4</sub> (287 mg, 7.6 mmol, 12.6 equiv) in MeOH, stirred at room temperature for 1h, was followed as general procedure of reduction. Compound **13c** as off-white powder (151 mg, 77.0%). FT-IR (cm<sup>-1</sup>),  $\nu$ : 3313 (N-H str.), 3311 board (O-H str.), 3058 (sp<sup>2</sup> C-H), 3029 (sp<sup>2</sup> C-H), 1658 (C=O str. in amide), 1184, 1112(C-O str.); <sup>1</sup>H NMR (300 MHz), CD<sub>3</sub>OD,  $\delta$  (ppm): 7.68 -7.55 (5H, m, Ar-H), 7.44 -7.19 (10H, m, Ar-H), 6.78 (1H, d, CH=CH), 5.74 (1H, s, CH-OH); <sup>13</sup>C NMR (75 MHz, CD<sub>3</sub>OD),  $\delta$  (ppm): 166.78 (C=O), 146.02 -121.23 (Ar-C), 76.71 (C-OH).

### 3.3 Evaluation of antitubercular activities

#### Determination of minimum inhibitory concentration by agar dilution method

Synthesized chemical compounds were tested for their antitubercular activities against *M.tuberculosis* H37Rv and 20 MTB clinical isolates at National Center for Genetic Engineering and Biotechnology (BIOTEC), using agar dilution method. [90] This is standard method to find minimum inhibitory concentration (MIC) for antimycobacterial drug-susceptibility testing. In agar dilution method, MIC means the lowest drug concentration inhibiting visible growth of a bacterial population of *M.tuberculosis* on solid Middlebrook agar medium within 21 days of incubation at 37°C. The *in vitro* bioassay method for investigating MIC-based structure activity relationship of different synthesized compounds is one of the promising methods in

the early stage of drug discovery process. Proposed general protocol for agar dilution method is presented as follows:

### **(1) Preparation of inoculums**

Inoculums were prepared by scraping colonies of exponential growth *M.tuberculosis* H37Rv from solid medium. Colonies were dispersed in a 20x150 mm screw-cap tube containing 2-3 ml of Middlebrook7H9 broth supplemented with 10% oleic acid-albumin-dextrose-catalase (OADC) and 0.05% Tween 80 and 5-8 glass beads (diameter of 6 mm). The mixture was vortexed for 2-3 min, and stood for 20 min to allow large clumps of cells to settle. Cell suspension was transferred to a new sterile tube and adjusted to a turbidity equivalent to a McFarland Standard No.1 (ca.  $3 \times 10^7$  cells/mL) with M7H9 broth. Then, it was diluted to reach standard inoculums (ca.  $1.5 \times 10^5$  cells/mL).

### **(2) Preparation of test compounds and antibiotic-containing Middlebrook7H10 agar dilution plates**

Middlebrook 7H10-10% oleic acid-albumin-dextrose-catalase (OADC) (Difco, USA) agar plates with different concentrations of test compounds (Final concentration: 20, 40 or 80  $\mu\text{g/mL}$ ) and kanamycin was used as positive controls.

### **(3) Inoculation of 7H10 agar plates**

McFarland ( $1.5 \times 10^5$  cells) of each *M.tuberculosis* strain standard inoculums 5  $\mu\text{l}$  was spotted onto both test compound, antibiotic containing and drug-free control 7H10 agar plates. Plates were sealed in CO<sub>2</sub>-permeable polyethylene bags and incubated at 37 °C for 3 weeks.

### **(4) Determination of MIC**

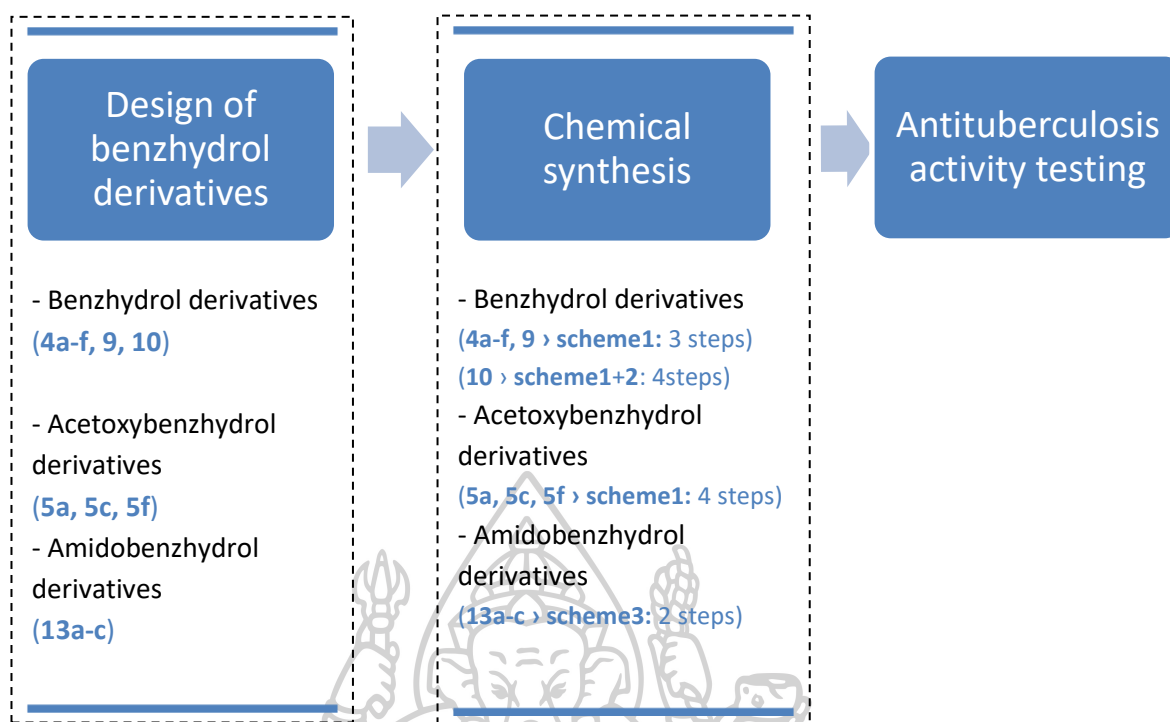
MIC was determined as the concentration of not detecting any colony (% resistance bacteria) compared with the control plate without drug.

$$\% \text{ Resistance bacteria} = \frac{\text{Number of colonies on drug containing medium}}{\text{Number of colonies on drug free medium}} \times 100$$

## CHAPTER 4

### RESULTS AND DISCUSSION

This research was included two experimental portions i.e. chemical synthesis and activity testing for antituberculosis activity. The scope of the research project was illustrated in Figure 22. Total fourteen benzhydrol derivatives compounds were designed and synthesized. The chemical structures, molecular weights and formulae of proposed benzhydrol compounds are displayed in Table 1. In order to synthesize those compounds, firstly, substituted benzoic acids were used as starting materials and their carboxylic acids were coupled with phenol to form esters by using EDC·HCl and DMAP as catalysts. The benzoate derivatives were changed to 4-hydroxy benzophenone by performing Fries rearrangement reaction. In order to determine the heating energy of the combustion in Fries rearrangement reaction using  $\text{AlCl}_3$  as catalyst for synthesis of benzophenone, DSC was used to investigate the optimum temperatures for progression of the reaction and show how the products evolve with respect to temperature. After that, 4-hydroxy benzophenones were converted to benzhydrols by reduction using  $\text{NaBH}_4$  to give benzhydrol derivatives. Based on their significant anti-TB properties, benzhydrol derivatives (**4a**, **4c**, and **4f**) were chosen as starting materials for the synthesis of diacetate compounds (**5a**, **5c**, and **5f**). Diacetylation was performed by acetylating hydroxyl groups of benzhydrol derivatives using acetic anhydride as an acetylating agent. All synthesized target compounds were purified by column chromatography and elucidated by means of FT IR,  $^1\text{H}$  NMR,  $^{13}\text{C}$  NMR and MS spectroscopic methods. General reaction pathways for synthesizing compounds **4a-f**, **5a**, **5c**, **5f**, **9**, **10** and **13a-c** were shown in Scheme 1-3. Then, the synthesized target compounds **3a-b**, **4a-f**, **5a**, **5c**, **5f**, **9**, **10** and **13a-c** were tested for their antituberculosis activities.

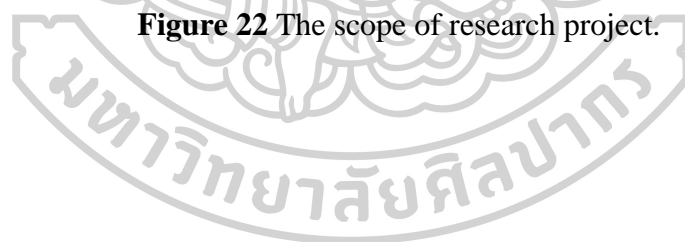


Scheme 1 : esterification + Fries rearrangement + reduction

Scheme 2 : base-catalyzed hydrolysis

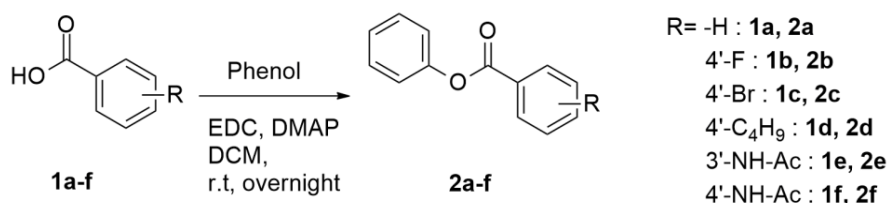
Scheme 3 : amide formation + reduction

**Figure 22** The scope of research project.

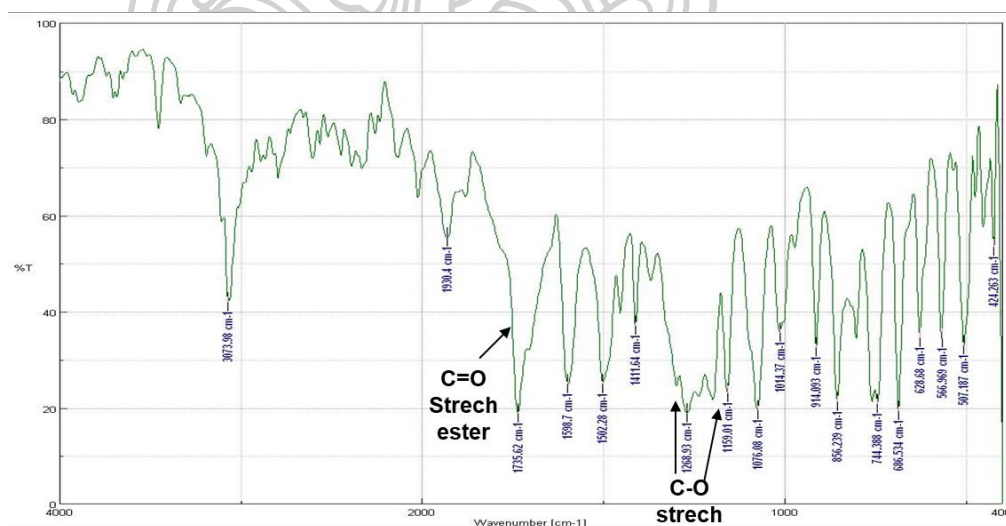


## 4.1 Chemical synthesis

### 4.1.1 Phenyl benzoate compounds (2a-f)



For this reaction, substituted benzoic acids (**1a-f**) were used as starting materials to afford compounds **2a-f**. The aim of this step was to preparing esters before the next step i.e. Fries Rearrangement reaction. The reaction was accelerated by the presence of carbodiimide activator (EDC·HCl) with catalytic amount of DMAP in dried dichloromethane. The reaction was completed at room temperature after 12-24 h to afford compound **2a-f** in 78.9 to 96.7 % yield. The reaction mechanism for esterification was described in Figure 23.[91] The ester compounds were identified by IR spectrum to confirm ester functional groups.



IR spectrum of phenyl benzoate compounds showed characteristic vibration bands of stretching of functional groups. The bands of ester moiety were displayed carbonyl C=O stretching at  $1735\text{ cm}^{-1}$ , C-O stretching at  $1269\text{ cm}^{-1}$  and  $1159\text{ cm}^{-1}$ .



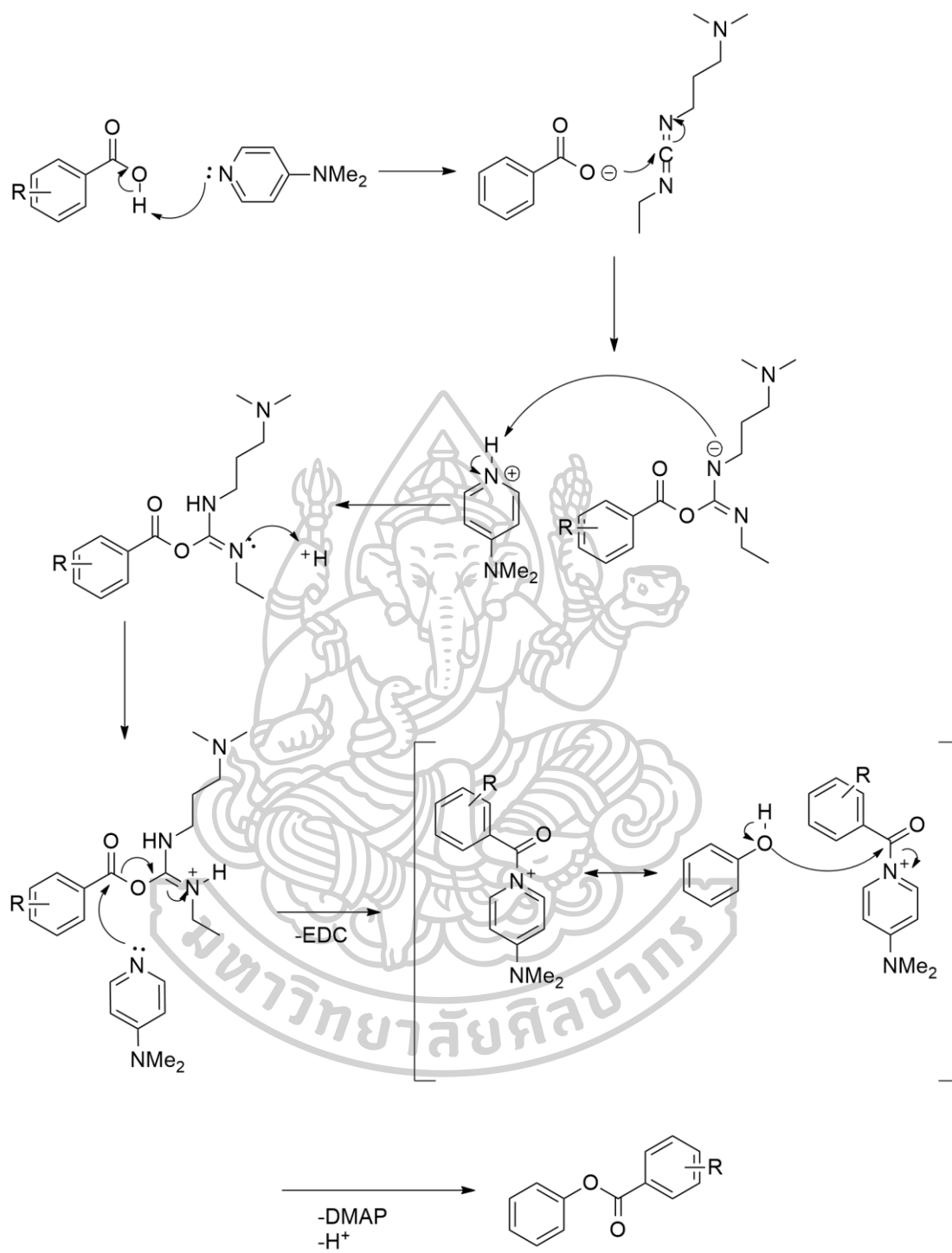
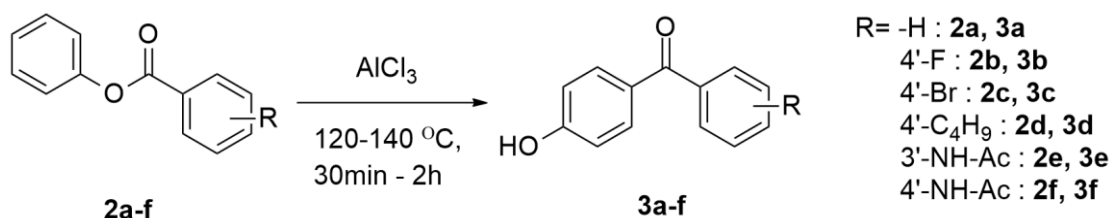


**Figure 23** The reaction mechanism of the esterification.

#### 4.1.2 Benzophenone compounds (3a-m)



This step is one of the critical reaction steps of the chemical synthesis in this study. Fries rearrangement reaction was chosen to create the formation of benzophenone compounds. In the previous experiment, benzhydrol compounds were prepared by coupling reaction between aryl bromide and aryl aldehyde using organolithium reagents as reported in [92] with overall yield of 52.7%. However, it was difficult to control the reaction to acquire the desirable product since the reaction needed to be done at very low temperature and the reactive aryl anion intermediate was easily decomposed when exposed to moisture. Using Fries rearrangement, a more straightforward synthesis method for synthesizing benzhydrol compounds derived from benzophenones with a higher yield has been developed in order to circumvent the aforementioned synthetic difficulty.

##### 4.1.2.1 Fries rearrangement reaction investigation by DSC analysis

The Fries rearrangement reaction was convenient to use as a nonsolvent method for synthesis. In order to specify the appropriate temperature for Fries rearrangement reaction, the reaction mixtures of selected phenyl benzoates **2b**, **2e**, **2f** and AlCl<sub>3</sub> heated at a heating rate of 5 °C/min under nitrogen atmosphere were studied using a DSC 823e (Mettler Toledo, Switzerland). Phenyl benzoates **2b**, **2e**, and **2f** were representatively phenyl benzoate substrates for the Fries rearrangement reaction because they were synthesized with high yields. The mixtures of compounds **2b**, **2e**, **2f** and AlCl<sub>3</sub> were inspected by heating from 40 °C to 400 °C which cover endothermic and exothermic temperatures of these mixtures during the progress of the Fries rearrangement reaction. The obtained products were assayed by employing LC-

MS to determine the optimal temperatures in order to get the highest yields of compounds **3b**, **3e** and **3f**.

### DSC analysis method used for investigation of temperature on the Fries rearrangement reaction.

On the basis of calorimetry technique, DSC is a thermal analysis equipment examining the changes in physical properties of a sample upon increasing temperature against time. This technique has been used to gain insight the thermodynamics of reaction intermediates. [93] In this study, phenyl benzoates **2b**, **2e** and **2f** were subjected to react with  $\text{AlCl}_3$  and determined by using DSC at heating from 40 °C to 400 °C. The range of temperatures used in the Fries rearrangement reaction covered endothermic and exothermic changes of these compounds. The resulted products were subjected to LC-MS analysis to determine the optimal temperatures for the preparation of compounds **3b**, **3e** and **3f**.

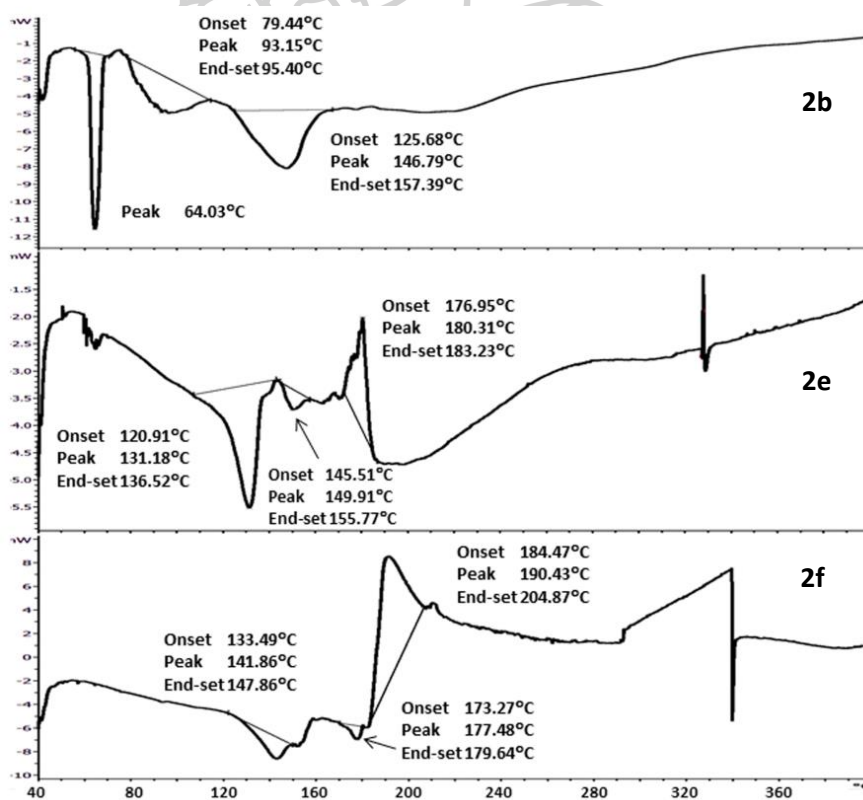


Figure 24 DSC curves of the mixtures of compounds **2b**, **2e**, **2f** and  $\text{AlCl}_3$

Figure 24 illustrates the DSC curves of reaction mixtures of compounds **2b**, **2e**, **2f** and  $\text{AlCl}_3$ . The sharp endothermic peak shown at  $64.0\text{ }^\circ\text{C}$  is the melting point of compound **2b**. The thermograph of compound **2b** also includes two broad endothermic peaks about  $79\text{-}95\text{ }^\circ\text{C}$  and  $126\text{-}157\text{ }^\circ\text{C}$ . The DSC curves of compounds **2e** and **2f** show the endothermic peaks at about  $121\text{-}137\text{ }^\circ\text{C}$  and  $146\text{-}156\text{ }^\circ\text{C}$  and at about  $133\text{-}148\text{ }^\circ\text{C}$  and  $173\text{-}180\text{ }^\circ\text{C}$ , respectively. The endothermic peaks may correspond to the interaction between phenyl benzoates and  $\text{AlCl}_3$ . The exothermic peaks at about  $177\text{-}183\text{ }^\circ\text{C}$  and  $184\text{-}205\text{ }^\circ\text{C}$  of compounds **2e-f**, consecutively, are related to their thermal decomposition [74].

**Table 3** % Compositions of Fries rearrangement products by LC-MS analysis at variable temperatures

Starting materials (Compounds)	Compounds	% Compositions <sup>a</sup>					
		Temperature of Fries rearrangement reaction ( $^\circ\text{C}$ )					
		60	95	130	140	180	190
2b	3b	$4.24 \pm 0.76$	$55.77 \pm 8.55$	$60.80 \pm 3.18$	$44.39 \pm 0.72$	$46.89 \pm 7.72$	$43.34 \pm 1.86$
	2b	$90.90 \pm 4.40$	$1.32 \pm 0.50$	$1.93 \pm 0.19$	$12.63 \pm 0.67$	$4.68 \pm 3.83$	$4.69 \pm 0.25$
2e	3e	-	$21.83 \pm 1.71$	$69.70 \pm 4.70$	$84.28 \pm 4.75$	$24.72 \pm 3.41$	$17.18 \pm 1.18$
	2e	$92.80 \pm 2.76$	$32.07 \pm 2.97$	-	-	-	$6.45 \pm 0.79$
2f	3f	-	$21.23 \pm 1.95$	$27.21 \pm 2.60$	$17.42 \pm 1.67$	$2.93 \pm 1.66$	$10.54 \pm 3.15$
	2f	$93.23 \pm 5.94$	$30.56 \pm 3.53$	$18.42 \pm 6.45$	$36.03 \pm 4.48$	$64.65 \pm 2.81$	$14.44 \pm 2.05$

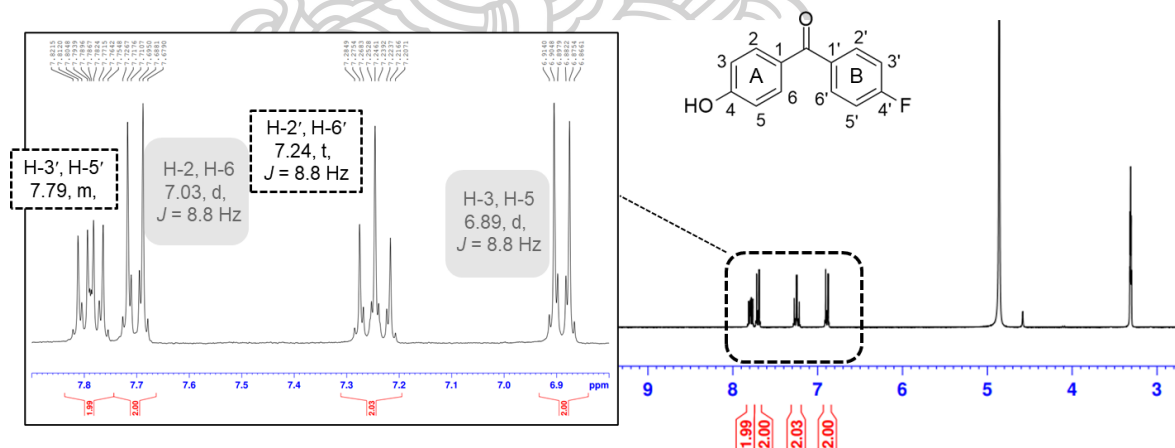
<sup>a</sup> % Compositions represent means  $\pm$  SD of triplicate samples from three independent experiments.

As displayed in Table 3, raising the reaction temperature from  $140\text{ }^\circ\text{C}$  to  $180\text{ }^\circ\text{C}$  resulted in extremely lower yields of products **3b**, **3e**, **3f** while yield of product **3b** increased a few percent. This could have been perceived from the presupposition that amide functional groups existed in compounds **2e-f** and **3e-f** might reacted with the excess chloride of  $\text{AlCl}_3$  and such changes in enthalpy leading to exothermic reactions.[94] Therefore, the exothermic peaks in the DSC curve of amido compounds **2e-f** and **3e-f** could be evidences of the product decomposition. [94-96] This supposition was attested by the fact that fluoro compounds **2b** and **3b** with no amido group did not show an exothermic process in the DSC thermograph.

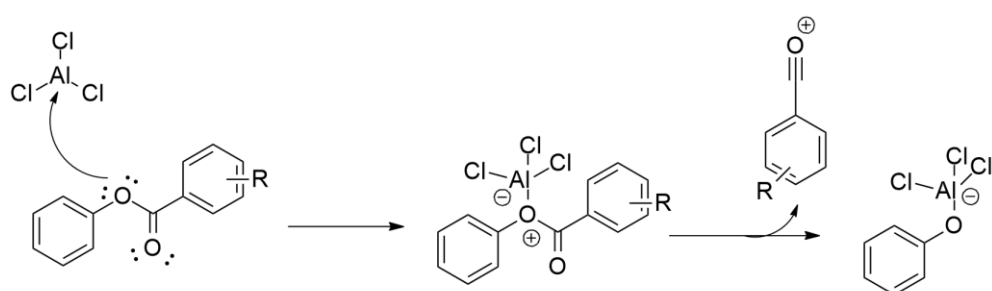
According to DSC and LC-MS results, DSC curves could inform that Fries rearrangement reactions between ester compounds and  $\text{AlCl}_3$  commenced at

endothermic temperature, followed by the decomposition of products occurring at exothermic temperature. As published works, the effective temperature for running Fries rearrangement of phenyl benzoate compounds (**2b**, **2e**, **2f**) was assumed around 130-140°C for 1 hour. Benzophenone compounds (**3b**, **3e**, **3f**) were generated from this condition with high to moderate percent yield (33.7 - 78.9 %).<sup>[97]</sup> The reaction mechanism of this step was described in Figure 25. As the results of this study, we assumed the optimal reaction temperatures of Fries rearrangement of phenylbenzoate compounds to attain high percent yields for the preparation of benzophenone derivatives (**3a-f**, **8**) were 130-140 °C for 30-60 min as shown in Table 4.

The mechanism of the Fries rearrangement reaction is illustrated in Figure 25. The acylium carbocation starts to attack the aromatic ring via an electrophilic aromatic substitution reaction. It is noted that the orientation of this electrophilic aromatic substitution is temperature-dependent. Low reaction temperatures favor para position substitutions while relatively high temperatures favor ortho position substitutions. <sup>[98-100]</sup> The obtained benzophenone derivatives were identified as *para*- isomers using the <sup>1</sup>H-NMR spectrum.



There are two signals of proton on aromatic ring A showed as representative *para*- substitution of hydroxyl group. The signal of the symmetry protons at 2 and 6 positions showed at the chemical shift of 7.03 ppm as a doublet with a coupling constant of 8.8 Hz, the same as the coupling constant of the proton signal at 3 and 5 positions was 8.8 Hz at the chemical shift of 6.89 ppm. The appearance of two symmetry signals of protons on aromatic ring A implies that the obtained product was a *para*-isomer.



Two possible pathways

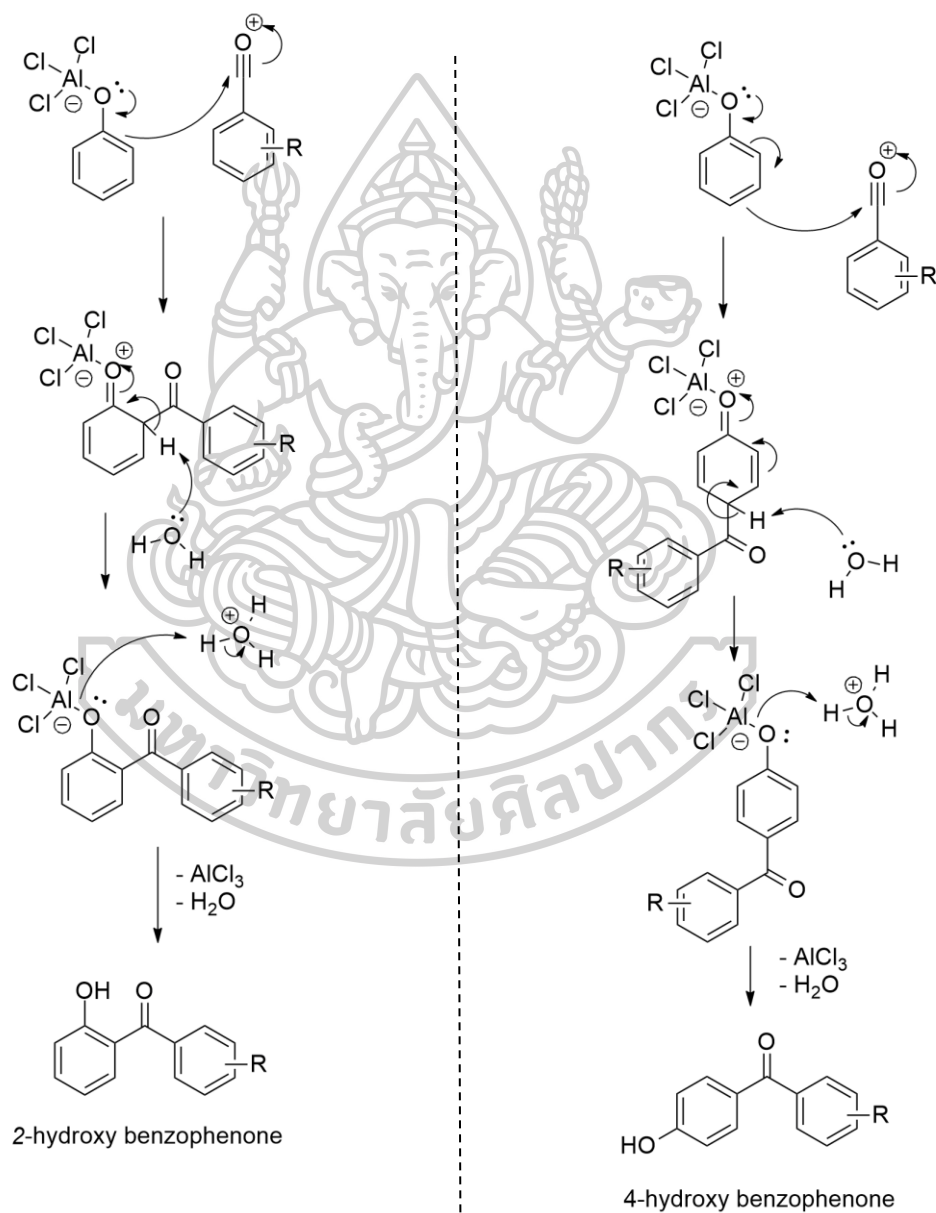


**Figure 25** The reaction mechanism of Fries rearrangement.

**Table 4** The reaction conditions and percent yields of compounds 3a-f and 8.

Entry	Compd	Product	Temp (°C)	Time (min)	Yield (%)	Physical state
1	2a	3a	140	45	33.7	white powder
2	2b	3b	140	45	47.5	white powder
3	2c	3c	140	30	65.1	pale-yellow powder
4	2d	3d	130	30	78.9	white powder
5	2e	3e	140	30	44.9	pale yellow liquid
6	2f	3f	140	60	43.1	pale yellow liquid
7	7	8	130	60	59.7	Off-white powder

#### 4.1.3 Benzhydrol compounds (4a-f) and 9

The aim of this step is to convert from ketone functional group of compounds **3a-f** and **8** to hydroxyl group of compounds **4a-f** and **9**. The ketone compounds can be reduced by the hydride nucleophile of sodium borohydride ( $\text{NaBH}_4$ ). First, hydride anion attacked carbonyl to generate an alkoxide anion intermediate. Then, the alkoxide was protonated by methanol as a proton source to provide secondary alcohol. In the reduction by sodium borohydride hydrolysis occurs automatically when methanol is used as a solvent. [101] The reaction mechanism of reduction step was described in Figure 26. This reaction created the stereogenic carbon, and the alcohol products were assumed to be a racemic mixture due to the low effect of steric hindrance surrounding carbonyl carbon. In a further study, chiral benzhydrol derivatives can be determined the degree of enantiomers excess by using a polarimeter.

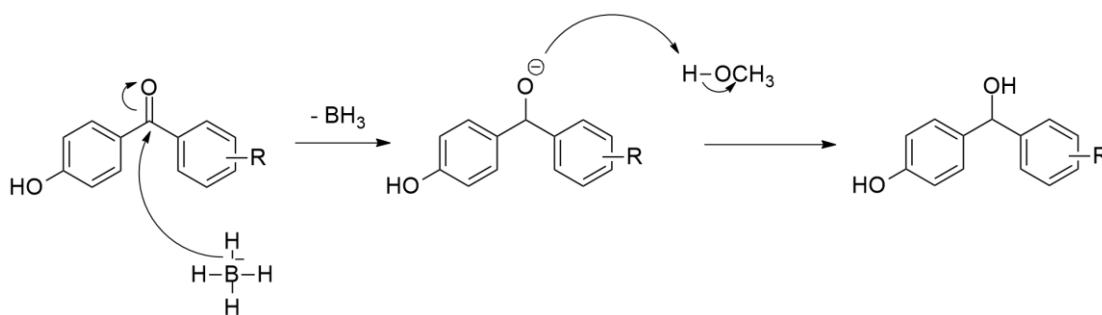


**Figure 26** The reaction mechanism of sodium borohydride reduction

#### 4.1.4 Diacetyl benzhydrol compounds (**5a**, **5c**, **5f**)

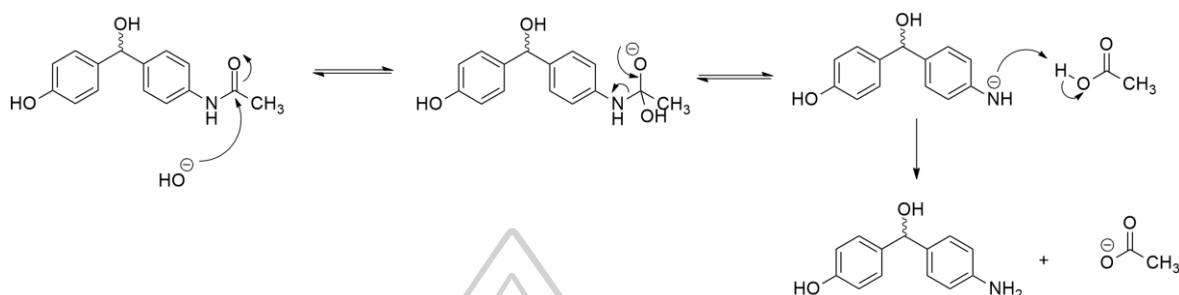
The aim of this step was to change the active hydroxyl group of compound 4-hydroxy- $\alpha$ -(phenyl)benzyl alcohol (**4a**), 4-hydroxy- $\alpha$ -(4'-bromophenyl)benzyl alcohol (**4c**) and 4-hydroxy- $\alpha$ -(4'-acetamido phenyl)benzyl alcohol (**4f**) to ester group in order to mimic the structure of ACA (I), chemical constituent of *Alpinia galanga*. For acetylation, alcohol was acylated using acetic anhydride as a source of acyl groups. Carbodiimide activator (EDC) with a catalytic quantity of DMAP in dichloromethane enhanced the process. The reaction was completed at room temperature for 12 hours to obtain compound **5a**, **5c**, **5f** with yields of 69.3 to 92.9 percent.

#### 4.1.5 4-hydroxy- $\alpha$ -(4'-amino phenyl)benzyl alcohol (**10**)

The aim of this step is to cleave the acetyl functional group from compound **4f** to afford the amino compound **10**. The carbonyl carbon of the amide can be removed by acid or base hydrolysis. Normally, amide is difficult to be hydrolyzed; even heating for a long time, amide does not react with water molecules to decompose. However, amide can be interacted with water molecules either in an acidic or a basic medium. In a basic medium, amide is hydrolyzed to attain a carboxylic acid and the salt of ammonia or amine salt. The mechanism of base-catalyzed hydrolysis is shown in Figure 27. The reaction mechanism of amide hydrolysis in basic medium starts with the nucleophilic attack at the carbonyl carbon by a hydroxide ion to form a tetrahedral alkoxide intermediate. This step is reversible intermediate. The carbonyl



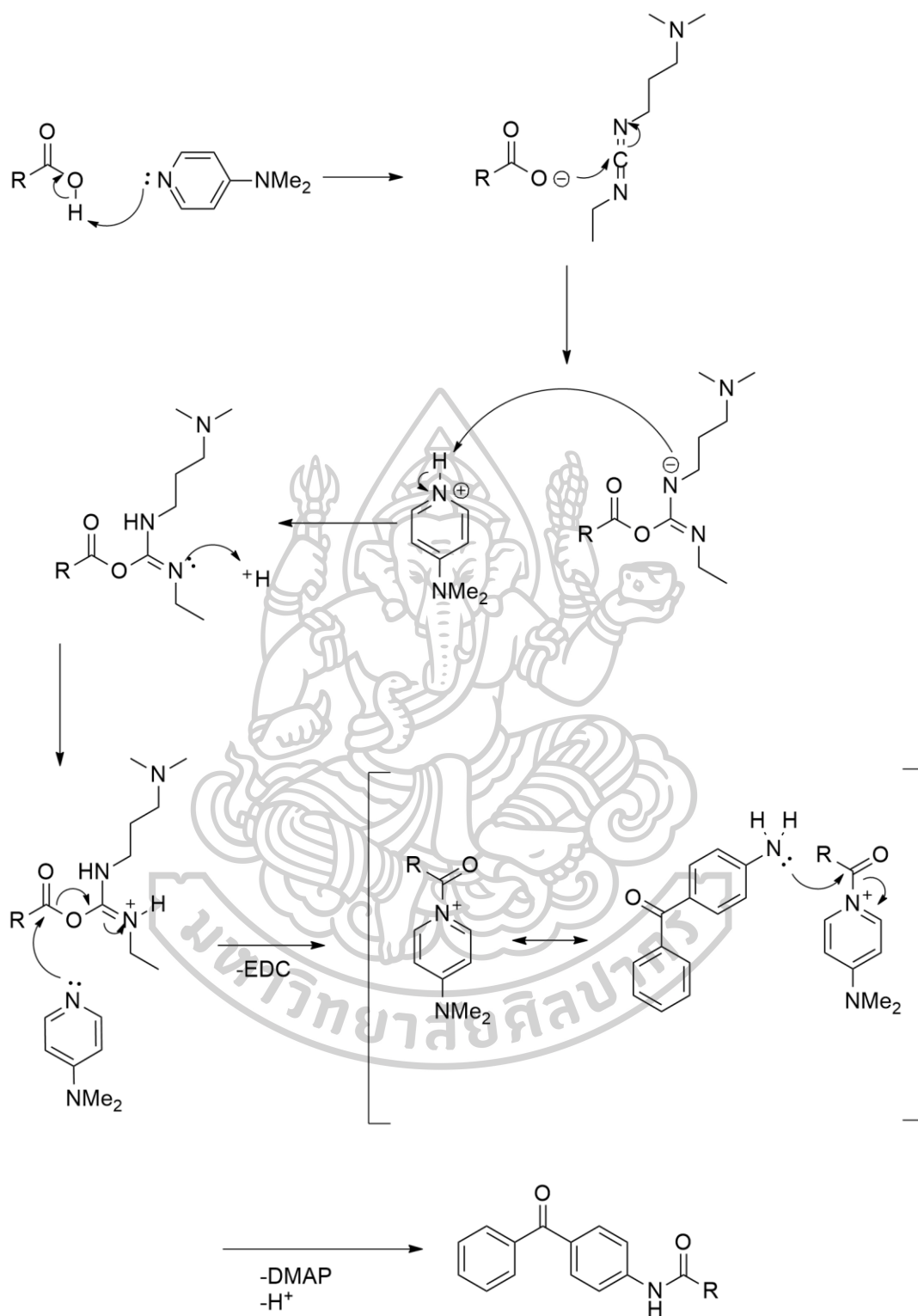
bond is reformed along with the elimination of an amide ion ( $\text{-NHR}$ ) leaving group, forming a carboxylic acid. In the final step, the amide ion is protonated by a proton from the carboxylic acid to form a carboxylate salt and an amine as products.[102]



**Figure 27** The reaction mechanism of the base-catalyzed hydrolysis

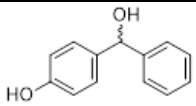
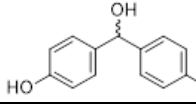
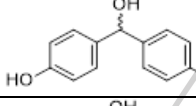
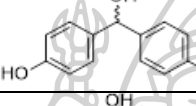
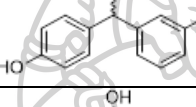
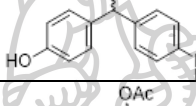
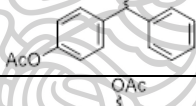
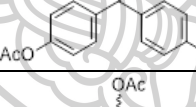
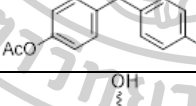
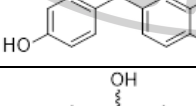
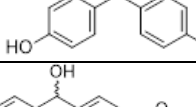
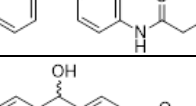
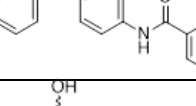
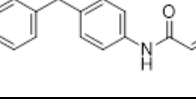
#### 4.1.6 Amidobenzhydryl compounds (13a-c)

The aim of this step was to link the various types of functional groups (i.e. alkyl, aryl and long chain) to amine group by amide bond in order to explore the binding target of anti-TB. For amide formation, the substituted acids (**11a-c**) were used as reagents for coupling with 4-aminobenzophenone. The reaction was accelerated in the presence of carbodiimide activator (EDC) with catalytic amount of DMAP in  $\text{CH}_2\text{Cl}_2$  [103]. The reaction was completed at room temperature after 12 h to afford compound **12a-c** as off-white solid in 31.5 to 72.0 % yield. The reaction mechanism for amide formation was described in Figure 28 [91]. Next, converting the ketone group to benzhydryl compounds (13a-c) was done by reduction reaction using  $\text{NaBH}_4$  as hydride nucleophile.



**Figure 28** The reaction mechanism of the amide formation

**Table 5** The physical properties and percent yield of benzhydryl derivatives

Entry	Compound	Product	Overall Yield (%) <sup>a</sup>	Physical state
1	4a		20.26	white solid
2	4b		26.98	white solid
3	4c		56.59	pale yellow solid
4	4d		49.71	pale yellow liquid
5	4e		31.41	pale yellow liquid
6	4f		23.97	pale yellow liquid
7	5a		18.82	white solid
8	5c		39.22	pale yellow solid
9	5f		21.96	pale yellow liquid
10	9		40.54	off-white solid
11	10		6.57	pale yellow solid
12	13a		57.53	off-white solid
13	13b		29.74	off-white solid
14	13c		24.26	off-white solid

<sup>a</sup>The overall yield of this convergent synthesis was calculated based on overall steps starting from compound 1 or 6 or 11 to afford final products

## 4.2 Structural characterizations

### 4.2.1 IR spectroscopic characterization

IR spectroscopy was used to determine the functional group and possibly identify components of benzhydrol derivatives. IR spectra of some benzhydrol derivatives were recorded (Neat or KBR pellets or nujol mulllets) on a Jasco FT-IR spectrophotometer (Japan) and a Thermo Scientific Nicolet FI IR spectrophotometer (USA) reported as a wavenumber ( $\text{cm}^{-1}$ ).

#### 4.2.1.1 IR Characterization of 4-hydroxy- $\alpha$ -(phenyl)benzyl alcohol (4a)

Characteristic vibration bands of functional groups were displayed in IR spectrum of 4-hydroxy- $\alpha$ -(phenyl)benzyl alcohol (4a). A spectrum of 4a was used as a representative spectrum to explain the compound's significant vibration bands of functional groups. The characteristic O-H stretching for intra-molecular hydrogen bonding of alcohol was displayed at 3399 and 3165  $\text{cm}^{-1}$  (strong). The strong aromatic C-O stretching bands was 1611  $\text{cm}^{-1}$ . The bands of aromatic ring included aromatic C=C stretching band at 1513 and 1448  $\text{cm}^{-1}$ , C-O stretching band of alcohol at 1005  $\text{cm}^{-1}$ , =C-H out of plane bending at 698  $\text{cm}^{-1}$ .

#### 4.2.1.2 IR Characterization of 4-hydroxy- $\alpha$ -(4'-fluorophenyl)benzyl alcohol (4b)

The characteristic O-H stretching for intra-molecular hydrogen bonding of alcohol was displayed at 3386 and 3180  $\text{cm}^{-1}$  (broad). The strong C-O stretching band of aromatic was 1600  $\text{cm}^{-1}$ . The bands of the aromatic ring included aromatic C=C stretching band at 1510 and 1454  $\text{cm}^{-1}$ . The strong C-F stretching band was indicated at 1230  $\text{cm}^{-1}$ .

#### 4.2.1.3 IR Characterization of 4-hydroxy- $\alpha$ -(4'-bromophenyl)benzyl alcohol (4c)

The characteristic O-H stretching for intra-molecular hydrogen bonding of alcohol was displayed at 3385 and 3153  $\text{cm}^{-1}$  (strong). The bands of aromatic ring included aromatic C=C stretching band at 1510 and 1453  $\text{cm}^{-1}$ . The strong C-O stretching bands of alcohol and strong C-Br stretching bands were indicated in the region of 1002 and 554  $\text{cm}^{-1}$ .

#### **4.2.1.4 IR Characterization of 4-hydroxy- $\alpha$ -(4'-butylphenyl)benzyl alcohol (4d)**

The characteristic O-H stretching for intra-molecular hydrogen bonding of alcohol was displayed at 3400 and 3168  $\text{cm}^{-1}$  (broad). The aliphatic C-H stretching bands in butyl were seen at 2958, 2925 and 2856  $\text{cm}^{-1}$ . The aliphatic C-H bending vibration was observed at 1362 and 1225  $\text{cm}^{-1}$ . The strong C-O stretching bands of alcohol showed at 1001  $\text{cm}^{-1}$ .

#### **4.2.1.5 IR Characterization of 4-hydroxy- $\alpha$ -(3'-acetamido phenyl)benzyl alcohol (4e)**

The characteristic O-H stretching for intra-molecular hydrogen bonding of alcohol was displayed at 3317 and 3190  $\text{cm}^{-1}$  (broad). The strong C-O stretching bands of alcohol showed at 995  $\text{cm}^{-1}$ . The strong C=O stretching at 1674  $\text{cm}^{-1}$ , N-H stretching in the region of approximate 3300  $\text{cm}^{-1}$  and N-H bending at 1605  $\text{cm}^{-1}$  indicated the presence of amide functional group.

#### **4.2.1.6 IR Characterization of 4-hydroxy- $\alpha$ -(4'-acetamido phenyl)benzyl alcohol (4f)**

The characteristic O-H stretching for intra-molecular hydrogen bonding of alcohol was displayed in the region at 3296 and 3103  $\text{cm}^{-1}$  (broad). The strong C-O stretching bands of alcohol showed at 1016  $\text{cm}^{-1}$ . The strong C=O stretching at 1666  $\text{cm}^{-1}$ , N-H stretching in the region of approximately 3300  $\text{cm}^{-1}$  and N-H bending at 1627  $\text{cm}^{-1}$  indicated the presence of an amide functional group.

#### **4.2.1.7 IR Characterization of 4-acetoxy- $\alpha$ -(phenyl)benzyl acetate (5a)**

The characteristic C=O stretching of acetyl groups was displayed at 1824, 1739  $\text{cm}^{-1}$  (strong). The aliphatic C-H stretching bands of methyl at 2935  $\text{cm}^{-1}$ . The bands of aromatic ring included aromatic C-H stretching at 3064, 3034  $\text{cm}^{-1}$ . The bands of aromatic ring included aromatic C=C stretching band at 1505 and 1455  $\text{cm}^{-1}$ .

#### **4.2.1.8 IR Characterization of 4-acetoxy- $\alpha$ -(4'-bromo phenyl)benzyl acetate (5c)**

The characteristic C=O stretching of acetyl groups was displayed at 1761, 1741  $\text{cm}^{-1}$  (strong). The aliphatic C-H stretching bands of methyl at 2922, 2895 and 2804  $\text{cm}^{-1}$ . The bands of aromatic ring included aromatic C-H stretching at about

3000  $\text{cm}^{-1}$ . The bands of aromatic ring included aromatic C=C stretching band at 1491 and 1448  $\text{cm}^{-1}$ . The C-Br stretching bands were indicated at 559  $\text{cm}^{-1}$ .

#### **4.2.1.9 IR Characterization of 4-acetoxy- $\alpha$ -(4'-acetamido phenyl)benzyl acetate (5f)**

The characteristic C=O stretching of acetyl groups was displayed at 1726, 1676  $\text{cm}^{-1}$  (strong). The aliphatic C-H stretching bands of methyl at 2983 and 2771  $\text{cm}^{-1}$ . The strong C=O stretching at about 1676  $\text{cm}^{-1}$ , N-H stretching at 3324  $\text{cm}^{-1}$  and N-H bending in the region of approximate 1600  $\text{cm}^{-1}$  indicated the presence of amide functional group. The bands of aromatic ring included aromatic C-H stretching at 3068  $\text{cm}^{-1}$ . The bands of aromatic ring included aromatic C=C stretching band at 1520 and 1408  $\text{cm}^{-1}$ .

#### **4.2.1.10 IR Characterization of 4-hydroxyphenyl(2-naphthyl)methanol (9)**

The characteristic O-H stretching for intra-molecular hydrogen bonding of alcohol was displayed at 3386 and 3164  $\text{cm}^{-1}$  (broad). The strong C-O stretching bands of alcohol showed at 1024  $\text{cm}^{-1}$ . The bands of aromatic ring included aromatic C-H stretching band at about 3000  $\text{cm}^{-1}$ , skeletal C=C stretching at 1511 and 1456  $\text{cm}^{-1}$ , =C-H out of plane bending at 785  $\text{cm}^{-1}$ .

#### **4.2.1.11 IR Characterization of 4-hydroxy- $\alpha$ -(4'-amino phenyl)benzyl alcohol (10)**

The bands of amine functional group included bands of N-H stretching at about 3300  $\text{cm}^{-1}$ , C-N stretching at 1081  $\text{cm}^{-1}$  with medium-weak intensity, medium intensity of N-H bending at 1618  $\text{cm}^{-1}$ . The characteristic O-H stretching for intra-molecular hydrogen bonding of alcohol was displayed around 3329  $\text{cm}^{-1}$  (broad). The strong C-O stretching bands of alcohol showed at 1022  $\text{cm}^{-1}$ . The bands of aromatic ring included aromatic C-H stretching band at about 3024  $\text{cm}^{-1}$ , skeletal C=C stretching at 1515 and 1450  $\text{cm}^{-1}$ . =C-H out of plane bending at 748  $\text{cm}^{-1}$ .

#### **4.2.1.12 IR Characterization of 4-butyramido- $\alpha$ -(phenyl)benzyl alcohol (13a)**

The bands of amide functional group included N-H stretching (strong) at about 3300  $\text{cm}^{-1}$ , C=O stretching (strong) at 1660  $\text{cm}^{-1}$ , N-H bending at 1601  $\text{cm}^{-1}$ . The characteristic O-H stretching for intra-molecular hydrogen bonding of alcohol was

displayed around  $3303\text{ cm}^{-1}$  (broad). The strong C-O stretching bands of alcohol showed at  $1016\text{ cm}^{-1}$ . The bands of aromatic ring included aromatic C-H stretching (medium) at  $3057\text{ cm}^{-1}$ , C-H out of plane bending at about  $727\text{ cm}^{-1}$ , skeletal C=C stretching at  $1533$  and  $1448\text{ cm}^{-1}$ . The aliphatic  $\text{sp}^3$  C-H stretching bands at  $2962$ ,  $2873\text{ cm}^{-1}$  and aliphatic C-H bending vibration at  $1309$ ,  $1271\text{ cm}^{-1}$  indicated the presence of butyl groups.

#### **4.2.1.13 IR Characterization of 4-benzamido- $\alpha$ -(phenyl)benzyl alcohol (13b)**

The bands of amide functional group included N-H stretching (strong) at about  $3300\text{ cm}^{-1}$ , C=O stretching (strong) at  $1651\text{ cm}^{-1}$ , N-H bending at  $1599\text{ cm}^{-1}$ . The characteristic O-H stretching for intra-molecular hydrogen bonding of alcohol was displayed around  $3319\text{ cm}^{-1}$  (broad). The strong C-O stretching bands of alcohol showed at  $1012\text{ cm}^{-1}$ . The bands of aromatic ring included aromatic C-H stretching (medium) at  $3060$ ,  $3030\text{ cm}^{-1}$ , skeletal C=C stretching at  $1523$ - $1446\text{ cm}^{-1}$ , =C-H out of plane bending at about  $731\text{ cm}^{-1}$ .

#### **4.2.1.14 IR Characterization of 4-cinnamido- $\alpha$ -(phenyl)benzyl alcohol (13c)**

The bands of amide functional group included N-H stretching (strong) at about  $3300\text{ cm}^{-1}$ , C=O stretching (strong) at  $1658\text{ cm}^{-1}$ , N-H bending at  $1601\text{ cm}^{-1}$ . The O-H stretching at about  $3313\text{ cm}^{-1}$  (broad), strong C-O stretching bands at  $1012\text{ cm}^{-1}$  revealed the presence of alcohol group. In the spectrum, unsaturated aliphatic C=C stretching at  $1533\text{ cm}^{-1}$ , the band of =C-H bending (strong) at  $729\text{ cm}^{-1}$ , the bands of aromatic ring included aromatic C-H stretching (medium) at  $3058$ ,  $3029\text{ cm}^{-1}$  were indicated the existence of cinnamic group.

**Table 6** Characteristic IR bands of important functional groups of synthesized compounds

Compd	Wavenumber (cm <sup>-1</sup> )											
	N-H st.	O-H st.	Aromatic C-H st.	Aliphatic C-H st.	C=O st.	N-H bend	Aromatic C-O st.	Aromatic C=C st.	Aliphatic C-H bend	C-O st.	=C-H bend	etc.
<b>4a</b>	-	3399, 3165	app 3000	-	-	-	1611	1513, 1448	-	1005	698	-
<b>4b</b>	-	3386, 3180	app 3000	-	-	-	1600	1510, 1454	-	1007	783	1230 (C-F st.)
<b>4c</b>	-	3385, 3153	app 3000	-	-	-	1600	1510, 1453	-	1002	785	554 (C-Br st.)
<b>4d</b>	-	3400, 3168	app 3000	2958, 2925, 2856	-	-	1597	1512, 1452	1362, 1225	1001	775	-
<b>4e</b>	app 3300	3317, 3190	app 3000	2810	1674	1605	1587	1512, 1441	1331, 1284	995	764	-
<b>4f</b>	app 3300	3296, 3103	app 3000	2910	1666	1627	1599	1525, 1404	1371, 1288	1016	771	-
<b>5a</b>	-	-	3064, 3034	2935	1824, 1739	-	1607	1505, 1455	1370, app 1200	1016	747	-
<b>5c</b>	-	-	app 3000	2922, 2895, 2804	1761, 1741	-	1620	1491, 1448	1369, 1234	1009	775	559 (C-Br st.)
<b>5f</b>	3324	-	3068	2983, 2771	1726, 1676	app 1600	1592	1520, 1408	1369, 1268	1000	767	-
<b>9</b>	-	3386, 3164	app 3000	-	-	-	1599	1511, 1456	-	1024	785	-
<b>10</b>	app 3000	3329	3024	-	-	app 1600	1617	1515, 1450	-	1022	748	1081 (C-N st.)
<b>13a</b>	app 3300	3303	3057	2962, 2873	1660	1601	-	1533, 1448	1309, 1271	1016	727	-
<b>13b</b>	app 3300	3319	3060, 3030	-	1651	1599	-	1523, 1446	-	1012	731	-
<b>13c</b>	app 3300	3313	3058, 3029	-	1658	1601	-	1495, 1448	-	1012	729	1533 (C=C st. cinnamic)



## 4.2.2 NMR spectroscopic characterization

NMR spectroscopy was used to determine the structure of benzhydrol derivatives. All of the  $^1\text{H}$ ,  $^{13}\text{C}$  NMR spectra were recorded on a Bruker-Ultra Shield (300 and 100 MHz for  $^1\text{H}$  and  $^{13}\text{C}$ , respectively), using  $\text{CD}_3\text{OH}$  or  $\text{CD}_3\text{COCD}_3$  as solvents with trace of  $\text{CH}_3\text{OH}$  or TMS as internal standards.

### 4.2.2.1 NMR Characterization of 4-hydroxy- $\alpha$ -(phenyl)benzyl alcohol (4a)

The  $^1\text{H}$  NMR spectroscopy was used to determine the structure of benzhydrol (4a) using  $\text{CD}_3\text{COCD}_3$  as a solvent with TMS as an internal standard. The C-H proton  $\alpha$  to the alcohol showed singlet signal at 5.73 ppm. The resonances of aromatic protons at positions of 3, 5 and 2, 6 showed at 6.76 ppm and 7.40 ppm as doublet splitting patterns with coupling constant 8.7 Hz, respectively. The chemical shifts of protons at 2', 6' appeared in the aromatic region of 7.26 to 7.32 ppm as multiplet. The resonances of 3', 4' and 5' protons appeared in the more upfield region between 7.16 to 7.22 ppm as multiplet.

### 4.2.2.2 NMR Characterization of 4-hydroxy- $\alpha$ -(4'-fluorophenyl)benzyl alcohol (4b)

The C-H proton  $\alpha$  to the alcohol showed singlet signal at 5.69 ppm. The resonances of aromatic protons at positions of 3, 5 and 2, 6 showed at 6.74 ppm and 7.15 ppm as doublet splitting patterns with coupling constant 8.6 Hz and 8.3 Hz, respectively. The chemical shifts of protons at 2', 6' appeared in the aromatic region of 6.98 to 7.05 ppm as triplet. The resonances of 3' and 5' protons appeared in the more downfield region between 7.32 to 7.37 ppm as multiplet due to electron withdrawing effect of fluorine.

The  $^{13}\text{C}$  NMR spectra showed the carbon of aromatic ring in the region of 115.71 - 165.01 ppm. The  $\alpha$ -carbon to OH group appeared at 76.07 ppm

### 4.2.2.3 NMR Characterization of 4-hydroxy- $\alpha$ -(4'-bromophenyl)benzyl alcohol (4c)

The C-H proton  $\alpha$  to the alcohol showed singlet signal at 5.73 ppm. The resonances of aromatic protons at positions of 3, 5 and 2, 6 showed at 6.77 ppm and 7.20 ppm as doublet splitting patterns with coupling constant 8.4 Hz. The chemical

shifts of protons at 2', 6' appeared in the aromatic region of 7.35 ppm as doublet. The resonances of 3' and 5' protons appeared in the more downfield region between 7.47 ppm as doublet due to electron withdrawing effect of bromine with the same coupling constants of 8.4 Hz.

#### **4.2.2.4 NMR Characterization of 4-hydroxy- $\alpha$ -(4'-butylphenyl)benzyl alcohol (4d)**

The signal of 4'' proton at butyl group showed at the chemical shift of 0.92 ppm as triplet with coupling constant 7.3 Hz. Two protons at position 3'' appeared resonance at 1.34 ppm as sextet resulting from the coupling of neighboring protons with coupling constant 7.6 Hz. The splitting pattern of 2'' proton was quintet due to coupling of 1'' and 3'' protons and its signal appeared at 1.57 ppm with coupling constant 7.6 Hz. The proton of 1'' showed chemical shift of 2.58 ppm as triplet with coupling constant 7.5 Hz. The C-H proton at  $\alpha$ -position to the alcohol showed singlet signal at 5.66 ppm. The resonances of two aromatic protons at positions of 3 and 5 showed at 6.73 ppm as doublet with coupling constant 8.6 Hz and two proton of 2 and 6 at 7.15 ppm as doublet. Two protons at position 2' and 6' appeared signals at 7.11 ppm as doublet. The resonances of two aromatic protons at positions of 3' and 5' attached to butyl group showed at 7.23 ppm as doublet with coupling constant 8.0 Hz.

The  $^{13}\text{C}$  NMR spectrum showed that the signals of carbons from butyl side chain appeared in the region of 14.42 ppm to 36.38 ppm. The signals of CH-OH carbon at  $\alpha$  to the alcohol showed at 76.66 ppm and aromatic ring carbons in the region of 116.04 to 157.70 ppm. The signals of CH-OH at aromatic rings appeared at 157.70 ppm

#### **4.2.2.5 NMR Characterization of 4-hydroxy- $\alpha$ -(3'-acetamido phenyl) benzyl alcohol (4e)**

The signal of  $\text{CH}_3$  proton at acetamido group showed at the chemical shift of 2.90 ppm as a singlet. The resonance of NH proton in acetamido group appeared at 4.65 ppm. The C-H proton at  $\alpha$ -position to the alcohol showed a singlet signal at 5.69 ppm. The resonances of two aromatic protons at positions 3 and 5 showed 6.76 ppm as a doublet with a coupling constant of 9.0 Hz. Two protons at positions 2 and 6 appeared signals at 7.58 ppm. The characteristic chemical shift for 2' proton in

aromatic ring attached to acetamido side chain showed at 7.08 ppm as doublet due to coupling with NH proton. The chemical shift of three protons of the aromatic ring at 4', 5' and 6' positions appeared in the region of 7.17 to 7.22 ppm.

#### **4.2.2.6 NMR Characterization of 4-hydroxy- $\alpha$ -(4'-acetamido phenyl)benzyl alcohol (4f)**

The signal of CH<sub>3</sub> proton at acetamido group showed the chemical shift of 2.94 ppm as singlet. The resonance of NH proton in acetamido group appeared at 4.82 ppm as a singlet. The C-H proton at  $\alpha$ -position to the alcohol showed a singlet signal at 5.73 ppm. The resonances of the symmetry protons at positions 3, 5 and 2, 6 on aromatic ring A showed at 6.77 ppm and 7.47 ppm as doublet splitting patterns with coupling constant 8.7 Hz. As doublet, the chemical shifts of protons at 3', 5' appeared in the aromatic region of 7.19 ppm. The resonances of 2' and 6' protons appeared in region 7.35 ppm as a doublet with the same coupling constants of 8.4 Hz.

#### **4.2.2.7 NMR Characterization of 4-acetoxy- $\alpha$ -(phenyl)benzyl acetate (5a)**

The signal of methyl proton in CH-OCOCH<sub>3</sub> and Ar-OCOCH<sub>3</sub> showed at the chemical shift of 2.15 ppm and 2.28 ppm as singlets, respectively. The C-H proton at  $\alpha$ -position to the alcohol showed a singlet signal at 6.88 ppm. The characteristic resonances for aromatic ring A in 3,5-positions appeared at 7.05 ppm as doublet splitting patterns with coupling constant 8.7 Hz. The splitting pattern resulting from the coupling with neighboring protons H-2, H-6, H-2', H-3', H-4', H-5' and H-6' was multiplet, and chemical shift appeared in the region of 7.26-7.36 ppm.

#### **4.2.2.8 NMR Characterization of 4-acetoxy- $\alpha$ -(4'-bromophenyl)benzyl acetate (5c)**

The signal of methyl proton in CH-OCOCH<sub>3</sub> and Ar-OCOCH<sub>3</sub> showed the chemical shift of 2.15 ppm and 2.28 ppm as singlets. The C-H proton at  $\alpha$ -position to the alcohol showed a singlet signal at 6.82 ppm. The resonances of aromatic protons at positions 3, 5 and 2, 6 showed at 7.06 ppm and 7.31 ppm as doublet splitting patterns with the same coupling constants of 8.7 Hz. The chemical shifts of protons at 2', 6' and 3', 5' appeared in the aromatic region of 7.20 ppm and 7.46 ppm as doublets with the same coupling constants of 8.4 Hz. The resonances of 3' and 5' protons

appeared in the more downfield region due to the electron-withdrawing effect of bromine.

#### **4.2.2.9 NMR Characterization of 4-hydroxyphenyl (2-naphthyl) methanol (9)**

The  $^1\text{H}$  NMR spectroscopic data showed that the characteristic resonances for C-H proton at  $\alpha$ -position to the alcohol appeared singlet signal at 5.86 ppm. The resonances of aromatic protons at positions of 3, 5 and 2, 6 showed at 6.75 ppm and 7.21 ppm as doublet splitting patterns with the coupling constants of 8.6 and 8.4 Hz, respectively. The resonances of three naphthalene protons at the positions of 2', 9' and 10' showed at 7.43 ppm as multiplet. Four protons of naphthalene ring at position 4', 5', 6', and 7' appeared signals at the region between 7.75 to 7.86 ppm as multiplet.

The  $^{13}\text{C}$  NMR spectrum showed that the signals  $\alpha$ -carbon to OH group appeared at 76.86 ppm. The carbons of aromatic rings were found in the region of 116.18 -157.90 ppm.

#### **4.2.2.10 NMR Characterization of 4-butyramido- $\alpha$ -(phenyl)benzyl alcohol (13a)**

The signal of  $\text{CH}_3$  proton at 3'' position of butyramide group showed at the chemical shift of 0.98 ppm as triplet with coupling constant 7.4 Hz. The splitting pattern of 2'' proton ( $\text{CH}_2$ ) was sextet due to coupling of 1'' and 3'' protons and its signal appeared at 1.70 ppm with coupling constant 7.4 Hz. The proton of 1'' showed chemical shift of 2.32 ppm as triplet with coupling constant 7.4 Hz. The proton of  $\alpha$ -carbon to OH group appeared at 5.74 ppm as a singlet. The resonances of five protons at aromatic ring-A and two protons at 2', 6' positions of aromatic ring-B showed in the region of 7.18-7.37 ppm as multiplet. The chemical shifts of protons at 3', 5' appeared in the aromatic region of 7.50 ppm as doublet. The differences of chemical shift of aromatic protons at 3', 5' positions were affected by inductive effect of amide group at *para*- position on aromatic ring.

The  $^{13}\text{C}$  NMR spectrum showed that the signals  $\alpha$ -carbon to OH group appeared at 76.68 ppm. The carbons of aromatic rings were found in the region of 121.25 -145.98 ppm. The carbon of amide group showed C=O signal in the most downfield at 174.68 ppm

#### 4.2.2.11 NMR Characterization of 4-benzamido- $\alpha$ -(phenyl)benzyl alcohol (13b)

The C-H proton  $\alpha$  to the alcohol showed singlet signal at 5.78 ppm. The resonances of seven protons at aromatic ring A (H-2, H-3, H-4, H-5, H-6) and ring B (H-2', H-6') showed in the region of 7.20 – 7.40 ppm as multiplet splitting patterns. The doublet signal at 7.64 ppm was the chemical shifts of protons at 3', 5' position of aromatic ring connected to amine group. The chemical shifts of protons at 3'', 4'', 5'' appeared in the aromatic region of 7.50 ppm as multiplet. The resonances of 2'' and 6'' protons appeared in the more downfield region of 7.92 ppm as doublet due to electron withdrawing effect of carbonyl group.

The  $^{13}\text{C}$  NMR spectrum showed that the signals  $\alpha$ -carbon to OH group appeared at 76.73 ppm. The carbons of aromatic rings were found in the region of 122.32 -146.04 ppm. The carbon of amide group showed C=O signal in the most downfield at 169.04 ppm

#### 4.2.2.12 NMR Characterization of 4-cinnamido- $\alpha$ -(phenyl)benzyl alcohol (13c)

The  $^1\text{H}$  NMR spectroscopic data showed that the characteristic resonances for C-H proton at  $\alpha$ -position to the alcohol appeared singlet signal at 5.74 ppm. The resonance of H-a position of CH=CH of cinnamide group appeared at 6.78 ppm as two broad singlets from the unlabelled isotopomer. The signal of H-b position of CH=CH group appeared in the region of 7.55 – 7.63 ppm. The resonances of aromatic protons at ring A and ring C showed in the region of 7.20 – 7.40 ppm as multiplet splitting patterns. The chemical shifts of protons at 2', 3', 4', 5' at ring B appeared in the aromatic region of 7.55 - 7.63 ppm as multiplet.

The  $^{13}\text{C}$  NMR spectrum showed that the signals  $\alpha$ -carbon to OH group appeared at 76.71 ppm. The unsaturated carbon including aromatics and alkenes showed in the region of 121.23 -146.02 ppm. The carbon of amide group showed C=O signal in the most downfield at 166.78 ppm

### 4.3 Structure-activity relationship of synthesized compounds and anti-tuberculosis activity

The synthesized compounds **4a-f**, **5a**, **5c**, **5f**, **9**, **10** and compound **13a-c** were investigated for antituberculosis activity on 20 clinical isolates and MTB H37Rv reference strains (ATCC 27294) according to the procedure described in section 3.3. The results of *in vitro* antituberculosis activities are summarized in Table 7.

It could be concluded that the inductive effects of substituents (fluorine or bromine atom) on a B-ring which significantly enhanced the anti-TB activity compared with unsubstituted 4-hydroxy benzhydrol **4a**. Firstly, we synthesized and investigated the high electronegativity of fluorine or bromine atom on aromatic benzene ring for the structure activity relationship of benzhydrol derivatives. It was found that fluorobenzhydrol **4b** and bromobenzhydrol **4c** had greater anti-TB efficacy than compound **4a** against all 20 MTB clinical isolates and MTB H37Rv reference strains with a MIC of 40  $\mu\text{g/ml}$ .

Secondly, we examined the significance of the hydroxy group at the  $\alpha$ -carbon for anti-TB activity by substituting the hydroxy group with a ketone group. It was found that ketone derivatives **3a** and **3b** were less active than their hydroxy derivatives **4a** and **4b**, respectively. Thus, the hydroxy group at the  $\alpha$ -carbon was essential for biological activity.

Thirdly, in our previous work, we synthesized 4-hydroxy- $\alpha$ -(3'-bromophenyl)benzyl alcohol, **14**, and examined its anti-tuberculosis (TB) activity for the *meta*-substitution of the electron-withdrawing bromo group with a MIC of 80  $\mu\text{g/ml}$  [92]. It showed lower anti-TB activity than compound **4c** with *para*-substituted bromine on B-ring (MIC of 40  $\mu\text{g/ml}$ ). As a result, the electronegativity effect of the bromine atom at *para* substitution on the B-ring could enhance the activities. In addition, the insertion of the acetamido group to either the *meta* or *para* position of the B-ring led to diminishing activity with MIC values  $>80$   $\mu\text{g/ml}$ .

Fourthly, we studied the effects of substitution of various functional groups on the B-ring on anti-TB activity. The compound with the highest activity was compound **4d**, which possessed an alkyl long chain substitution at *para*-position of B-ring with MIC value of 20-40  $\mu\text{g/ml}$ . Furthermore, compound **13c** containing *trans*-cinnamyl group at the *para*-position of ring B showed effective anti-TB activity with

a MIC of 40  $\mu\text{g/ml}$ . These results showed that phenyl substitution with an alkyl linker could enhance the activity. However, the presence of bulky groups (i.e., *p*-benzamide substitution, naphthalene) of compounds **13b** and **9** decreased anti-TB effectiveness. These may be the results of the steric hindrance of compounds to access the target site.

Finally, we examined the effect of acetylation on hydroxyl groups of benzhydrol derivatives. The result revealed that diacetylated derivatives **5c** and **5f** failed to inhibit MTB. The MIC values of dihydroxy benzhydrols **4a**, **4c**, and **4f** were 40-80  $\mu\text{g/ml}$ ; however, diacetylated analogue of **4a** (compound **5a**) showed better anti-TB activity than its dihydroxy compound, with a MIC value  $< 40$   $\mu\text{g/ml}$ . The result of acetoxy substitution was reported in previous presentation [104].

The effects of the structural modification of benzhydrol derivatives on anti-TB activity could be concluded to the structure-activity relationship (SAR) as follows.

1.  $\alpha$ -carbon anti-TB activity increased in the order of  $-\overset{\text{OH}}{\text{C}}- > -\overset{\text{OAc}}{\text{C}}- > -\overset{\text{O}}{\text{C}}-$ .
2. Substituting the hydroxyl group or leaving it unsubstituted (H atom) at the *para*-position of A-ring exhibited anti-TB activity.
3. The *para*-substitution of halide, such as fluoride or bromide atom at the B-ring, could improve anti-TB activity.
4. The *para*-substitution of bromide showed higher anti-TB activity than the *meta*-substitution.
5. The presence of acetamido groups ( $\text{NHCOCH}_3$ ) at the B-ring reduced the activity.
6. Enlarging with the bulky aromatic ring scaffold on the B-ring caused low activities.
7. Elongating the benzhydrol core structure attached to the alkyl or phenyl long chains at the *para*-position led to higher activities.

In this series, the *n*-butyl compound (**4d**) exhibited the highest anti-TB activity with a MIC of 20-40  $\mu\text{g/ml}$ . A long chain alkyl substituents of compound **4d** may have more appropriate physical properties than other moieties for accessing the target site. The butyl elongation chains with flexible conformation were added to the

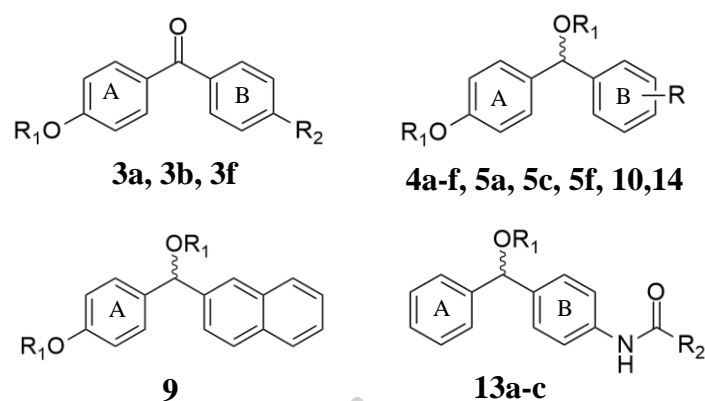
benzhydrol scaffold which might reach into the binding pocket with a high or long cavity. Furthermore, the similarity between the lipophilic nature of the alkyl long chain in molecule **4d** and the high fatty acid content (mycolic acid) of the cell wall of tuberculosis strains might hint at the target of action. Therefore, one promising mechanism of action for benzhydrol **4d** might be the inhibition of mycolic acid biosynthesis. Substrates of mycolic acid biosynthesis containing a large number of carbon units interact with an enzyme involved in the elongation of long-chain fatty acids with hydrophobic interaction.[105] The lipophilic nature of alkyl in the proposed compound **4d** might interact with the target in mycolic acid synthesis.

The chemical constituent of ACA from natural source responsible for antituberculosis activity is *S*-configuration i.e., 1'-*S*-1'-Acetoxychavicol acetate. According to the literature, MIC of synthetic ACA was higher than natural *S*-form of ACA on *M. tuberculosis* stains (63). Therefore, it can be postulated that the racemic form of synthetic 4-hydroxy- $\alpha$ -(4'-butylphenyl)benzyl alcohol (**4d**) contributed to lower antituberculosis activity and chirality may play an important role in the intermolecular interaction with binding sites of biological targets.

In order to develop a new candidate for an anti-Tb drug, the logarithm of the partition coefficient between n-octanol and water (cLog*P*) calculation and molecular weight (MW) were used in defining drug ability.[106] Candidate **4d** was a small molecule with an MW value of 256.34 and showed hydrophobic property with a cLog*P* value of 3.871. The cLog*P* values of **4d** and **13c** were higher than clog*P* values of other benzhydrols due to their greater hydrophobicity. In addition, ACA modification data [43] indicated that compounds of greater lipophilicity were much more likely to have high antituberculosis activity. However, since their cLog*P* values are more than three, it is concerned that aqueous solubility would be limited.

According to the results, it is concluded that compound **4d** showed the highest potential in the series to be a new lead for further structural modification in an attempt to improve the antituberculosis activity and drug-like properties.



**Table 7** *In vitro* antitubercular activities of synthesized compounds against MTB<sup>a</sup>

Cpds	R <sub>1</sub>	R <sub>2</sub>	MIC (µg/mL) <sup>a</sup>	MW	cLogP
3a	H	H	80	199.23	3.054
3b	H	F	80	217.22	3.272
3f	H	NH-CO-CH <sub>3</sub>	> 80	256.28	2.213
4a	H	4-H	40 - 80	200.23	1.785
4b	H	4-F	40	218.22	1.928
4c	H	4-Br	40	279.13	2.648
4d	H	4-C <sub>4</sub> H <sub>9</sub>	20 - 40	256.34	3.871
4e	H	3-NH-CO-CH <sub>3</sub>	> 80	257.28	0.804
4f	H	4-NH-CO-CH <sub>3</sub>	> 80	257.28	0.804
5a	-CO-CH <sub>3</sub>	H	< 40	284.31	2.657
5c	-CO-CH <sub>3</sub>	4-Br	Inactive	363.20	3.520
5f	-CO-CH <sub>3</sub>	4-NH-CO-CH <sub>3</sub>	> 80	341.36	1.676
9	H	-	80	250.29	2.959
10	H	4-NH <sub>2</sub>	-	215.25	0.558
13a	H	C <sub>3</sub> H <sub>7</sub>	80	240.28	2.529
13b	H	C <sub>6</sub> H <sub>6</sub>	80	303.35	2.960
13c	H	CH=CH-C <sub>6</sub> H <sub>6</sub>	40 - 80	329.39	3.974
14	H	3-Br	80	279.13	2.648
Kanamycin (control)			10	484.50	-3.88 <sup>b</sup>

<sup>a</sup> 20 MTB clinical isolates and MTB H37Rv reference strains (ATCC 27294).<sup>b</sup> Data is available on the website (<http://drugcentral.org>).

## CHAPTER 5 CONCLUSION

The structure-based design and synthesis of benzhydrol derivatives were developed and assessed for their *in vitro* antituberculosis activity. The various substituents, such as halide atoms, alkyl, aryl, acetamido, and amide derivatives, were connected to the B-ring of benzhydrol structure. Three main structural groups were designed for this series. First, designing 4-hydroxybenzhydrols (**4a-f**, **9**, **10**) contained the hydroxy group at ring A, focusing on varying substituents to explore the target binding site of *M. tuberculosis* inhibition mainly on the B-ring. The second group was benzhydrol diacetates (**5a**, **5c**, **5f**) designed to mimic ACA structure containing acetoxy groups. The last group, 4-amidobenzhydrols (**13a-c**), were generated from connecting benzhydrol to various alkyl, aryl, or cinnamyl groups that might interact on binding pockets of target sites.

The synthesis pathways to afford designed benzhydrol derivatives **4a-f**, **9** included three steps, the benzoic acid and substituted benzoic acid compounds were coupled with phenol by esterification reaction to form benzoate derivatives **2a-f** and **7** provided 78.9 to 96.7 percent yields. Next, the connection between two benzene rings by a ketone group to form benzophenone derivatives was performed via the Fries rearrangement reaction. The optimal temperatures for the synthesis of Fries rearrangement products with moderate to good yields (33.7 - 78.9 %) were 120 to 140 °C investigated by DSC analysis. The DSC data were effectively applied to estimate the optimal reaction temperatures to attain high percent yields for the Fries rearrangement reaction. The reduction step was achieved by sodium borohydride in methanol within one hour with high percent yields, 59.3% to 89.9%. The overall percent yields of benzhydrol derivatives **4a-f** and compound **9** were 20.3% to 56.6%. Compound **10** was obtained from amide hydrolysis of **4f** and provided low percent yields (6.57%). The synthesis of diacetyl products **5a**, **5c** and **5f** was completed by acetylation of the compound **4a**, **4c** and **4f** by EDC, DMAP and acetic anhydride with the overall yields of 18.8% to 39.2%. For the synthesis of acetamido products **13a-c**, 4-aminobenzophenone was coupled with various acids by amide bond linkage, followed by NaBH<sub>4</sub> reduction with overall percent yields of 24.3% to 57.5%. All the

structures of synthesized designed compounds were confirmed by FT-IR,  $^1\text{H}$  NMR, and  $^{13}\text{C}$  NMR methods and tested for antituberculosis activities.

According to MIC results, five compounds (**3a**, **3b**, **9**, **13a** and **13b**) had low activity against *M. tuberculosis* with MICs of 80  $\mu\text{g/ml}$ . Compounds **4a**, **4b**, **4c**, **5a**, and **13c** with MICs between 40 and 80  $\mu\text{g/ml}$  exhibited moderate activity. The highest efficacy of this series was compound **4d** with a MIC of 20-40  $\mu\text{g/ml}$ . The chemical structures of active benzhydrol derivatives of this series are shown in Figure 29. The structure-activity relationship study revealed that the most potent compound for anti-TB activity was compound **4d** with alkyl long chain substituent at the *para*-position, at which alkyl side chain was similar to the fatty acid content of cell walls of tuberculosis strains. At the *para* position of the B-ring, electron-withdrawing groups like fluorine and bromine could provide electron-withdrawing groups that might interact with complementary of binding sites. Halide derivatives showed moderate to good potential to inhibit mycobacterial growth. The active 11 compounds could imply that the benzhydrol derivatives offered promising new leads for further development. Significantly, compound **4d** exhibited the highest potential for further structural modification as a new antituberculosis agent.

For additional research on benzhydrol's antituberculosis activity, the expansion of the alkyl/aryl chain could influence the activity. As previously stated, ACA data showed high activity in *S*-form. The chirality effect at the  $\alpha$ -carbon of benzhydrol is an intriguing topic for further study. Upon chiral separation of the products, we expect that one of the enantiomers could achieve higher activity than their racemates. According to the activities of benzhydrol derivatives against 20 clinical MTB strains, it is possible to combat MDR-TB; however, future research suggests modifying the substituent's chemical structure at the *para*-position on the B-ring. In order to obtain information on how benzhydrol derivatives bind to their targets, target enzymes involved in mycolic acid biosynthesis should be further investigated. Once the target enzyme is known further design on modification of benzhydrol derivatives based on their binding affinities a target enzyme could be done.

Although, benzhydrol derivatives showed good activity against mycobacterial tuberculosis *in vitro*, inhibitory properties may not correlate with antimycobacterial *in*

*in vivo* results. Next step of study should include *in vivo* testing since *in vivo* studies are essential to drug development to provide the information on drug's properties, including in pharmacokinetic and pharmacodynamic processes of drug action.

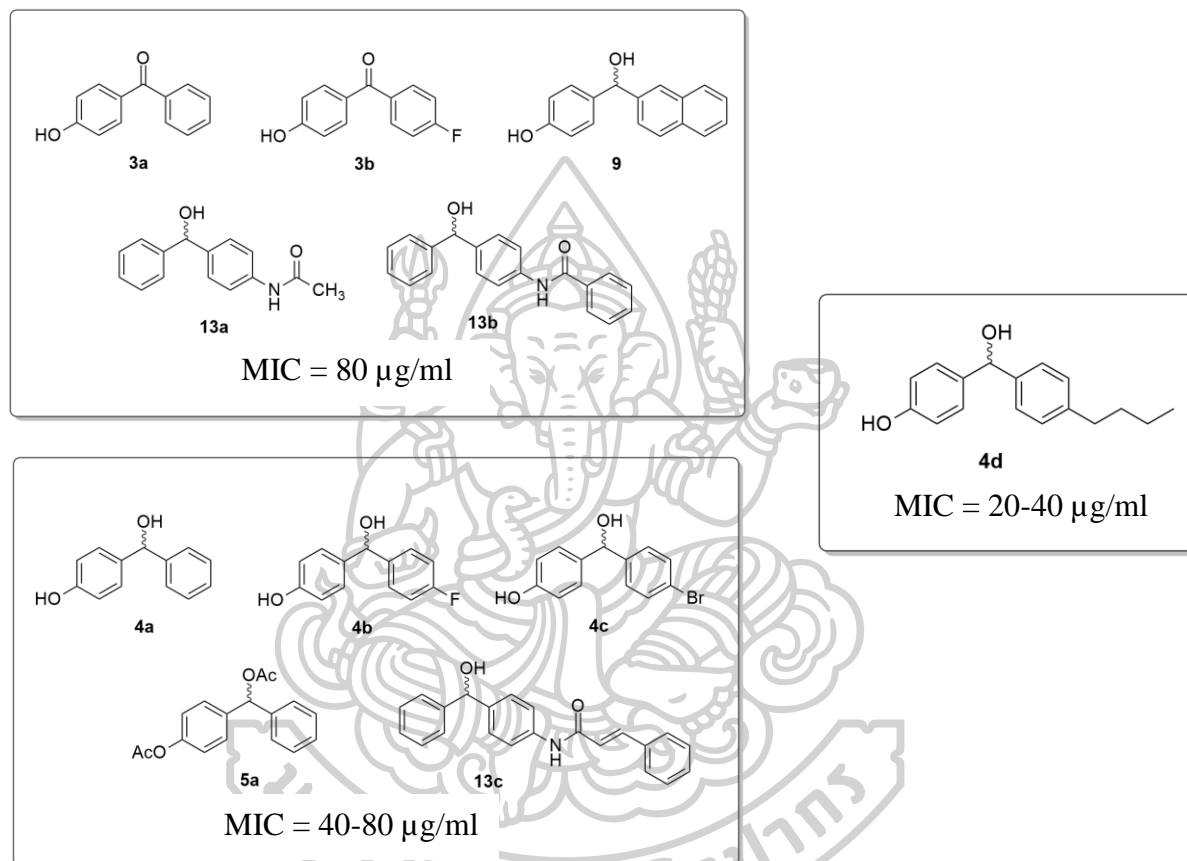


**Figure 29** The structure of active benzhydrol derivatives of this series

## REFERENCES

1. World Health Organization. *Global tuberculosis report 2021* [cited 2022 10 September 2022]; Available from: <https://www.who.int/publications/i/item/9789240037021>.
2. Palittapongarnpim, P., et al., *1'-Acetoxychavicol acetate for tuberculosis treatment*. 2002, National Science and Technology Development Agency, Klong 1, KlongLuang, Prathumthani (TH)
3. Misawa, T., et al., *Structural Development of Benzhydrol-Type 1 & prime;-Acetoxychavicol Acetate (ACA) Analogs as Human Leukemia Cell-Growth Inhibitors Based on Quantitative Structure & dash;Activity Relationship (QSAR) Analysis*. Chemical and Pharmaceutical Bulletin, 2008. **56**(10): p. 1490-1495.
4. Venugopala, K.N., et al., *Benzothiazole analogs as potential anti-TB agents: computational input and molecular dynamics*. Journal of Biomolecular Structure and Dynamics, 2019. **37**(7): p. 1830-1842.
5. Michio, K. and C.C. Dean, *MenA Is a Promising Drug Target for Developing Novel Lead Molecules to Combat Mycobacterium tuberculosis*. Medicinal Chemistry, 2009. **5**(2): p. 197-207.
6. Das, S.K., et al., *Design, synthesis and antitubercular activity of diarylmethylnaphthol derivatives*. Bioorganic & Medicinal Chemistry Letters, 2007. **17**(20): p. 5586-5589.
7. Seung, K.J., S. Keshayjee, and M.L. Rich, *Multidrug-Resistant Tuberculosis and Extensively Drug-Resistant Tuberculosis*. (2157-1422 (Electronic)).
8. Davies, P.D., *The role of DOTS in tuberculosis treatment and control*. (1175-6365 (Print)).
9. Zumla, A., et al., *Drug-Resistant Tuberculosis—Current Dilemmas, Unanswered Questions, Challenges, and Priority Needs*. The Journal of Infectious Diseases, 2012. **205**(suppl\_2): p. S228-S240.
10. Cox, E. and K. Laessig, *FDA Approval of Bedaquiline — The Benefit–Risk Balance for Drug-Resistant Tuberculosis*. New England Journal of Medicine, 2014. **371**(8): p. 689-691.
11. Xavier, A.S. and M. Lakshmanan, *Delamanid: A new armor in combating drug-resistant tuberculosis*. (0976-500X (Print)).
12. Kim, C.T., et al., *Bedaquiline and delamanid for the treatment of multidrug-resistant tuberculosis: a multicentre cohort study in Korea*. LID - 1702467 [pii] LID - 10.1183/13993003.02467-2017 [doi]. (1399-3003 (Electronic)).
13. Schaaf, H.S., et al., *Adverse effects of oral second-line antituberculosis drugs in children*. Expert Opinion on Drug Safety, 2016. **15**(10): p. 1369-1381.
14. Gupta, A., et al., *Adverse drug reactions & drug interactions in MDR-TB patients*. Indian Journal of Tuberculosis, 2020. **67**(4, Supplement): p. S69-S78.
15. Isralls, S., et al., *QT Interval Prolongation in People Treated With Bedaquiline for Drug-Resistant Tuberculosis Under Programmatic Conditions: A Retrospective Cohort Study*. Open Forum Infectious Diseases, 2021. **8**(8): p. ofab413.
16. Conradie, F., et al., *Treatment of Highly Drug-Resistant Pulmonary Tuberculosis*. (1533-4406 (Electronic)).
17. Fu, L.M. and C.S. Fu-Liu, *Is Mycobacterium tuberculosis a closer relative to*

- Gram-positive or Gram-negative bacterial pathogens?* Tuberculosis, 2002. **82**(2): p. 85-90.
18. Alderwick, L.J., et al., *The Mycobacterial Cell Wall--Peptidoglycan and Arabinogalactan*. (2157-1422 (Electronic)).
  19. Bhamidi, S., et al., *Detailed structural and quantitative analysis reveals the spatial organization of the cell walls of in vivo grown Mycobacterium leprae and in vitro grown Mycobacterium tuberculosis*. (1083-351X (Electronic)).
  20. Alderwick, L.J., et al., *Structure, function and biosynthesis of the Mycobacterium tuberculosis cell wall: arabinogalactan and lipoarabinomannan assembly with a view to discovering new drug targets*. (0300-5127 (Print)).
  21. Brennan, P.J., *Structure, function, and biogenesis of the cell wall of Mycobacterium tuberculosis*. (1472-9792 (Print)).
  22. Lambert, P.A., *Cellular impermeability and uptake of biocides and antibiotics in Gram-positive bacteria and mycobacteria*. (1364-5072 (Print)).
  23. Hartkoorn, R.C., et al., *Towards a new tuberculosis drug: pyridomycin - nature's isoniazid*. (1757-4684 (Electronic)).
  24. Mikušová, K. and S. Ekins, *Learning from the past for TB drug discovery in the future*. (1878-5832 (Electronic)).
  25. AlMatar, M., et al., *New drugs for the treatment of Mycobacterium tuberculosis infection*. (1950-6007 (Electronic)).
  26. Tiberi, S., et al., *The challenge of the new tuberculosis drugs*. La Presse Médicale, 2017. **46**(2, Part 2): p. e41-e51.
  27. Prasad, M.S., et al., *Mycobacterium enoyl acyl carrier protein reductase (InhA): A key target for antitubercular drug discovery*. Bioorganic Chemistry, 2021. **115**: p. 105242.
  28. Arbex, M.A., et al., *Antituberculosis drugs: drug interactions, adverse effects, and use in special situations. Part 1: first-line drugs*. Jornal brasileiro de pneumologia : publicacao oficial da Sociedade Brasileira de Pneumologia e Tisiologia, 2010. **36** **5**: p. 626-40.
  29. Lee, H.W., et al., *Pharmacokinetics of prothionamide in patients with multidrug-resistant tuberculosis*. (1815-7920 (Electronic)).
  30. Chen, C.H., et al., *Minimal inhibitory concentrations of rifabutin, ciprofloxacin, and ofloxacin against Mycobacterium tuberculosis isolated before treatment of patients in Taiwan*. (0003-0805 (Print)).
  31. Bemer-Melchior, P., H.B. Bryskier A Fau - Drugeon, and H.B. Drugeon, *Comparison of the in vitro activities of rifapentine and rifampicin against Mycobacterium tuberculosis complex*. (0305-7453 (Print)).
  32. Torrea, G., et al., *Bedaquiline susceptibility testing of Mycobacterium tuberculosis in an automated liquid culture system*. (1460-2091 (Electronic)).
  33. Kwon, Y.S., *Clinical Implications of New Drugs and Regimens for the Treatment of Drug-resistant Tuberculosis*. (2233-7385 (Print)).
  34. Ermertcan, S., et al., *In vitro activity of linezolid against Mycobacterium tuberculosis strains isoalted from Western Turkey*. (1344-6304 (Print)).
  35. Alahari, A., et al., *Thiacetazone, an antitubercular drug that inhibits cyclopropanation of cell wall mycolic acids in mycobacteria*. (1932-6203 (Electronic)).
  36. Ruiz, P., et al., *In Vitro Activity of Tedizolid against Mycobacterium*

- tuberculosis*. LID - 10.1128/AAC.01939-18 [doi] LID - e01939-18. (1098-6596 (Electronic)).
37. Zhu, T., et al., *Population pharmacokinetic/pharmacodynamic analysis of the bactericidal activities of sutezolid (PNU-100480) and its major metabolite against intracellular Mycobacterium tuberculosis in ex vivo whole-blood cultures of patients with pulmonary tuberculosis*. (1098-6596 (Electronic)).
  38. Protopopova, M., et al., *Identification of a new antitubercular drug candidate, SQ109, from a combinatorial library of 1,2-ethylenediamines*. (0305-7453 (Print)).
  39. Upton, A.M., et al., *In vitro and in vivo activities of the nitroimidazole TBA-354 against Mycobacterium tuberculosis*. (1098-6596 (Electronic)).
  40. Hanif, S.N., L. Hickey Aj Fau - Garcia-Contreras, and L. Garcia-Contreras, *Liquid chromatographic determination of CPZEN-45, a novel anti-tubercular drug, in biological samples*. (1873-264X (Electronic)).
  41. Lu, P., et al., *The anti-mycobacterial activity of the cytochrome bcc inhibitor Q203 can be enhanced by small-molecule inhibition of cytochrome bd*. Scientific Reports, 2018. **8**(1): p. 2625.
  42. Kumar, D., B. Negi, and D.S. Rawat, *The anti-tuberculosis agents under development and the challenges ahead*. (1756-8927 (Electronic)).
  43. Bunthitsakda, W., *The Study of Structure-activity Relationship of 1-Acetoxychavicol Acetate Analogs and Tendency Against Mycobacterium Tuberculosis*, in Department of Chemistry, Faculty of Science in and Technology, . 2010, Thammasat University.
  44. Phongpaichit, S., et al., *Evaluation of the antimycobacterial activity of extracts from plants used as self-medication by AIDS patients in Thailand*. Pharmaceutical Biology, 2006. **44**(1): p. 71-75.
  45. Roy, S.K., et al., *Phenylpropanoids of Alpinia galanga as efflux pump inhibitors in Mycobacterium smegmatis mc2 155*. Fitoterapia, 2012. **83**(7): p. 1248-1255.
  46. Yasuhara, T., et al., *Acetoxybenzhydrols as highly active and stable analogues of 1'S-1'-acetoxychavicol, a potent anti-allergic principal from Alpinia galanga*. Bioorganic & Medicinal Chemistry Letters, 2009. **19**(11): p. 2944-2946.
  47. Awang, K., et al., *The apoptotic effect of 1's-1'-acetoxychavicol acetate from Alpinia conchigera on human cancer cells*. Molecules (Basel, Switzerland), 2010. **15**(11): p. 8048-8059.
  48. Azuma, H., et al., *Lipase-catalyzed preparation of optically active 1'-acetoxychavicol acetates and their structure-activity relationships in apoptotic activity against human leukemia HL-60 cells*. Bioorganic & Medicinal Chemistry, 2006. **14**(6): p. 1811-1818.
  49. Xu, S., et al., *Comparison of glutathione reductase activity and the intracellular glutathione reducing effects of 13 derivatives of 1'-acetoxychavicol acetate in Ehrlich ascites tumor cells*. Chemico-Biological Interactions, 2010. **185**(3): p. 235-240.
  50. Xu, S., et al., *(1'S)-Acetoxychavicol acetate and its enantiomer inhibit tumor cells proliferation via different mechanisms*. Chemico-Biological Interactions, 2008. **172**(3): p. 216-223.
  51. Murakami, A., et al., *Structure-Activity Relationships of (1'S)-1'-Acetoxychavicol Acetate, a Major Constituent of a Southeast Asian Condiment*

- Plant Languas galanga, on the Inhibition of Tumor-Promoter-Induced Epstein–Barr Virus Activation.* Journal of Agricultural and Food Chemistry, 2000. **48**(5): p. 1518-1523.
52. Matsuda, H., et al., *Antiallergic principles from Alpinia galanga: structural requirements of phenylpropanoids for inhibition of degranulation and release of TNF- $\alpha$  and IL-4 in RBL-2H3 cells.* Bioorganic & Medicinal Chemistry Letters, 2003. **13**(19): p. 3197-3202.
  53. Latha, C., et al., *Antiplasmodic activity of 1'-acetoxychavicol acetate from Alpinia galanga against multi-drug resistant bacteria.* Journal of Ethnopharmacology, 2009. **123**(3): p. 522-525.
  54. Janssen, A.M. and J.J.C. Scheffer, *Acetoxychavicol Acetate, an Antifungal Component of Alpinia galanga.* Planta Med, 1985. **51**(6): p. 507-511.
  55. Matsuda, H., et al., *Gastroprotective effects of phenylpropanoids from the rhizomes of Alpinia galanga in rats: structural requirements and mode of action.* European Journal of Pharmacology, 2003. **471**(1): p. 59-67.
  56. Matsuda, H., et al., *Structure–activity relationships of 1'S-1'-acetoxychavicol acetate for inhibitory effect on NO production in lipopolysaccharide-activated mouse peritoneal macrophages.* Bioorganic & Medicinal Chemistry Letters, 2005. **15**(7): p. 1949-1953.
  57. Ando, S., et al., *1'S-1'-Acetoxychavicol acetate as a new type inhibitor of interferon- $\beta$  production in lipopolysaccharide-activated mouse peritoneal macrophages.* Bioorganic & Medicinal Chemistry, 2005. **13**(9): p. 3289-3294.
  58. Ye, Y. and B. Li, *1'S-1'-Acetoxychavicol acetate isolated from Alpinia galanga inhibits human immunodeficiency virus type 1 replication by blocking Rev transport.* Journal of General Virology, 2006. **87**(7): p. 2047-2053.
  59. Bunthitsakda, W. *The study of structure-activity relationship of 1'-acetoxylchavicol acetate analogs and tendency against mycobacterium tuberculosis (MTB).* in *1<sup>st</sup> Current Drug Development International Conference 2010.* Phuket, Thailand.
  60. Warit, S., et al., *In Vitro Activities of Enantiopure and Racemic 1'-Acetoxychavicol Acetate against Clinical Isolates of Mycobacterium tuberculosis.* Scientia Pharmaceutica, 2017. **85**(3): p. 32.
  61. Kubota, K., et al., *Occurrence and antioxidative activity of 1'-acetoxychavicol acetate and its related compounds in the rhizomes of Alpinia Galanga during cooking,* in *Food Flavors and Chemistry: Advances of the New Millennium,* A.M. Spanier, et al., Editors. 2001, The Royal Society of Chemistry. p. 601-608.
  62. Kwon, E.M., et al., *Preparation of benzoyloxy benzophenone derivatives and their inhibitory effects of ICAM-1 expression.* Bull. Korean Chem. Soc., 2012. **33**(6): p. 1939-1944.
  63. Dewar, M.J.S. and J. Michl, *Synthesis and 19F NMR spectra of fluoroanthracenes, fluoroacenaphthylenes, and fluorofluoranthenes, and a practical synthesis of 7-substituted fluoranthenes.* Tetrahedron, 1970. **26**(2): p. 375-384.
  64. Yerande, S., et al., *ChemInform Abstract: Fries Rearrangement: Scalable Synthesis of Key Fluoro Building Blocks 3-Fluoro-4-methoxybenzoyl Chloride (IV) and 1,2-Diethoxy-3-fluorobenzene (V).* Tetrahedron Letters, 2014. **55**: p. 2426–2429.



65. Liu, T., et al., *Influence of coordinating groups of organotin compounds on the Fries rearrangement of diphenyl carbonate*. RSC Advances, 2019. **9**(48): p. 28112-28118.
66. Skoog, D.A., F.J. Holler, and S.R. Crouch, *Principles of Instrumental Analysis*, ed. 6th. 1985, Canada: David Harris.
67. Nikolaev, E.V., et al., *Investigation of interactions in the mechanically activated  $\alpha$ -Fe<sub>2</sub>O<sub>3</sub>/Li<sub>2</sub>CO<sub>3</sub> reagents by thermal analysis*. Journal of Thermal Analysis and Calorimetry, 2022.
68. Wang, Y., et al., *Torrefaction at 200 °C of Pubescens Pretreated with AlCl<sub>3</sub>(3) Aqueous Solution at Room Temperature*. (2470-1343 (Electronic)).
69. Ulkowski, M., M. Musialik, and G. Litwinienko, *Use of Differential Scanning Calorimetry To Study Lipid Oxidation. 1. Oxidative Stability of Lecithin and Linolenic Acid*. Journal of Agricultural and Food Chemistry, 2005. **53**(23): p. 9073-9077.
70. Sopade, P.A., P.J. Halley, and L.L. Junming, *Gelatinisation of starch in mixtures of sugars. II. Application of differential scanning calorimetry*. Carbohydrate Polymers, 2004. **58**(3): p. 311-321.
71. Madhav, H., N. Singh, and G. Jaiswar, *Chapter 4 - Thermoset, bioactive, metal-polymer composites for medical applications*, in *Materials for Biomedical Engineering*, V. Grumezescu and A.M. Grumezescu, Editors. 2019, Elsevier. p. 105-143.
72. Gill, P. and A. Ghaemi, *Nucleic Acid Isothermal Amplification Technologies—A Review*. Nucleosides, Nucleotides & Nucleic Acids, 2008. **27**(3): p. 224-243.
73. Peniche-Covas, C., W. Argüelles-Monal, and J. San Román, *A kinetic study of the thermal degradation of chitosan and a mercaptan derivative of chitosan*. Polymer Degradation and Stability, 1993. **39**(1): p. 21-28.
74. Xie, Y., X. Liu, and Q. Chen, *Synthesis and characterization of water-soluble chitosan derivate and its antibacterial activity*. Carbohydrate Polymers, 2007. **69**(1): p. 142-147.
75. Kayser, M.M., S. Eliev, and O. Eisenstein, *Reduction of ketones by sodium borohydride in the absence of protic solvents. Inter versus intramolecular mechanism*. Tetrahedron Letters, 1983. **24**(10): p. 1015-1018.
76. Prati, F., et al., *Screening of a Novel Fragment Library with Functional Complexity against Mycobacterium tuberculosis InhA*. ChemMedChem, 2018. **13**(7): p. 672-677.
77. Soutter, H.H., et al., *Discovery of cofactor-specific, bactericidal Mycobacterium tuberculosis InhA inhibitors using DNA-encoded library technology*. Proceedings of the National Academy of Sciences, 2016. **113**(49): p. E7880-E7889.
78. Sabbah, M., et al., *Fragment-Based Design of Mycobacterium tuberculosis InhA Inhibitors*. Journal of Medicinal Chemistry, 2020. **63**(9): p. 4749-4761.
79. Jun Cheng, Y.-y.X.I.A.E.-y.L.I.U.L.Z., *Thinking on the disposal of tuberculosis outbreak in schools*. Chinese Journal of Antituberculosis, 2018. **40**(2): p. 145-148.
80. Warbasse, J.P., *I. Cinnamic Acid in the Treatment of Tuberculosis*. (0003-4932 (Print)).
81. Rastogi, N., et al., *Synergistic activities of antituberculous drugs with cerulenin*

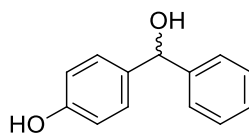
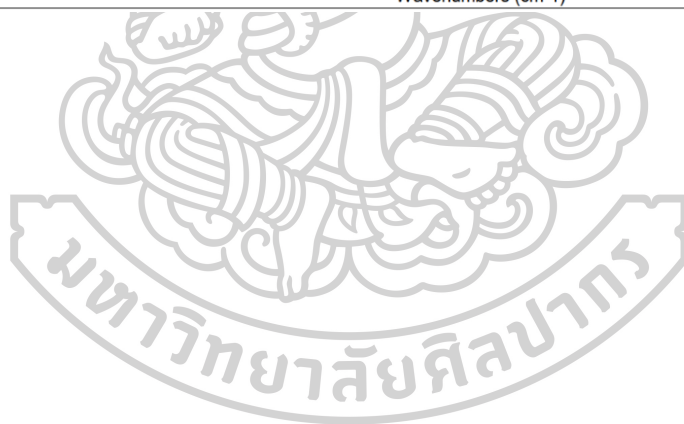
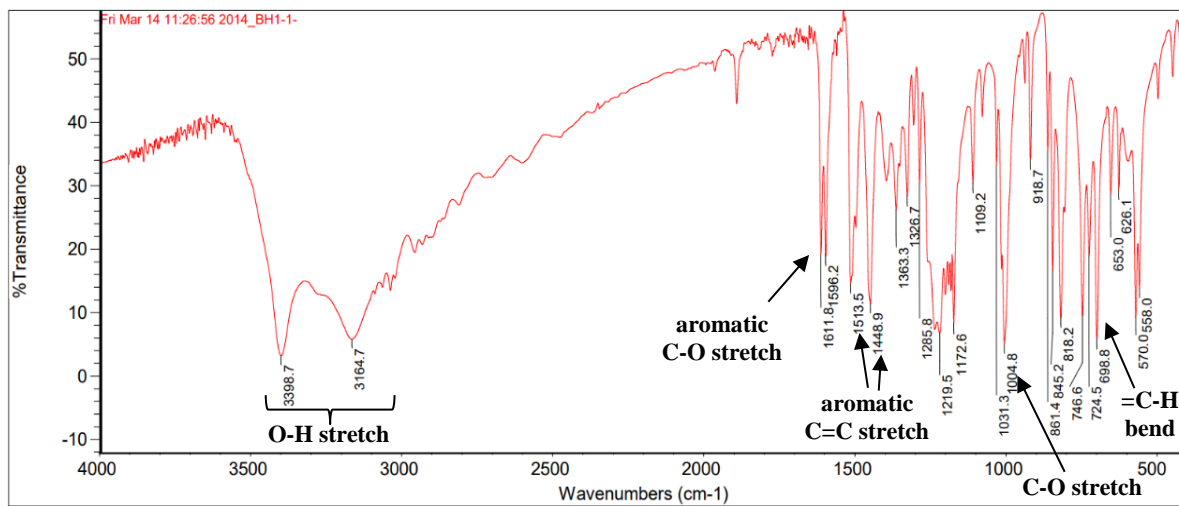
- and trans-cinnamic acid against Mycobacterium tuberculosis*. FEMS Immunology & Medical Microbiology, 1998. **21**(2): p. 149-157.
82. Carvalho, S.A., et al., *Synthesis and antimycobacterial evaluation of new trans-cinnamic acid hydrazide derivatives*. Bioorganic & Medicinal Chemistry Letters, 2008. **18**(2): p. 538-541.
83. Bairwa, R., et al., *Novel molecular hybrids of cinnamic acids and guanylhydrazones as potential antitubercular agents*. (1464-3405 (Electronic)).
84. Hett, E.C. and E.J. Rubin, *Bacterial growth and cell division: a mycobacterial perspective*. (1098-5557 (Electronic)).
85. Stec, J., et al., *Biological evaluation of potent triclosan-derived inhibitors of the enoyl-acyl carrier protein reductase InhA in drug-sensitive and drug-resistant strains of Mycobacterium tuberculosis*. (1860-7187 (Electronic)).
86. Tsakos, M., et al., *Ester coupling reactions – an enduring challenge in the chemical synthesis of bioactive natural products*. Natural Product Reports, 2015. **32**(4): p. 605-632.
87. Neises, B. and W. Steglich, *Simple Method for the Esterification of Carboxylic Acids*. Angewandte Chemie International Edition in English, 1978. **17**(7): p. 522-524.
88. Choukeb, P.B. and V.N. Ingle, *Synthesis and characterization of o-hydroxyarylalkylketones by using eco-friendly solvent free catalyst in fries rearrangement*. Der Pharma Chemica, 2012. **4**(1): p. 377-382.
89. Johnson, M.R. and B. Rickborn, *Sodium borohydride reduction of conjugated aldehydes and ketones*. The Journal of Organic Chemistry, 1970. **35**(4): p. 1041-1045.
90. Sirgel, F.A., I.J.F. Wiid, and P.D. van Helden, *Measuring Minimum Inhibitory Concentrations in Mycobacteria*, in *Mycobacteria Protocols: Second Edition*, T. Parish and A.C. Brown, Editors. 2009, Humana Press: Totowa, NJ. p. 173-186.
91. DeTar, D.F. and R. Silverstein, *Reactions of Carbodiimides. I. The Mechanisms of the Reactions of Acetic Acid with Dicyclohexylcarbodiimide 1,2*. Journal of the American Chemical Society, 1966. **88**(5): p. 1013-1019.
92. Kanjanapruk, P., S. Niratisai, and K. Pochanakom. *Synthesis of bromobenzhydrol derivatives as novel antituberculosis agents*. . in *The 3rd Current Drug Development International Conference*. 2014. Ao Nang Beach, Krabi, Thailand.
93. Gill, P., B. Moghadam Tt Fau - Ranjbar, and B. Ranjbar, *Differential scanning calorimetry techniques: applications in biology and nanoscience*. (1943-4731 (Electronic)).
94. Dreisch, S., et al., *Thermal stability of amine compounds and dichloromethane*. Chemical Engineering Transactions, 2016. **48**: p. 763-768.
95. Mossety-Leszczak, B., et al., *Analysis of curing reaction of liquid-crystalline epoxy compositions by using temperature-modulated DSC TOPEM®*. Journal of Thermal Analysis and Calorimetry, 2019. **138**(4): p. 2435-2444.
96. Safdari, A., et al., *Corrosion resistance evaluation of self-healing epoxy coating based on dual-component capsules containing resin and curing agent*. International Journal of Polymer Science, 2021. **2021**.
97. Kanjanapruk, P., et al., *Synthesis of Benzhydrol Derivatives as Antituberculosis Agents via Fries Rearrangement Method Investigated by DSC Analysis*. Key

- Engineering Materials, 2022. **914**: p. 141-146.
98. Sainsbury, M., *Aromatic chemistry (Oxford Chemistry Primers)*. 1992, North Carolina: Oxford University Press.
  99. Balkus, K.J., A.K. Khanmamedova, and R. Woo, *Fries rearrangement of acetanilide over zeolite catalysts* *Dedicated to Professor Herman van Bekkum on the occasion of his 65th birthday.1*. *Journal of Molecular Catalysis A: Chemical*, 1998. **134**(1): p. 137-143.
  100. Shihabaldain, N., *Fries rearrangement of 3,5-dimethoxyphenyl acetate*. 2012. **38**.
  101. Nayanapalli, P. and S. Tamraparni, *Pharmaceutical Organic Chemistry-Iii*. As Per PCI Regulations Second Year B Pharm Semester Iv. 2019: Educreation Publishing.
  102. East, A.L., *On the hydrolysis mechanisms of amides and peptides*. *International Journal of Chemical Kinetics*, 2018. **50**(10): p. 705-709.
  103. *Esterification: Methods, Reactions and Applications* By J. Otera. Wiley VCH: Weinheim. 2003. 303 pp. £100. ISBN 3-527-30490-8. *Organic Process Research & Development*, 2004. **8**(5): p. 814-814.
  104. Kanjanapruk, P., et al. *Synthesis of Benzhydrol and Its Acetamido Analogues as Antituberculosis Agents*. in *The 4th Current Drug Development International Conference*. 2016. Phuket, Thailand.
  105. Takayama, K., G.S. Wang C Fau - Besra, and G.S. Besra, *Pathway to synthesis and processing of mycolic acids in Mycobacterium tuberculosis*. (0893-8512 (Print)).
  106. Doak, Bradley C., et al., *Oral Druggable Space beyond the Rule of 5: Insights from Drugs and Clinical Candidates*. *Chemistry & Biology*, 2014. **21**(9): p. 1115-1142.

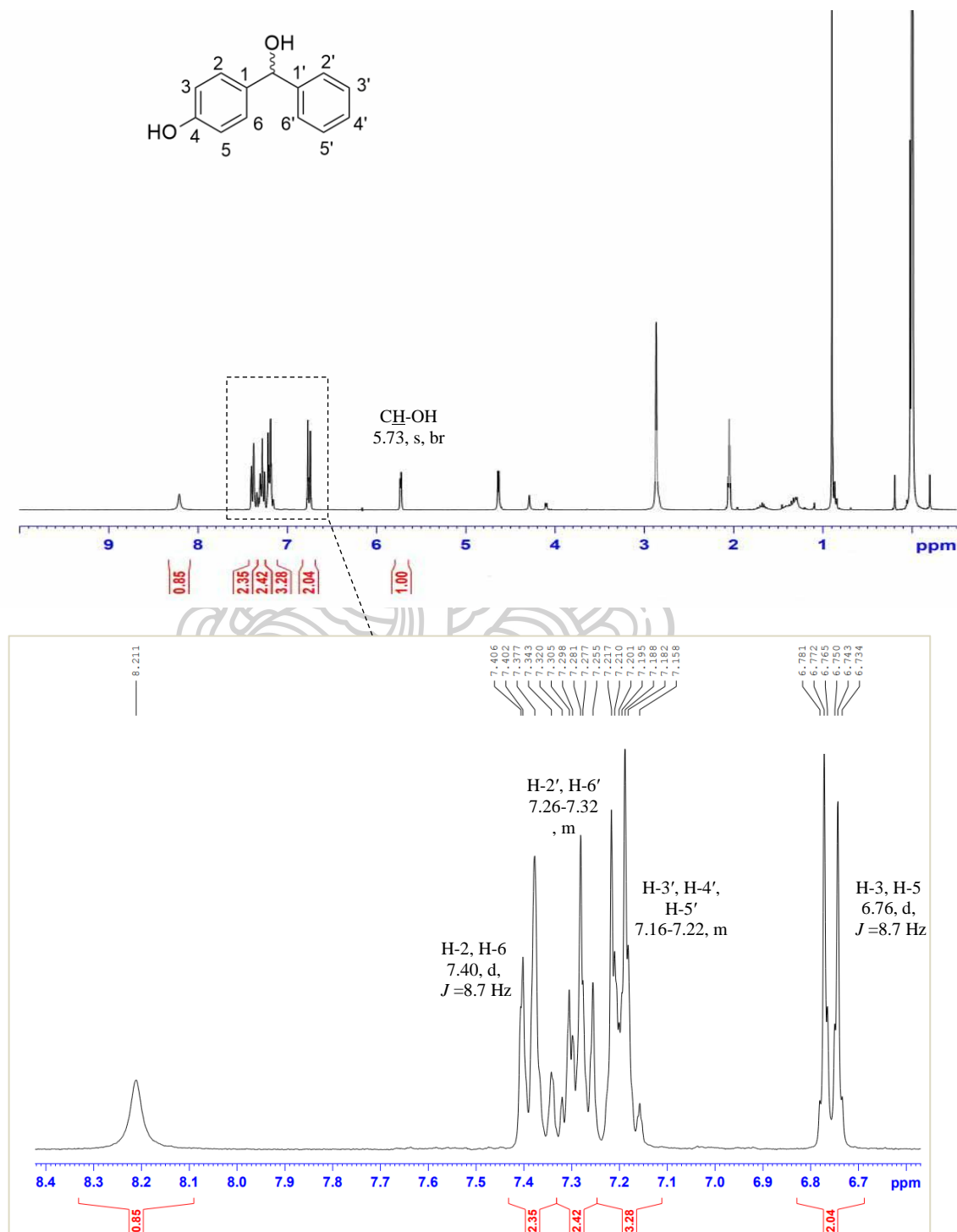


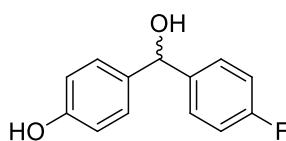
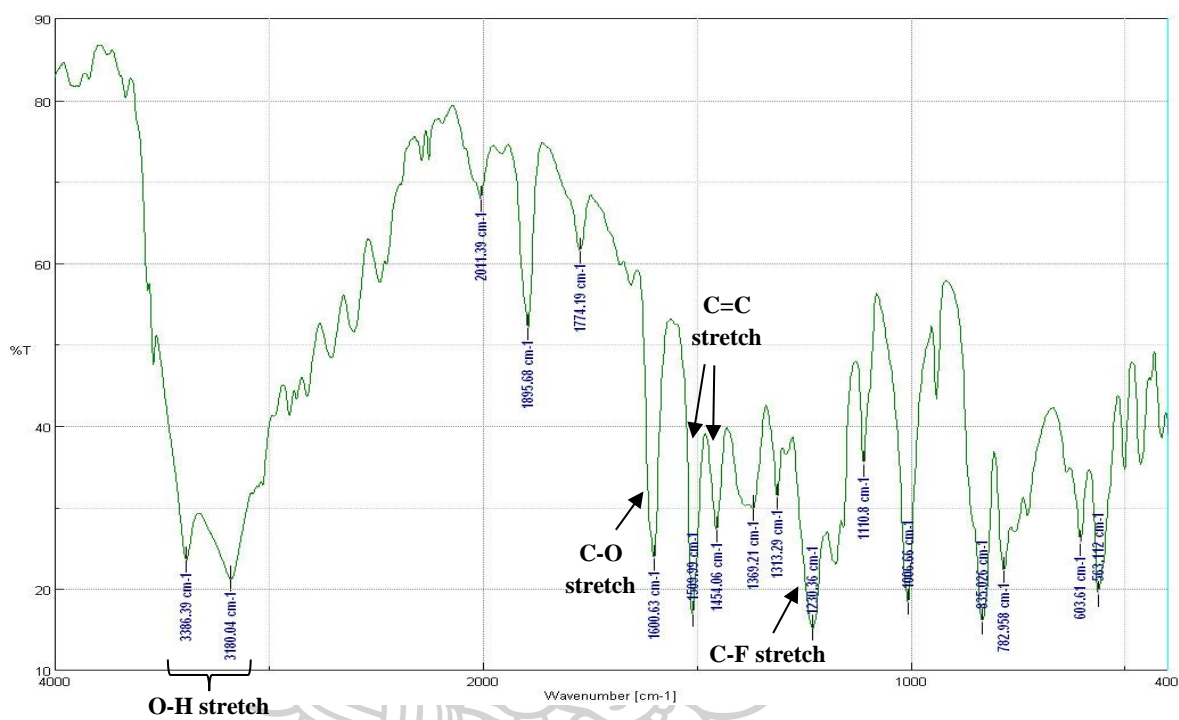
**APPENDIX**



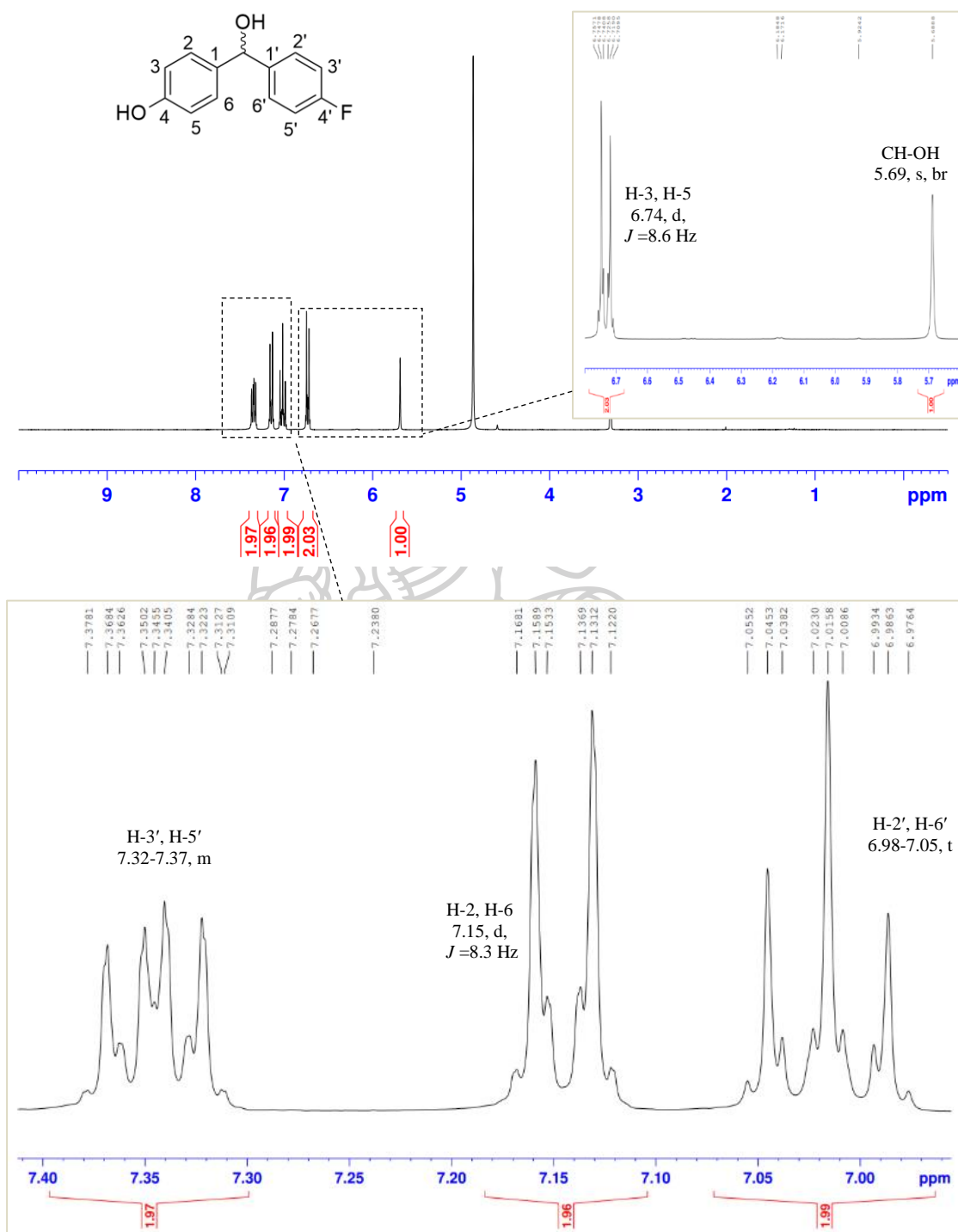
**4-hydroxy- $\alpha$ -(phenyl)benzyl alcohol (4a)****IR spectrum**

**<sup>1</sup>H NMR spectrum (300 MHz, CDCl<sub>3</sub>) of 4-hydroxy- $\alpha$ -(phenyl)benzyl alcohol (4a)**



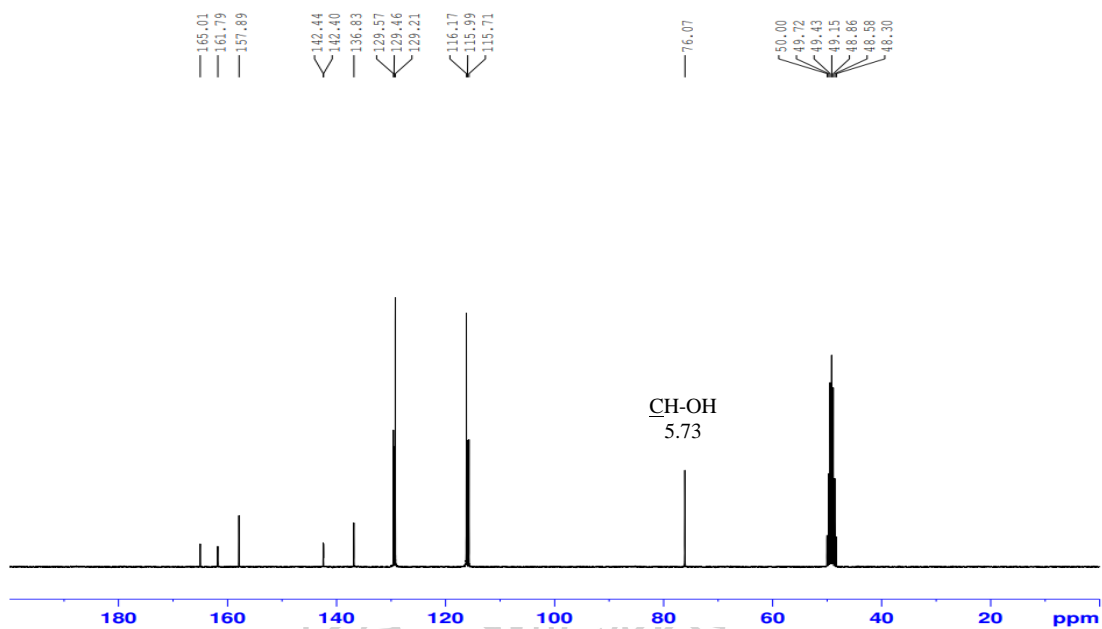
**4-hydroxy- $\alpha$ -(4'-fluorophenyl)benzyl alcohol (4b)****IR spectrum**

**$^1\text{H}$  NMR spectrum (300 MHz,  $\text{CD}_3\text{OD}$ ) of 4-hydroxy- $\alpha$ -(4'-fluorophenyl)benzyl alcohol (4b)**

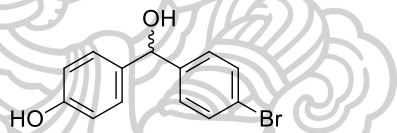




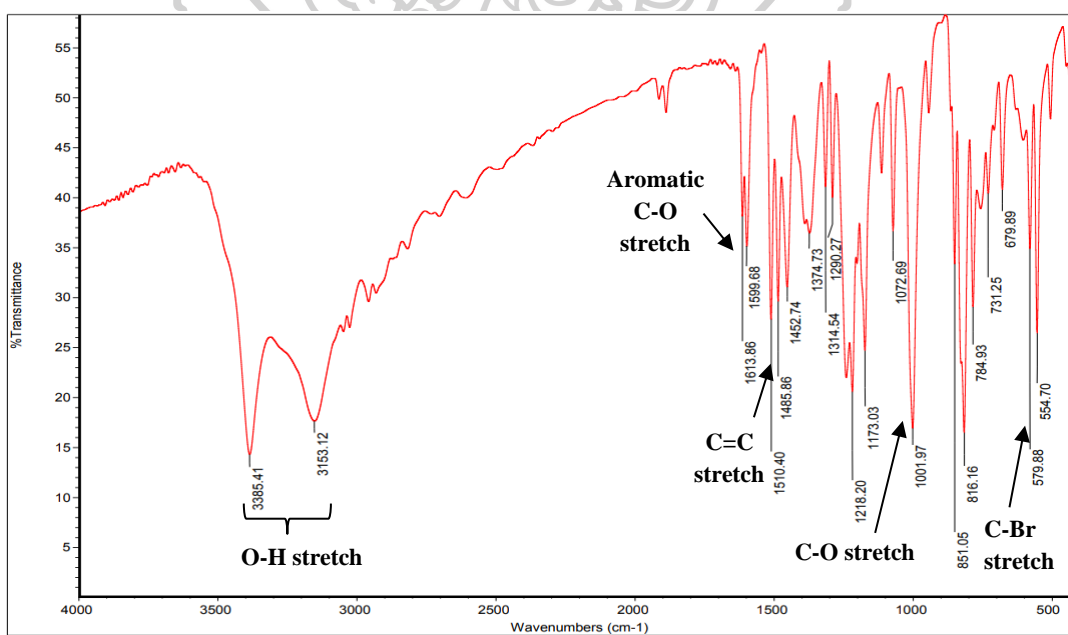
**$^{13}\text{C}$  NMR spectrum (75 MHz,  $\text{CD}_3\text{OD}$ ) of 4-hydroxy- $\alpha$ -(4'-fluorophenyl)benzyl alcohol (4b)**



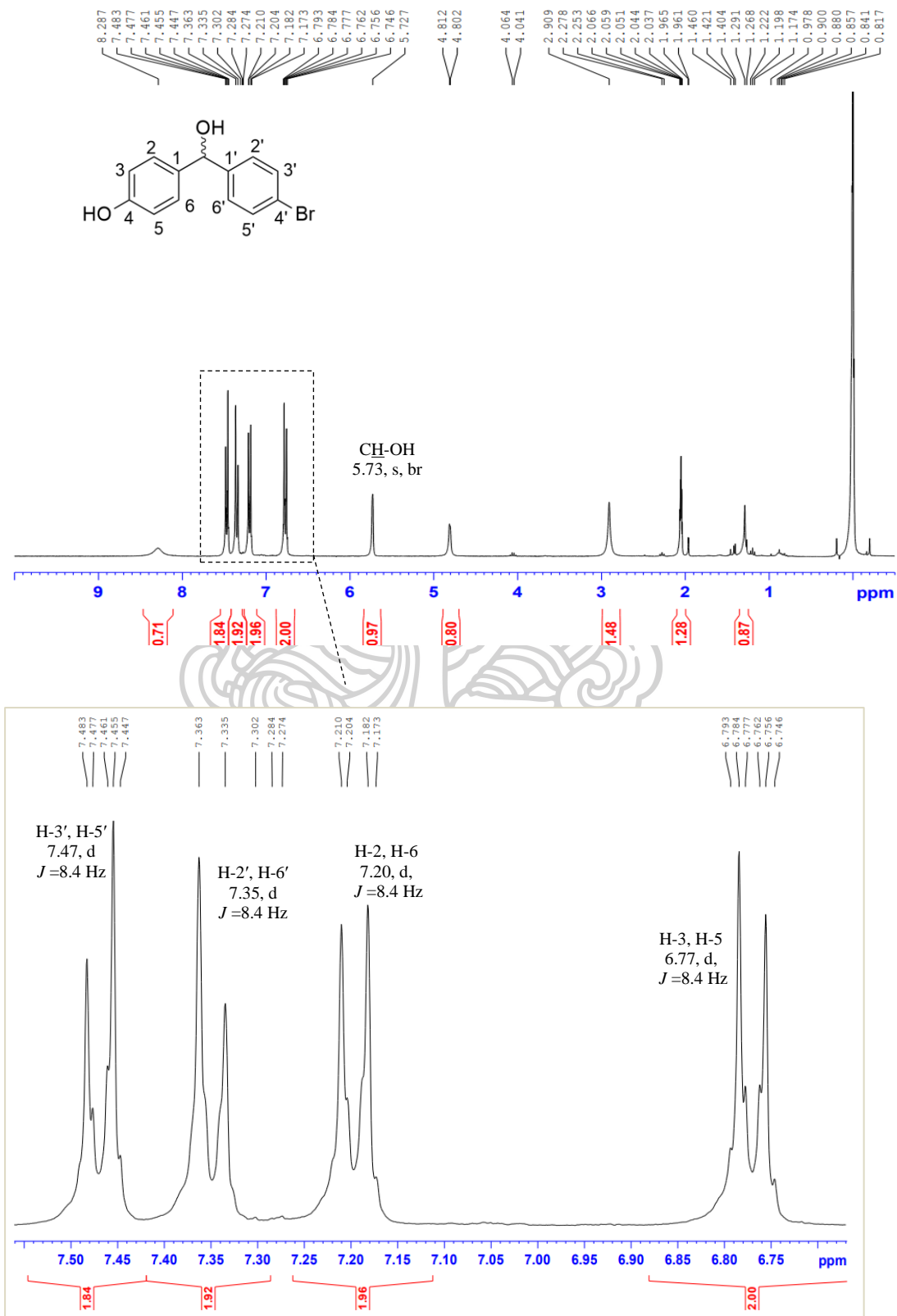
**4-hydroxy- $\alpha$ -(4'-bromophenyl)benzyl alcohol (4c)**

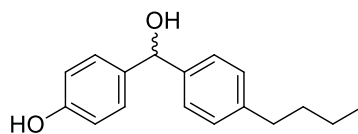
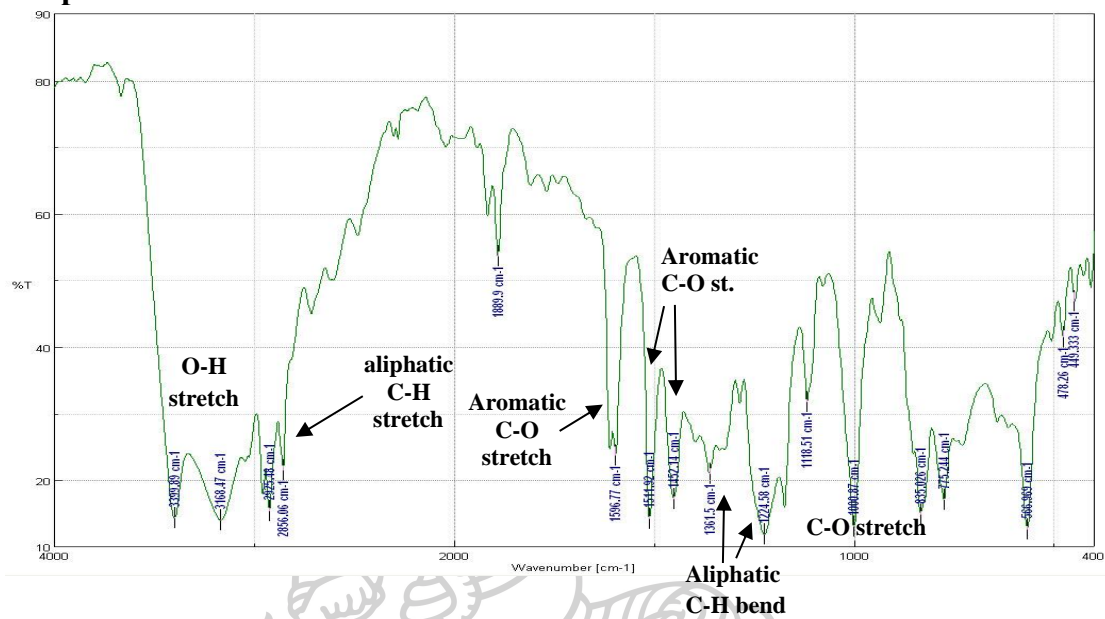


**IR spectrum**

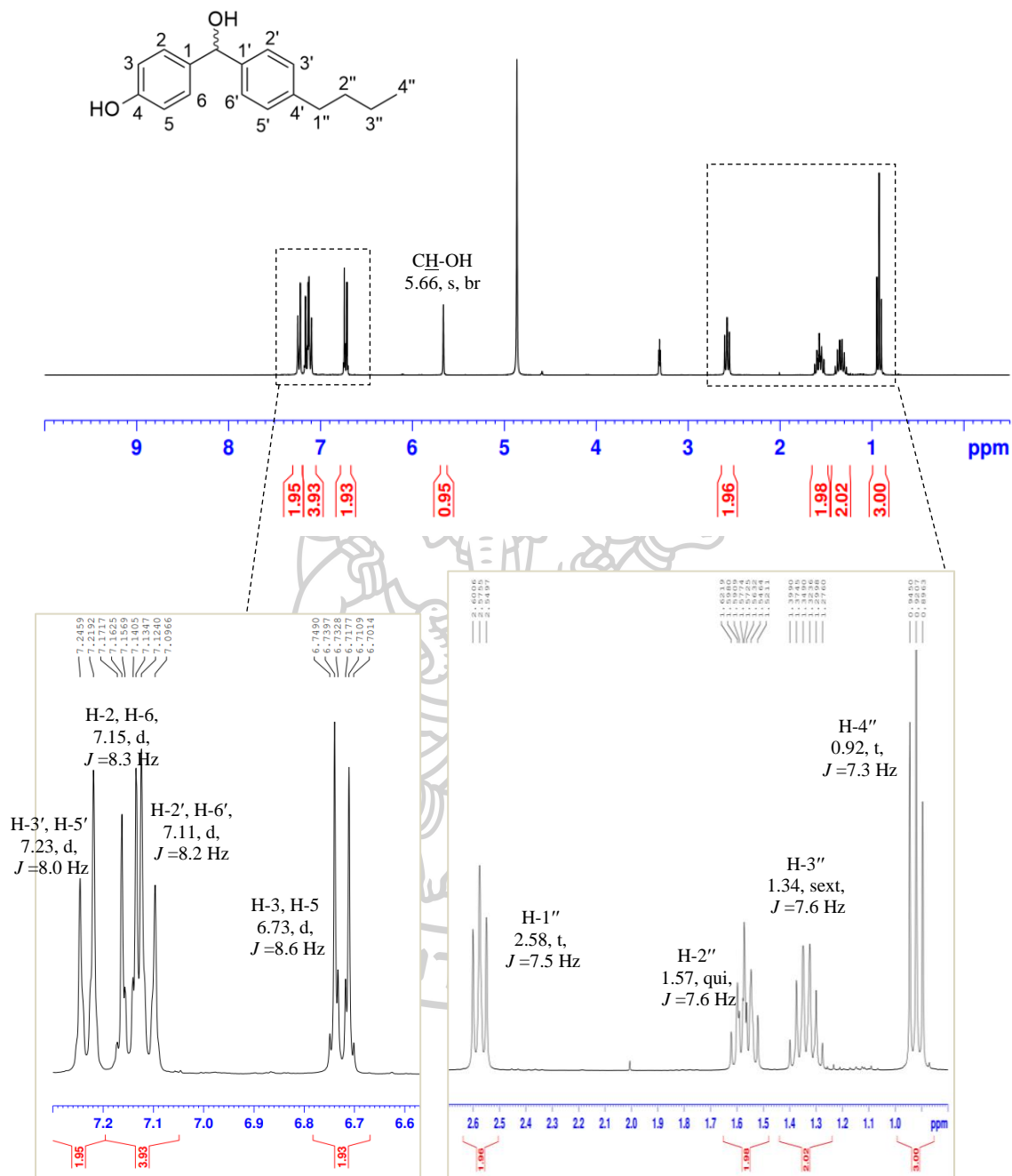


**$^1\text{H}$  NMR spectrum (300 MHz,  $\text{CD}_3\text{COCD}_3$ ) of 4-hydroxy- $\alpha$ -(4'-bromophenyl)benzyl alcohol (4c)**

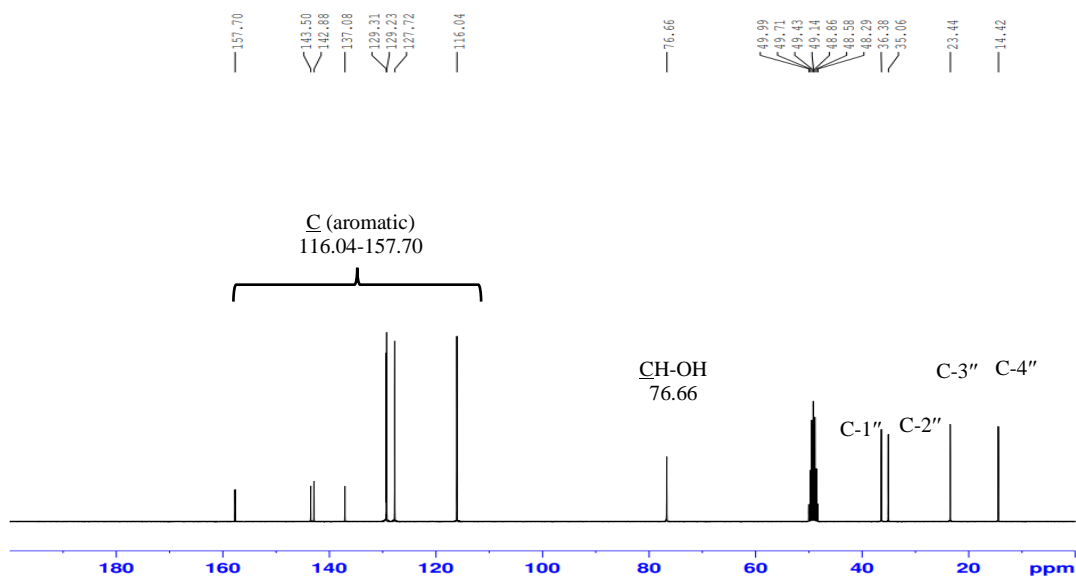


**4-hydroxy- $\alpha$ -(4'-butylphenyl)benzyl alcohol (4d)****IR spectrum**

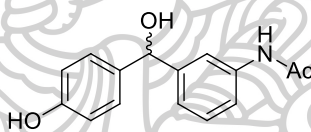
**<sup>1</sup>H NMR spectrum (300 MHz, CD<sub>3</sub>OD) of 4-hydroxy- $\alpha$ -(4'-butylphenyl)benzyl alcohol (4d)**



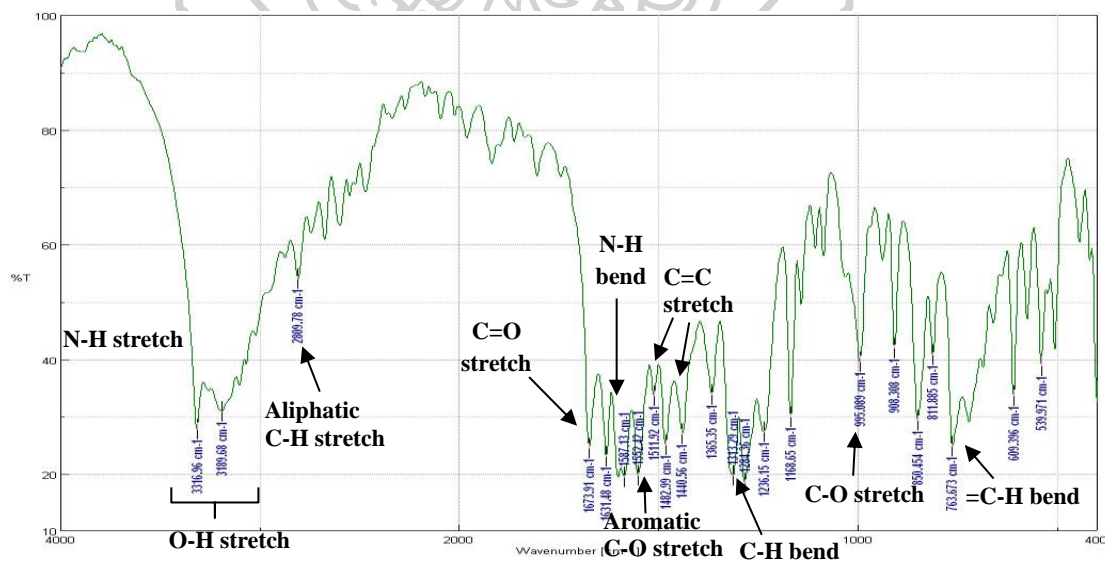
**$^{13}\text{C}$  NMR spectrum (75 MHz,  $\text{CD}_3\text{OD}$ ) of 4-hydroxy- $\alpha$ -(4'-butylphenyl)benzyl alcohol (4d)**



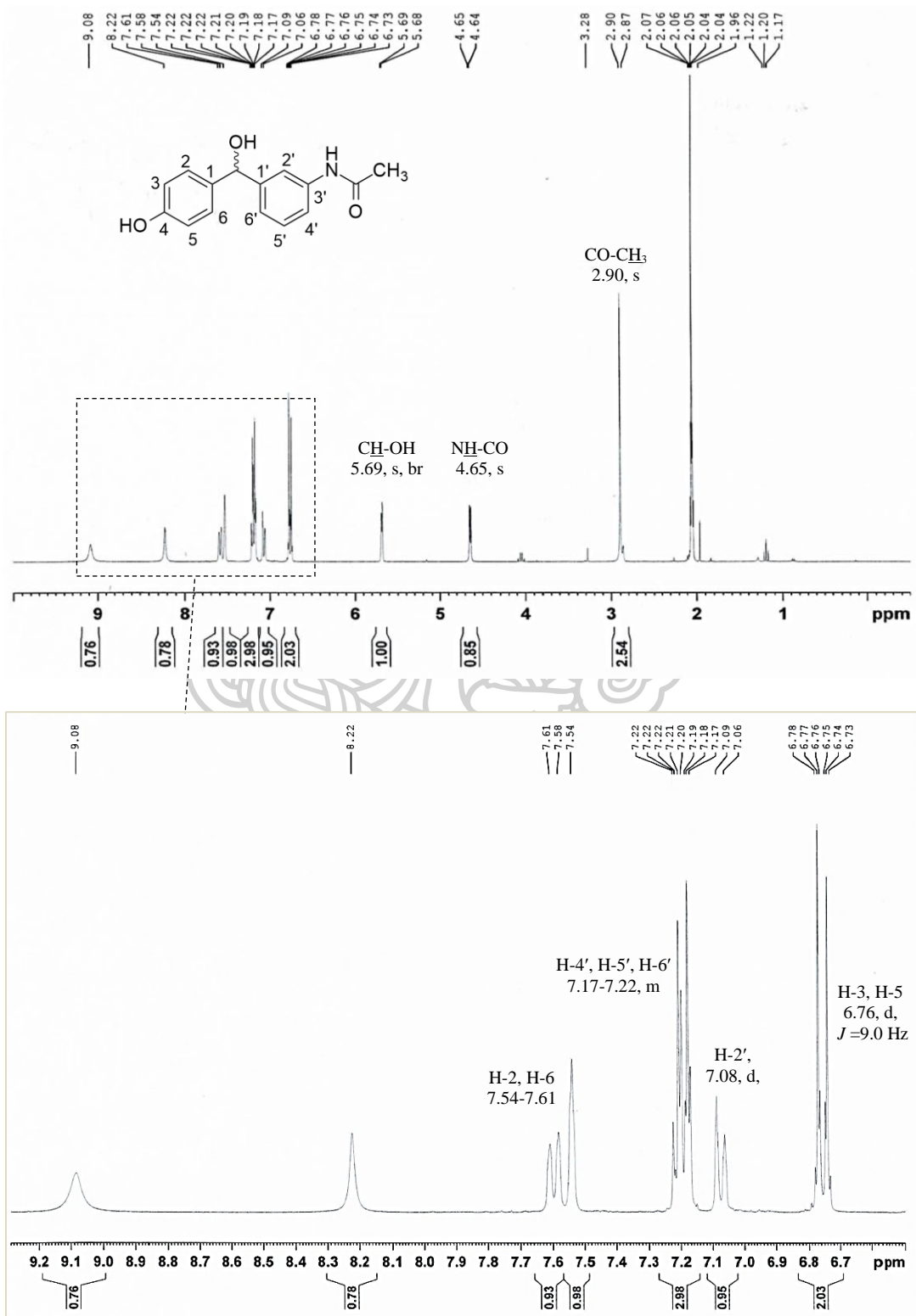
**4-hydroxy- $\alpha$ -(3'-acetamidophenyl)benzyl alcohol (4e)**



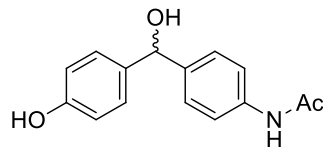
**IR spectrum**



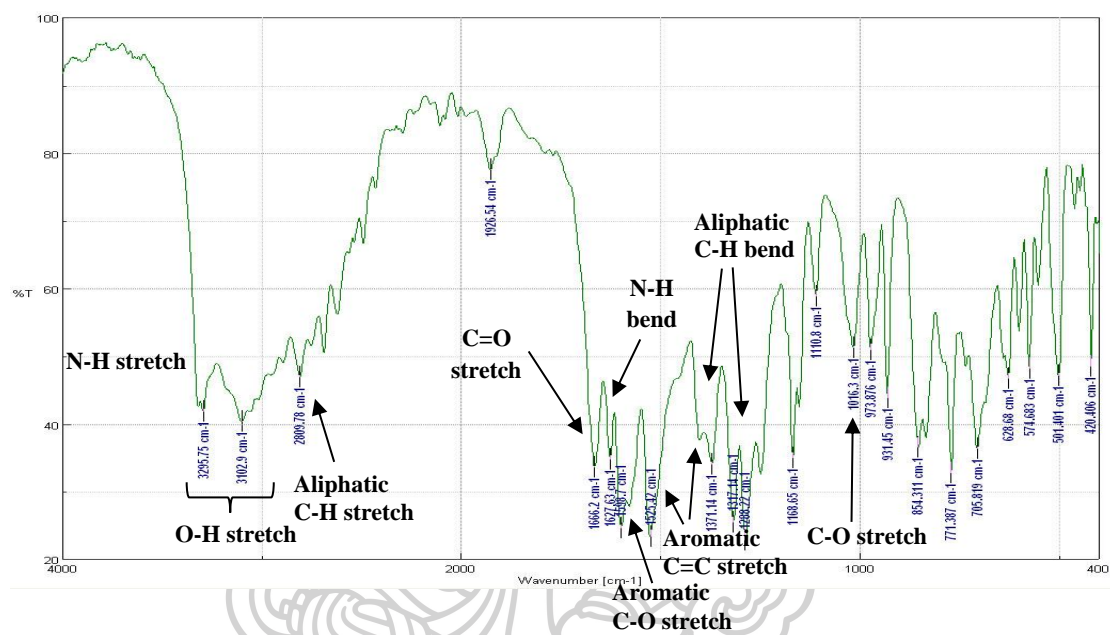
**<sup>1</sup>H NMR spectrum (300 MHz, CD<sub>3</sub>COCD<sub>3</sub>) of 4-hydroxy- $\alpha$ -(3'-acetamidophenyl)benzyl alcohol (4e)**



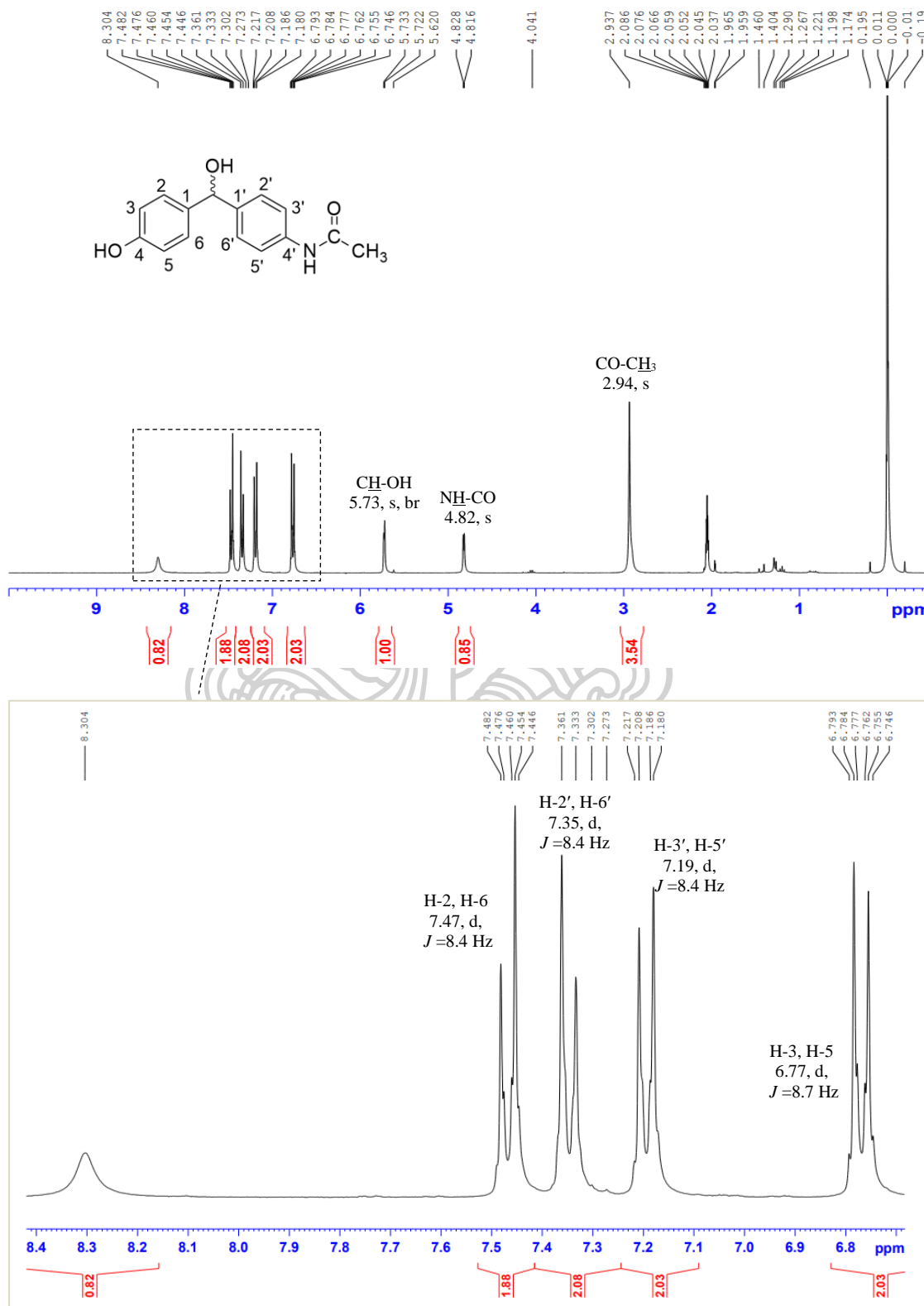
### 4-hydroxy- $\alpha$ -(4'-acetamidophenyl)benzyl alcohol (4f)



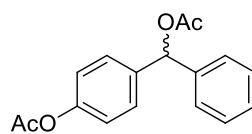
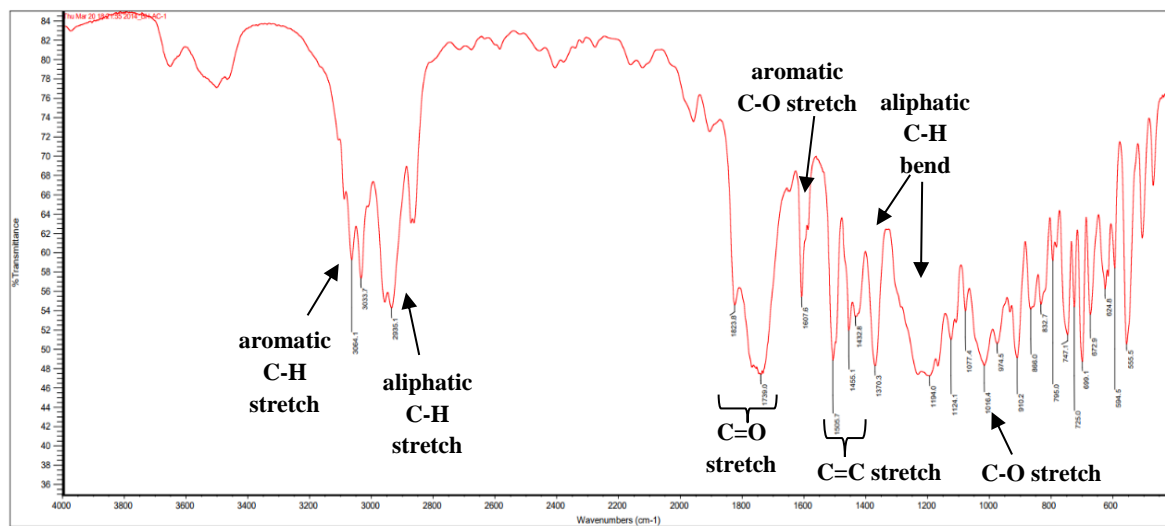
### IR spectrum

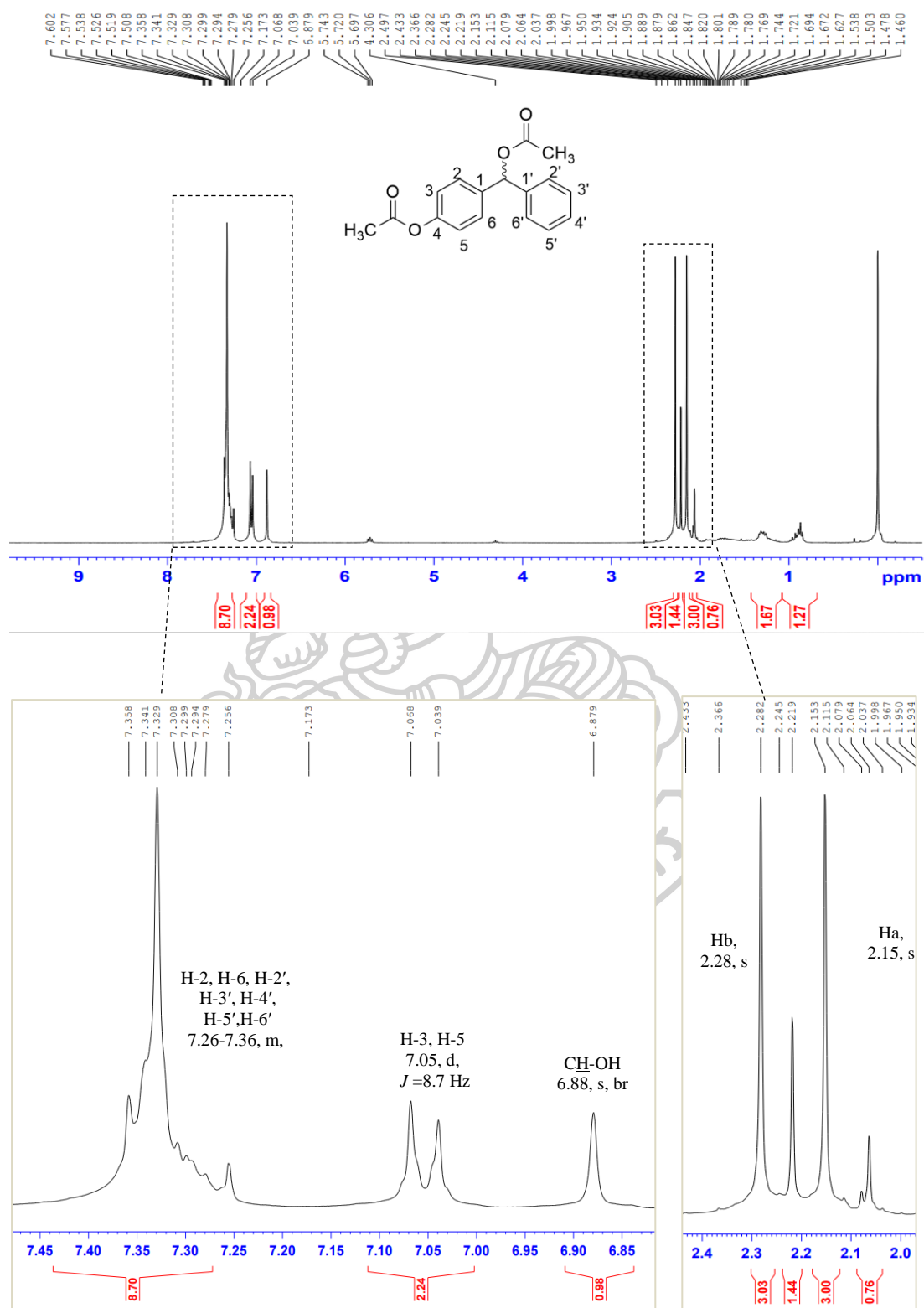


**$^1\text{H}$  NMR spectrum (300 MHz,  $\text{CD}_3\text{COCD}_3$ ) of 4-hydroxy- $\alpha$ -(4'-acetamidophenyl)benzyl alcohol (4f)**

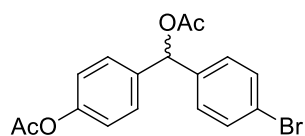




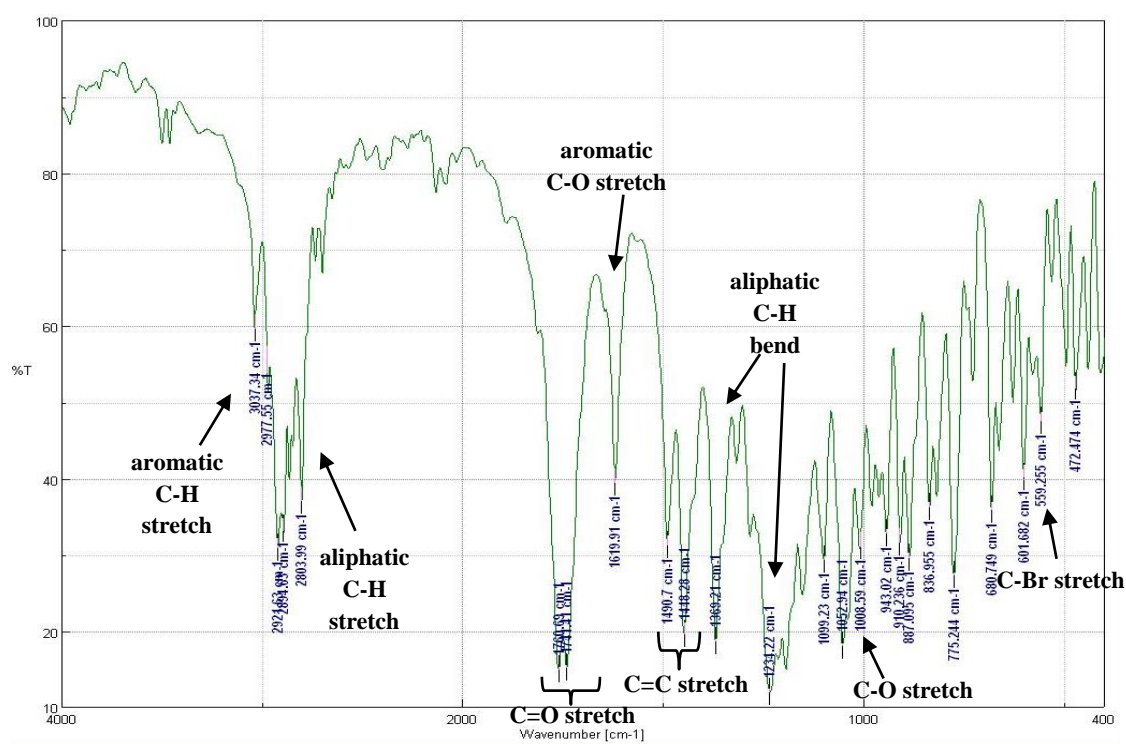
**4-acetoxy- $\alpha$ -(phenyl)benzyl acetate (5a)****IR spectrum**

**<sup>1</sup>H NMR spectrum (300 MHz, CDCl<sub>3</sub>) of 4-acetoxy- $\alpha$ -(phenyl)benzyl acetate (5a)**

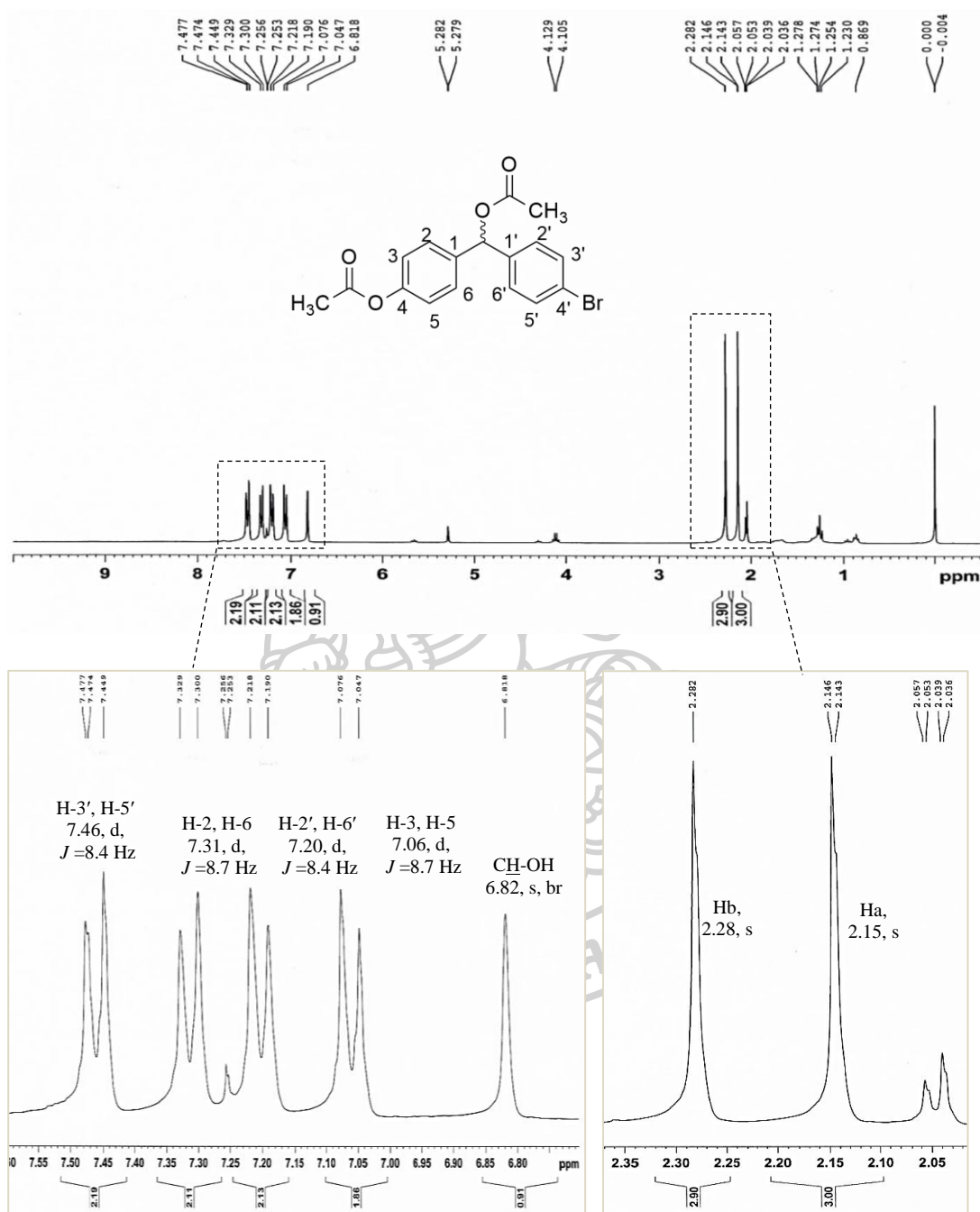
### 4-acetoxy- $\alpha$ -(4'-bromo phenyl)benzyl acetate (5c)

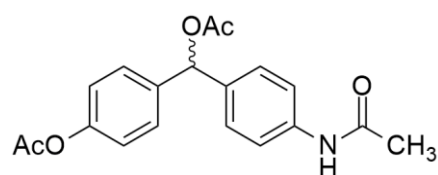


### IR spectrum

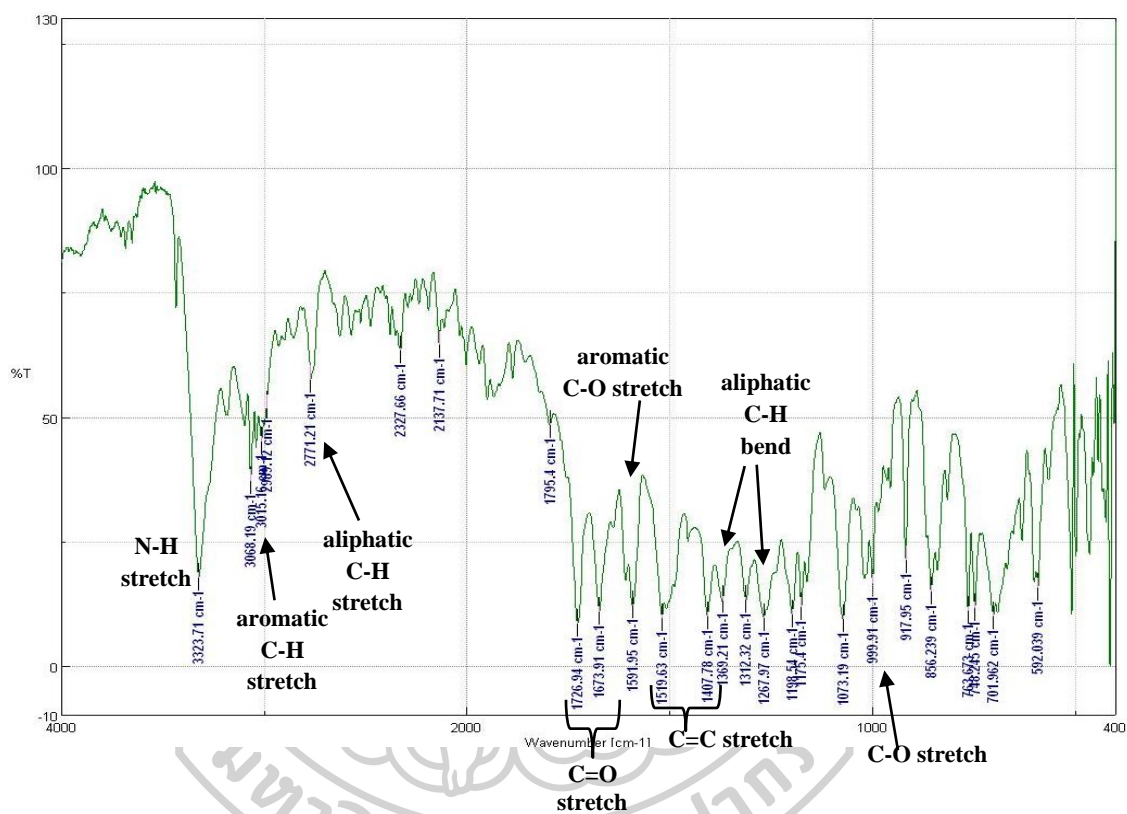


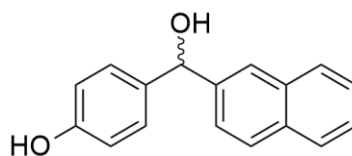
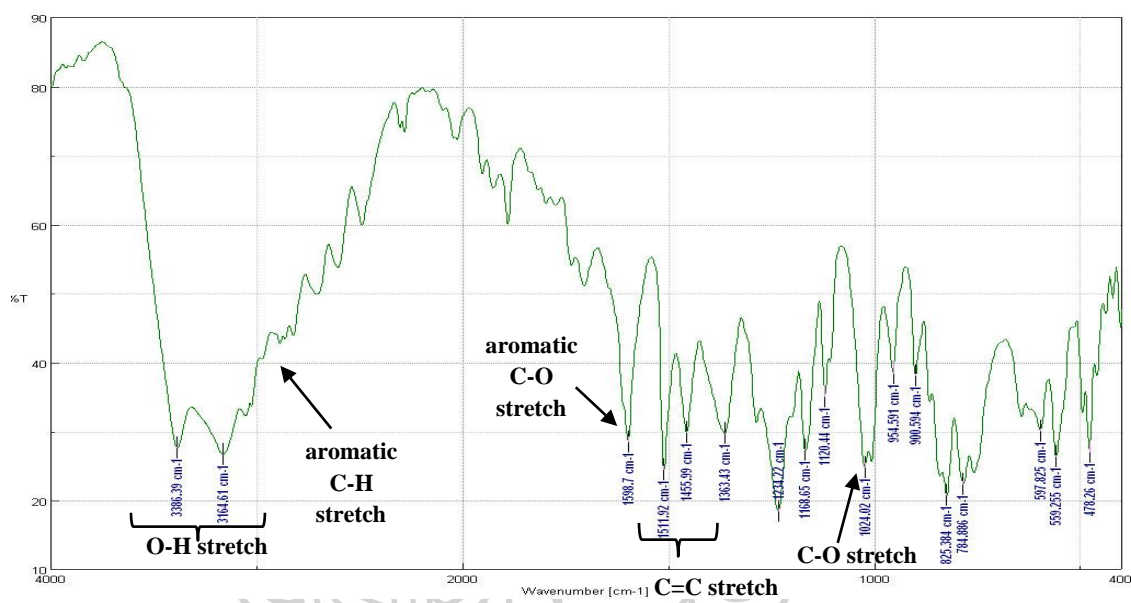
**<sup>1</sup>H NMR spectrum (300 MHz, CDCl<sub>3</sub>) of 4-acetoxy- $\alpha$ -(4'-bromophenyl)benzyl acetate (5c)**



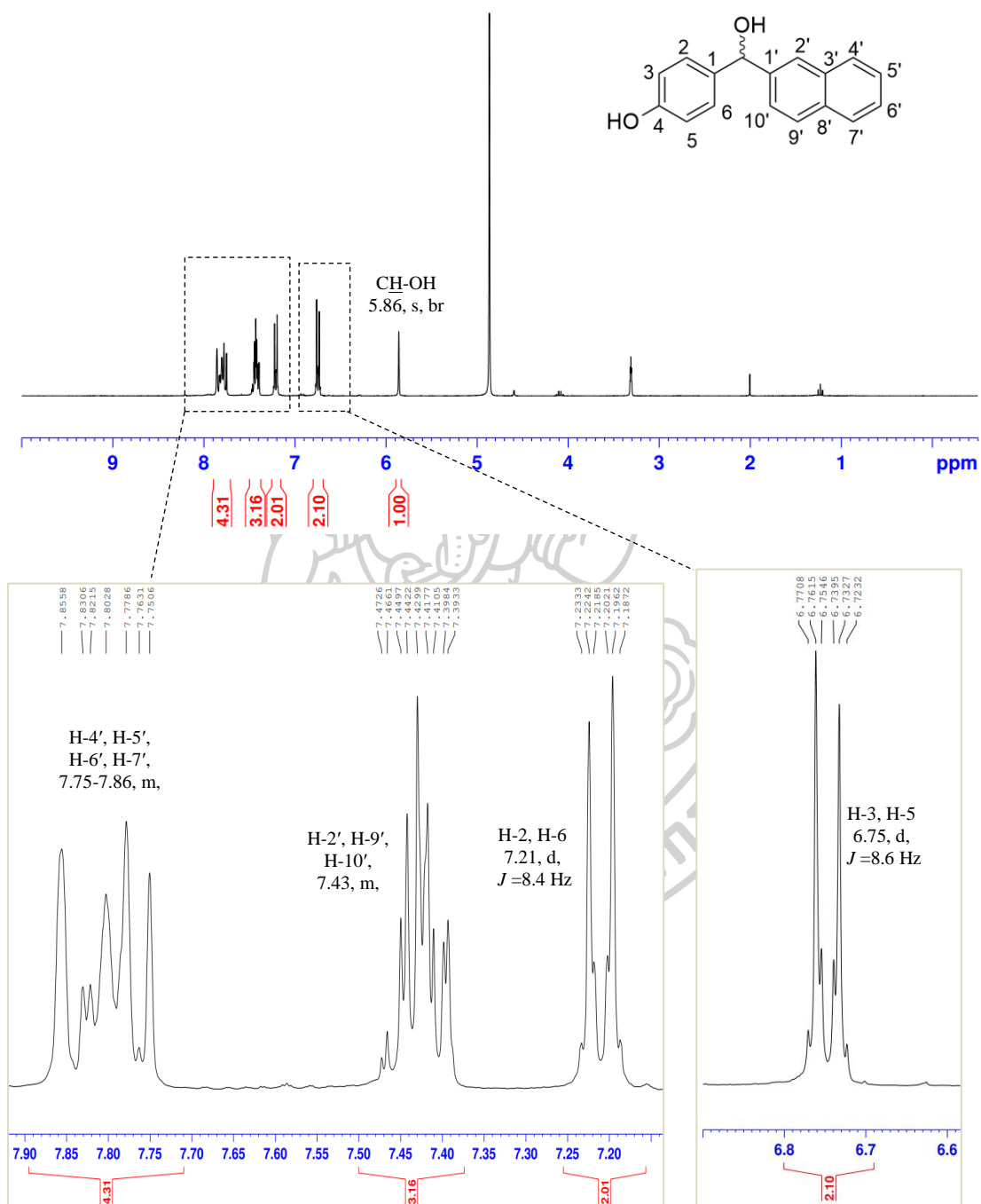
4-acetoxy- $\alpha$ -(4'-acetamido phenyl)benzyl acetate (5f)

## IR spectrum

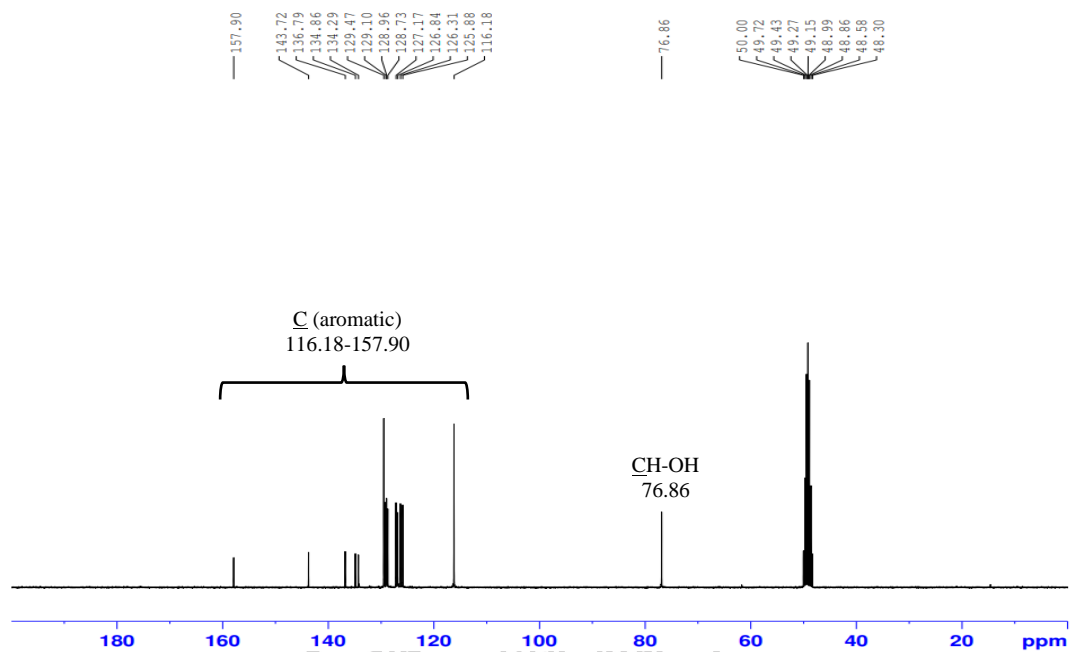


**4-hydroxyphenyl(2-naphthyl)methanol (9)****IR spectrum**

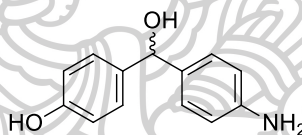
**<sup>1</sup>H NMR spectrum (300 MHz, CD<sub>3</sub>OD) of 4-hydroxyphenyl(2-naphthyl)methanol (9)**



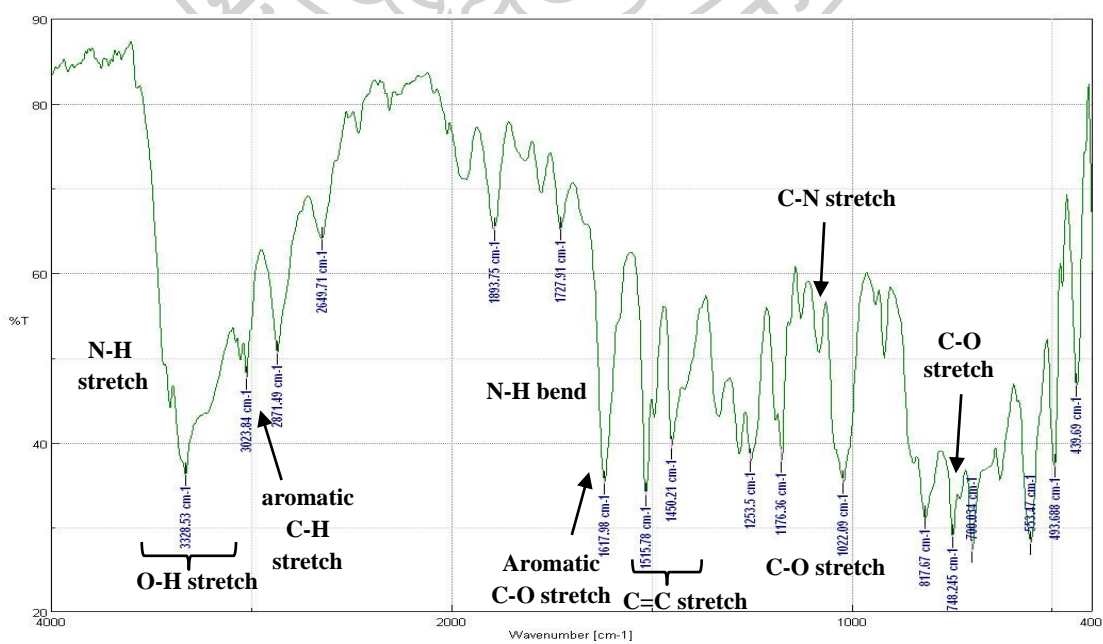
**$^{13}\text{C}$  NMR spectrum (75 MHz,  $\text{CD}_3\text{OD}$ ) of 4-hydroxyphenyl(2-naphthyl)methanol (9)**



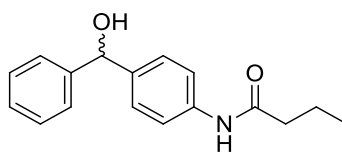
**4-hydroxy- $\alpha$ -(4'-amino phenyl)benzyl alcohol (10)**



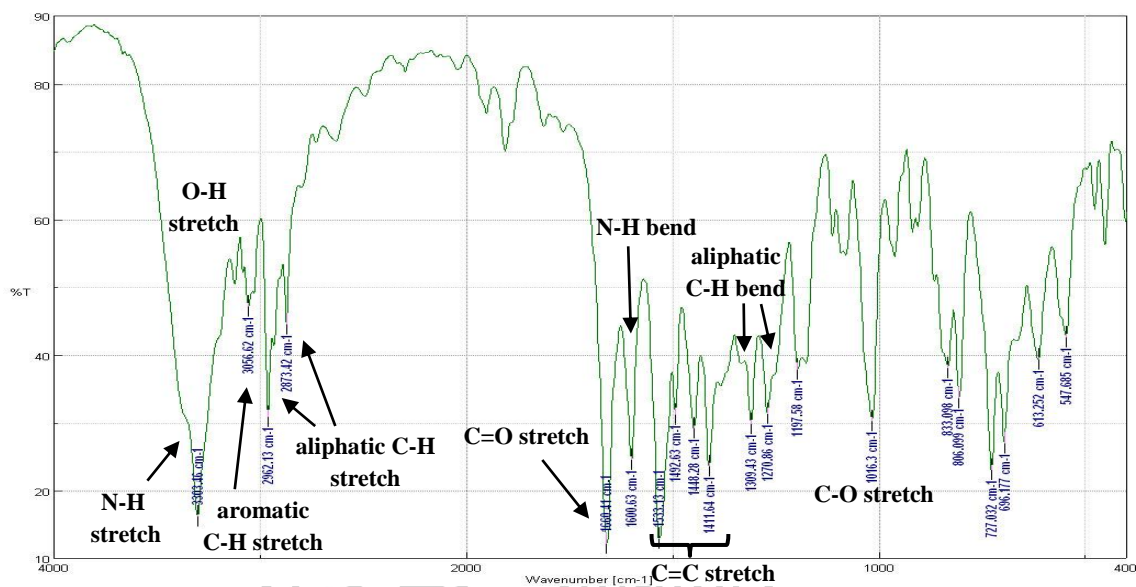
**IR spectrum**



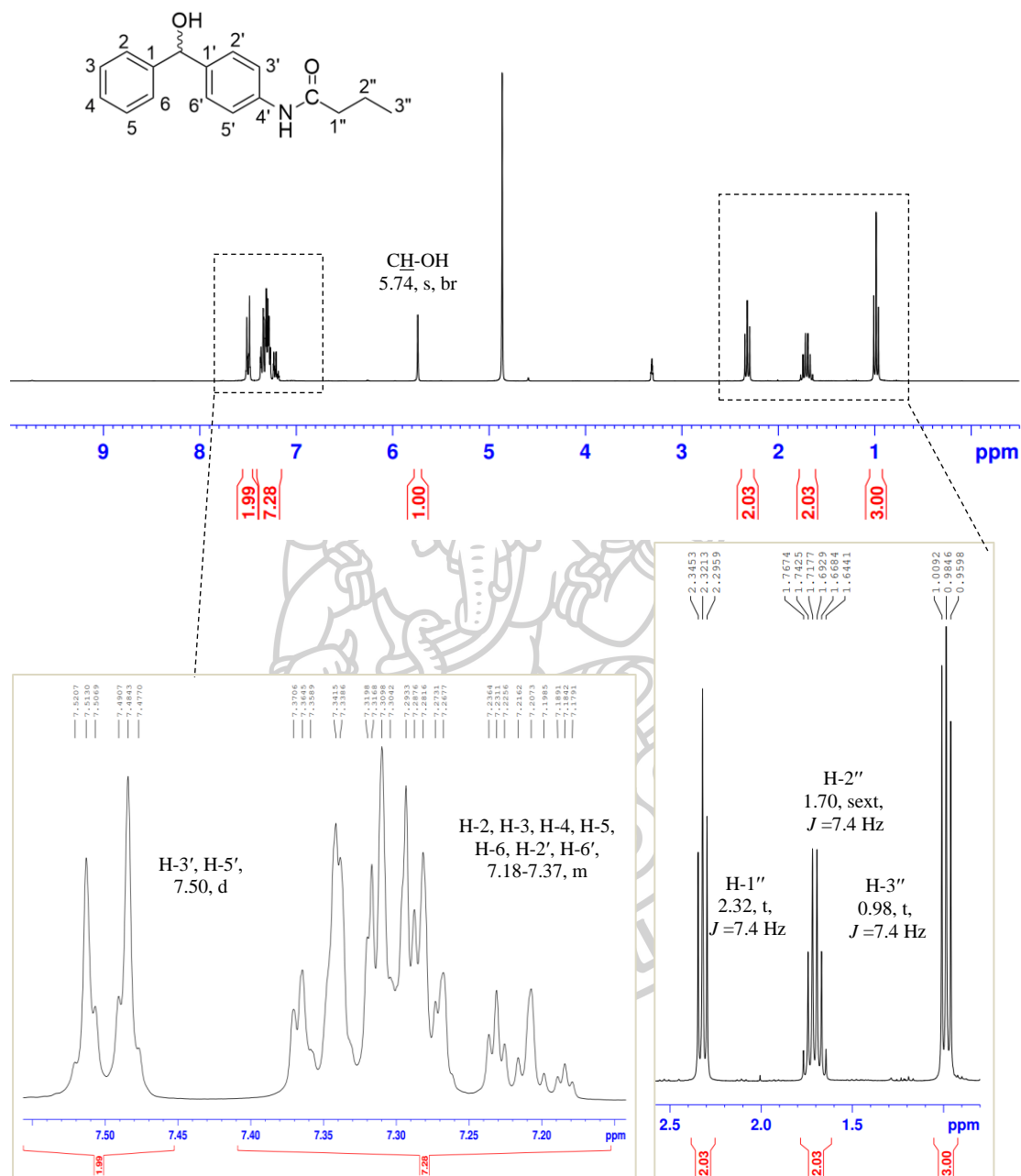


4-butylamido- $\alpha$ -(phenyl)benzyl alcohol (13a)

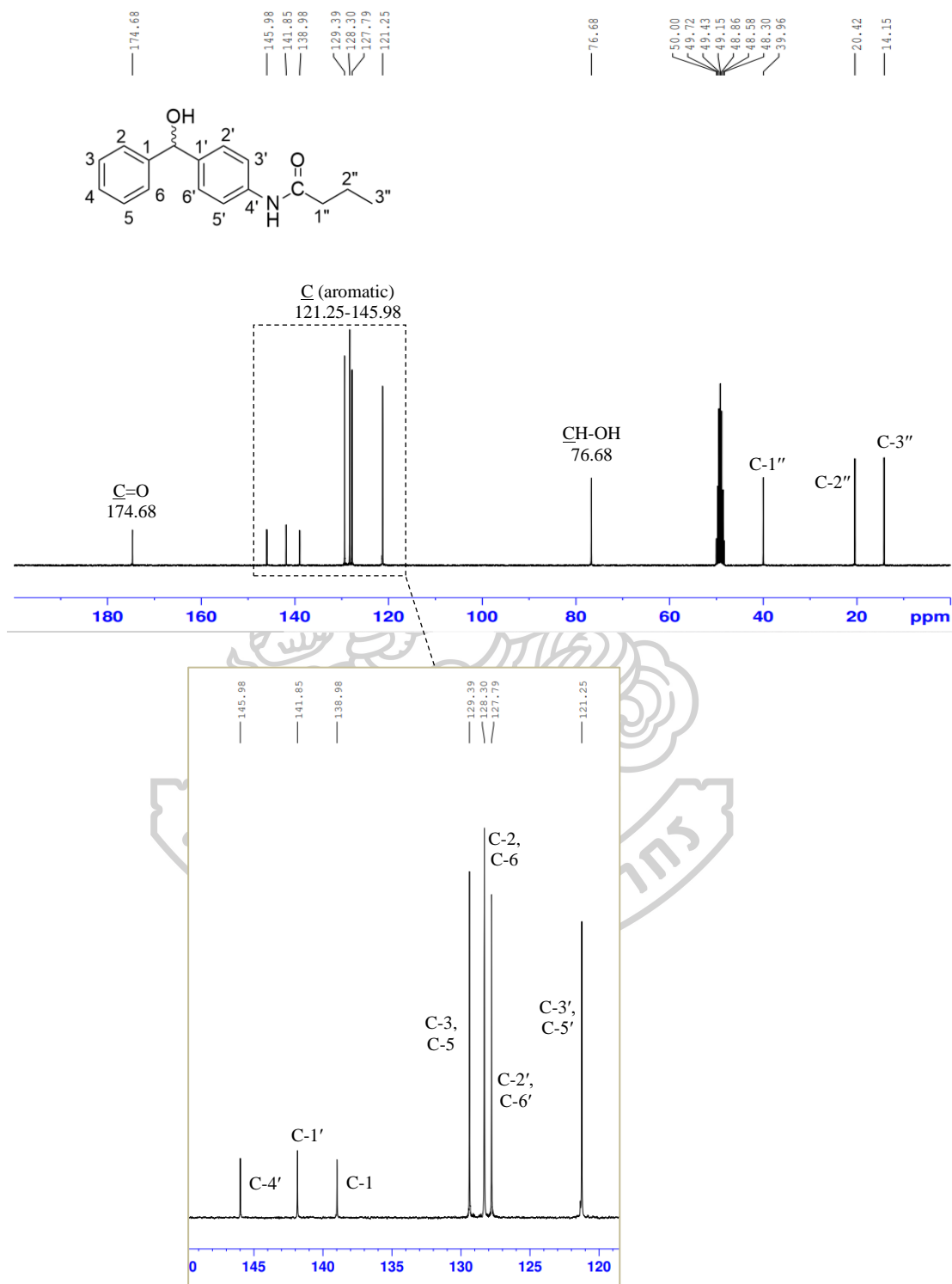
## IR spectrum

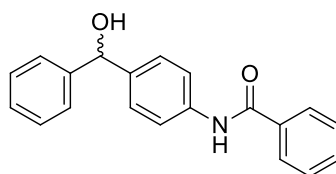
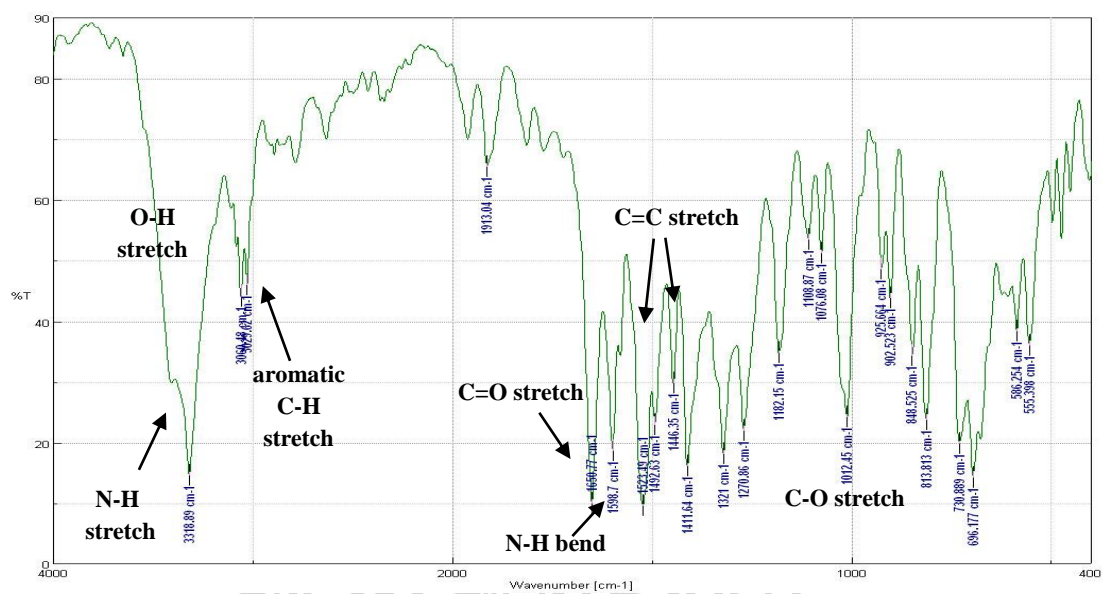


**$^1\text{H}$  NMR spectrum (300 MHz,  $\text{CD}_3\text{OD}$ ) of 4-butyramido- $\alpha$ -(phenyl)benzyl alcohol (13a)**

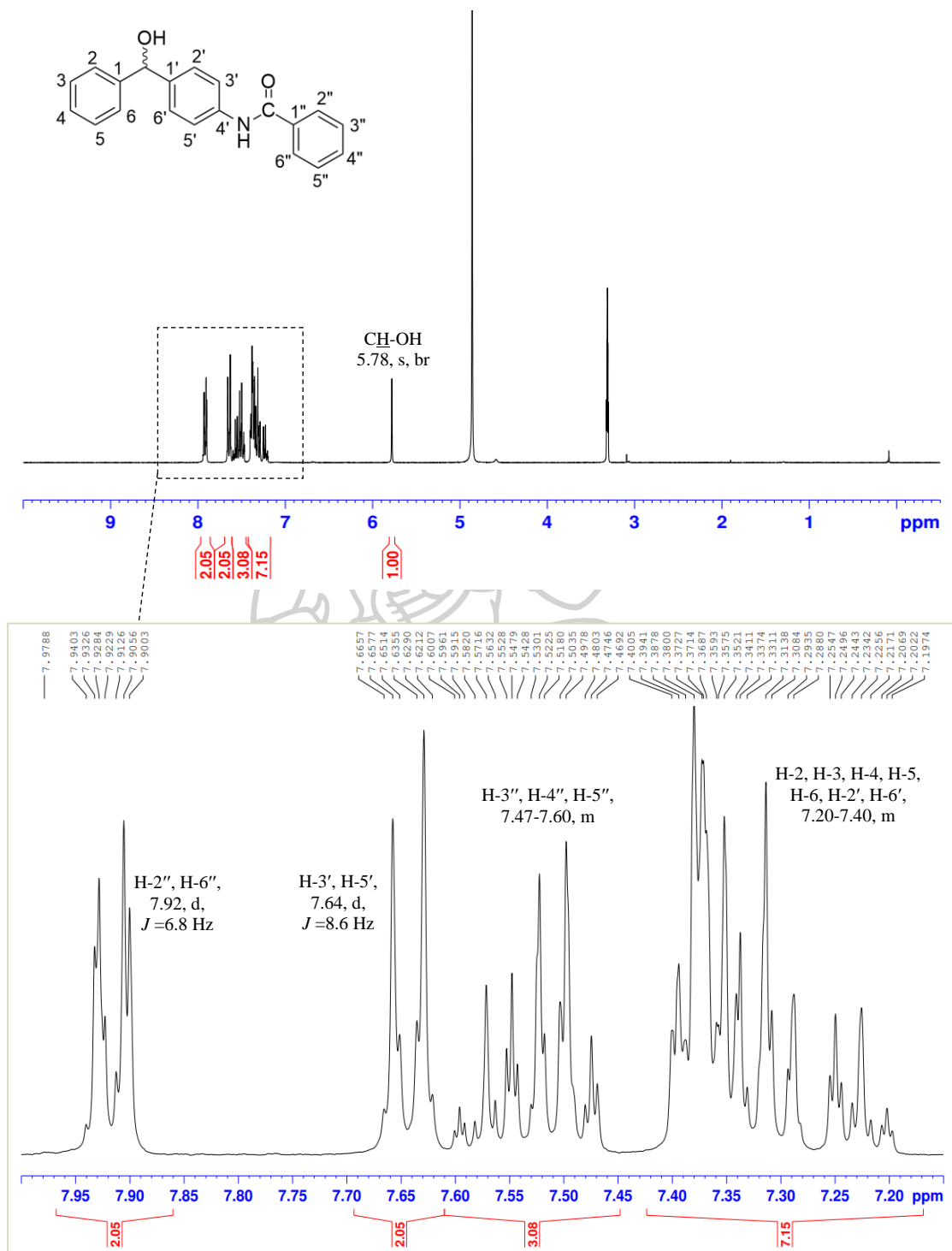


$^{13}\text{C}$  NMR spectrum (75 MHz,  $\text{CD}_3\text{OD}$ ) of 4-butyramido- $\alpha$ -(phenyl)benzyl alcohol (13a)

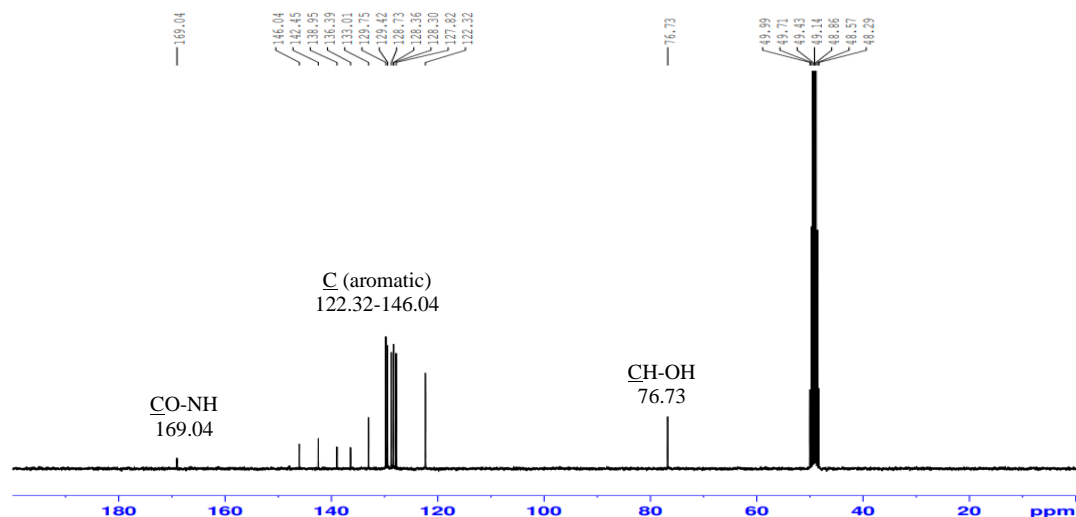


**4-benzamido- $\alpha$ -(phenyl)benzyl alcohol (13b)****IR spectrum**

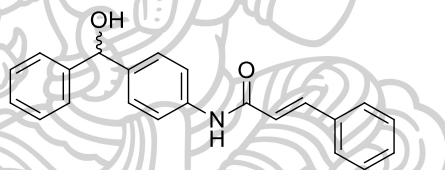
**<sup>1</sup>H NMR spectrum (300 MHz, CD<sub>3</sub>OD) of 4-benzamido- $\alpha$ -(phenyl)benzyl alcohol (13b)**



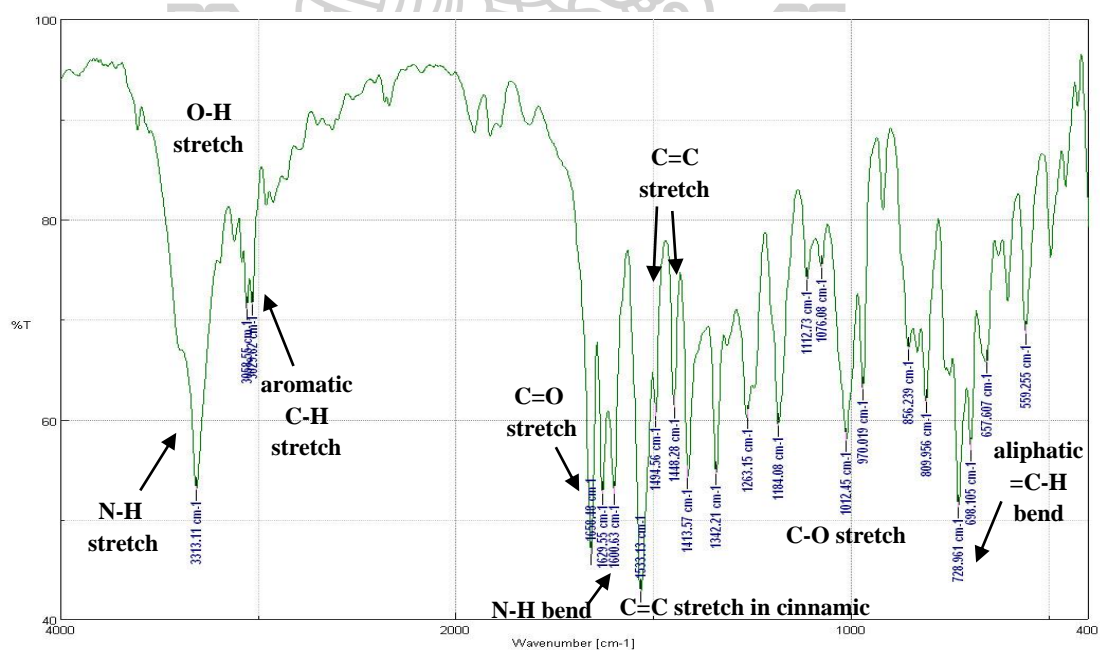
**$^{13}\text{C}$  NMR spectrum (75 MHz,  $\text{CD}_3\text{OD}$ ) of 4-benzamido- $\alpha$ -(phenyl)benzyl alcohol (13b)**



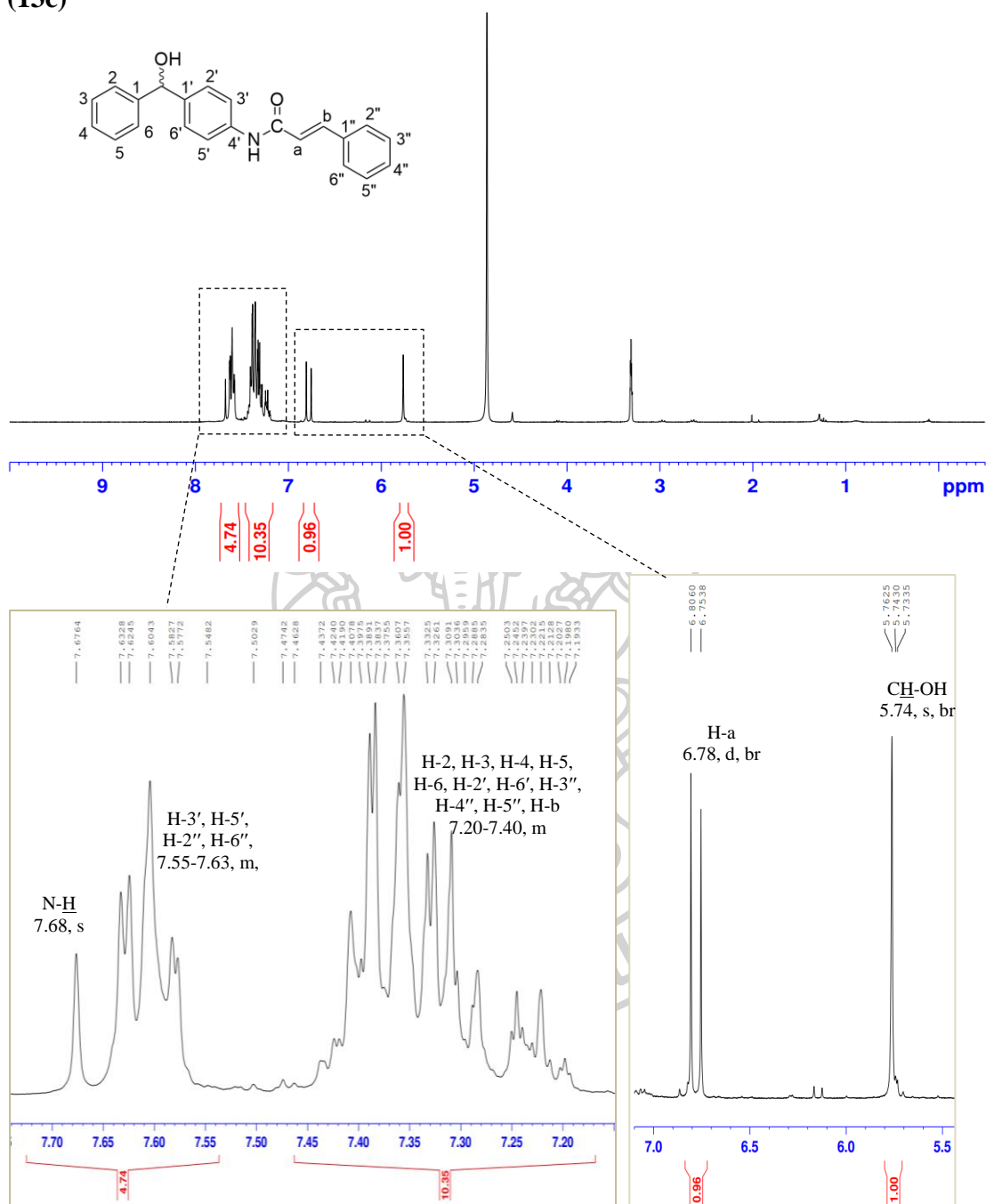
**4-cinnamido- $\alpha$ -(phenyl)benzyl alcohol (13c)**



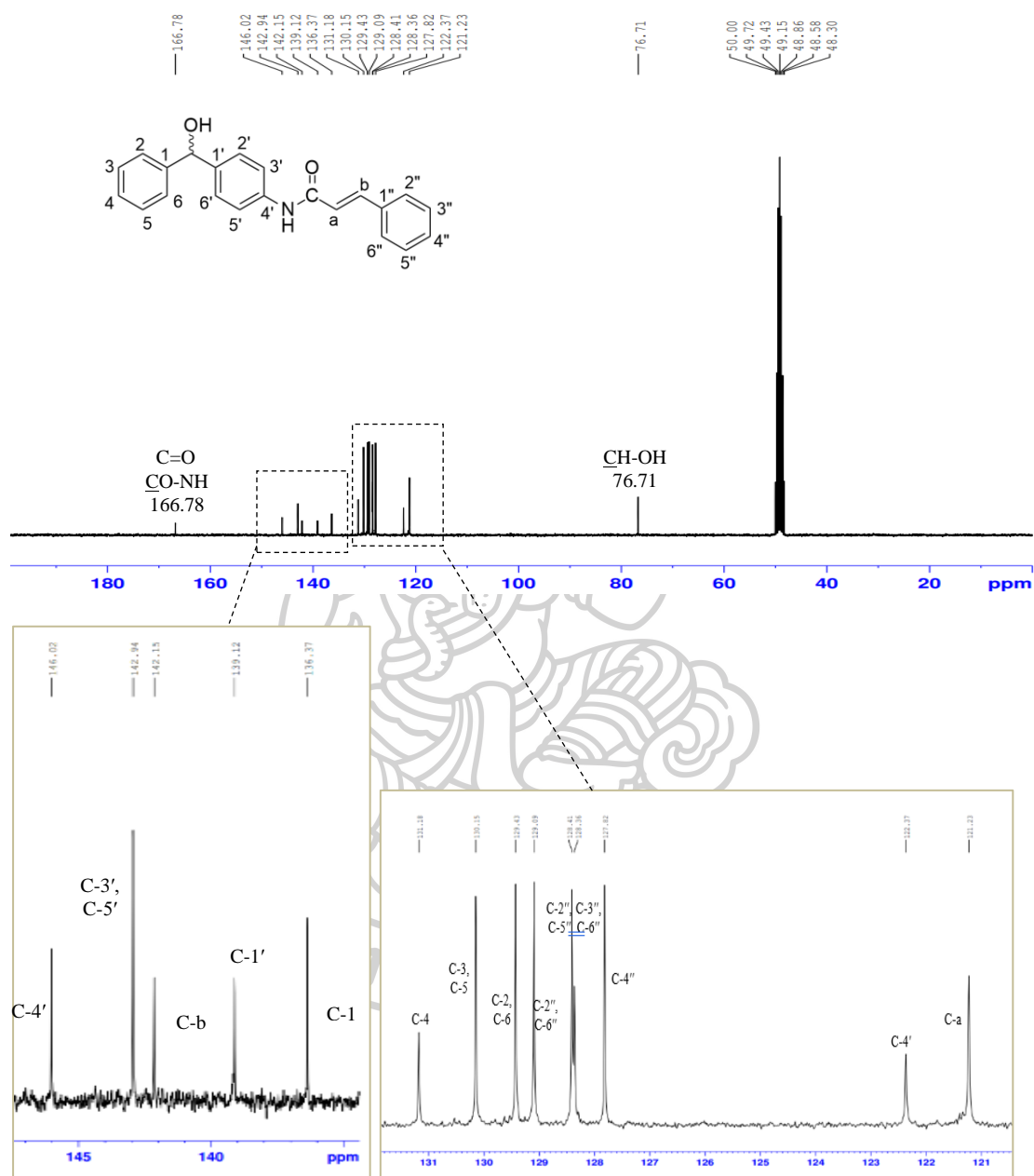
**IR spectrum**



**$^1\text{H}$  NMR spectrum (300 MHz,  $\text{CD}_3\text{OD}$ ) of 4-cinnamido- $\alpha$ -(phenyl)benzyl alcohol (13c)**



**$^{13}\text{C}$  NMR spectrum (75 MHz,  $\text{CD}_3\text{OD}$ ) of 4-benzamido- $\alpha$ -(phenyl)benzyl alcohol (13b)**





## VITA

**NAME** Pitikan Kanjanapruk

**DATE OF BIRTH** 3 August 1984

**PLACE OF BIRTH** Nakhon Pathom

**INSTITUTIONS ATTENDED** Faculty of Pharmacy, Silpakorn University

**HOME ADDRESS** 132/34 Casa Ville Ratchaphruek – Rama 5, Bang Krang, Mueang Nonthaburi, Nonthaburi 11000

**PUBLICATION** Kanjanapruk, P., Prammananan, T., Niratisai, S., & Pochanakom, K. (2022). Synthesis of Benzhydrol Derivatives as Antituberculosis Agents via Fries Rearrangement Method Investigated by DSC Analysis. In Key Engineering Materials (Vol. 914, pp. 141–146).

